ANKARA YILDIRIM BEYAZIT UNIVERSITY

GRADUATE SCHOOL OF NATURAL AND APPLIED SCIENCES

THERMAL MODELING AND ENERGY ANALYSIS OF SMALL SATELLITES AT LOW EARTH ORBITS

Ph.D. Thesis by

Cihan ATAR

Department of Energy Systems Engineering

January, 2024

ANKARA

THERMAL MODELING AND ENERGY ANALYSIS OF SMALL SATELLITES AT LOW EARTH ORBITS

A Thesis Submitted to

The Graduate School of Natural and Applied Sciences of

Ankara Yıldırım Beyazıt University

In Partial Fulfillment of the Requirements for the Degree of Doctor of Philosophy in Energy Systems Engineering, Department of Energy Systems Engineering

by

Cihan ATAR

January, 2024

ANKARA

Ph.D. THESIS EXAMINATION RESULT FORM

We have read the thesis entitled **"THERMAL MODELING AND ENERGY ANALYSIS OF SMALL SATELLITES AT LOW EARTH ORBITS"** completed by **CİHAN ATAR** under the supervision of **PROF. DR. METİN AKTAŞ** and **PROF. DR. NEDİM SÖZBİR** and we certify that in our opinion it is fully adequate, in scope and in quality, as a thesis for the degree of Doctor of Philosophy.

Prof. Dr. Metin AKTAŞ

Supervisor

Prof. Dr. Nedim SÖZBİR

Co-Supervisor

Prof. Dr. Ünal ÇAMDALI	Prof. Dr. Atilla BIYIKOĞLU
Jury Member	Jury Member
Assoc. Prof. Dr. Murat BULUT	Asst. Prof. Dr. Sıtkı KOCAOĞLU
Jury Member	Jury Member

Prof. Dr. Sadettin ORHAN

Director

Graduate School of Natural and Applied Sciences

ETHICAL DECLARATION

I hereby declare that, in this thesis which has been prepared in accordance with the Thesis Writing Manual of Graduate School of Natural and Applied Sciences,

- All data, information and documents are obtained in the framework of academic and ethical rules,
- All information, documents and assessments are presented in accordance with scientific ethics and morals,
- All the materials that have been utilized are fully cited and referenced,
- No change has been made on the utilized materials,
- All the works presented are original,

and in any contrary case of above statements, I accept to renounce all my legal rights.

Date: 11/01/2024 **Signature: ……..**

Name & Surname: Cihan ATAR

ACKNOWLEDGMENTS

First, I would like to express my sincere appreciation to my supervisor, Prof. Dr. Metin AKTAŞ for his tremendous support and motivation during my study. His immense knowledge and precious recommendations constituted the milestones of this study. His guidance helped me throughout my research and while drafting this dissertation.

I would like to express my deepest gratitude to my co-supervisor, Prof. Dr. Nedim SÖZBİR for his constant support, guidance, and constructive suggestions, which were determinant for the accomplishment of the work presented in this thesis from the very beginning of this journey.

I would also like to thank my committee members Prof. Dr. Bülent YEŞİLATA and Prof. Dr. Ünal ÇAMDALI for generously offering their time, support, patient guidance and useful critiques throughout the preparation of this research work.

I would like to thank Assoc. Prof. Dr. Murat BULUT not only for providing his expertise but also for his motivating and constructive approach.

I had the pleasure of collaborating with the STM Defense Technologies Engineering and Trade Inc. and Elif DİRGİN.

I would like to acknowledge all instructors that I took their classes during my studies. I learnt so many things in their classes and expanded my horizon with their teaching.

My very special thanks go to my parents for their endless support and encouragement. Your unconditional love and endless support have meant the world to me.

Last but not least, I would like to thank my family. My lovely wife has been extremely supportive during the entire process while my little son has provided all the motivation that I required to finish my degree.

2024, 11 January **Cihan ATAR**

THERMAL MODELING AND ENERGY ANALYSIS OF SMALL SATELLITES AT LOW EARTH ORBITS

ABSTRACT

The interest in small satellites, playing crucial role in various tasks from communication to scientific research, have been strongly increasing. The process of designing and developing small satellites requires detailed engineering approaches to ensure safe and reliable space missions. This research concentrates on thermal modeling and energy analysis of small satellites, specifically CubeSats, operating at various low Earth orbits by considering the thermal environment in space, orbital characteristics, and satellite design parameters, with respect to thermal behavior. The aims of this study include revealing relationships among the variables effecting thermal performance of satellites, investigating the effects of deployable solar panels, providing valuable insight for satellite thermal modeling, and developing a fast and accurate thermal analyzer tool for thermal testing in the early design stage. First, external heat loads and temperature distributions for CubeSats sizing from 1U to 12U were examined for orbital altitudes from 400 km to 2000 km, beta angles from 0 to 75 degrees, and different coating types. Then, the thermal effects associated with solar panel deployment angles were assessed in detail by changing deployment angles from -75 to +75 degrees. Finally, a spreadsheet thermal simulation tool for predicting and obtaining the temperature distribution of the satellite with an acceptable accuracy for preliminary design phases was developed by utilizing numerical methods. The results presented that orbital altitude, beta angle, satellite size and surface properties greatly influence the absorbed heat by satellite panels and temperature distribution across the satellite. It was also shown that the satellite heat budget is affected by deployment angles. Furthermore, the developed tool was found to be a cost-effective solution when compared to the real thermal test data. In conclusion, the findings of this study can be beneficial, particularly in developing small satellites and determining optimal orbital configurations, in the preliminary design phase.

Keywords: CubeSat, satellite thermal analysis, thermal modeling, space heat flux, low earth orbit, aerospace heat transfer, numerical methods.

ALÇAK DÜNYA YÖRÜNGELERİNDEKİ KÜÇÜK UYDULARIN TERMAL MODELLEMESİ VE ENERJİ ANALİZİ

ÖZ

İletişimden bilimsel araştırmalara kadar pek çok görevde hayati rol oynayan küçük uydulara olan ilgi giderek artmaktadır. Küçük uyduların tasarlanması ve geliştirilmesi süreci, güvenli ve güvenilir uzay görevlerini sağlamak için detaylı mühendislik yaklaşımlarını gerektirmektedir. Bu çalışma, uzaydaki termal ortamı, yörünge özelliklerini ve uydu tasarım parametrelerini termal davranış açısından dikkate alarak çeşitli alçak Dünya yörüngelerinde hizmet eden küçük uyduların, özellikle de küp uyduların, termal modellemesi ve enerji analizine odaklanmaktadır. Bu çalışmanın amaçları arasında; uyduların termal performansını etkileyen değişkenler arasındaki ilişkilerin ortaya çıkarılması, konuşlandırılabilir güneş panellerinin etkilerinin araştırılması, uydu termal modellemesi için değerli bilgiler sağlanması ve erken tasarım aşamasındaki termal testler için hızlı ve doğru bir termal analiz aracı geliştirilmesi yer almaktadır. Öncelikle, 1U'dan 12U'ya kadar boyutlara sahip küp uydular için dış ısı yükleri ve sıcaklık dağılımları, 400 km'den 2000 km'ye kadar olan yörünge yükseklikleri, 0'dan 75 dereceye kadar olan beta açıları ve farklı kaplama türleri için incelenmiştir. Daha sonra, güneş paneli konuşlandırma açılarıyla ilişkili termal etkiler, konuşlandırma açıları -75'ten +75 dereceye değiştirilerek ayrıntılı olarak değerlendirildi. Son olarak, sayısal yöntemler kullanılarak ön tasarım aşamaları için uydunun sıcaklık dağılımını kabul edilebilir bir doğrulukla tahmin etmek ve elde etmek için bir elektronik tablo termal simülasyon aracı geliştirilmiştir. Sonuçlar, yörünge yüksekliği, beta açısı, uydu boyutu ve yüzey özelliklerinin, uydu panelleri tarafından emilen ısıyı ve uydu boyunca sıcaklık dağılımını büyük ölçüde etkilediğini ortaya koydu. Uydu ısı bütçesinin, konuşlandırma açılarından etkilendiği de gösterilmiştir. Ayrıca, geliştirilen aracın, gerçek termal test verileriyle karşılaştırıldığında uygun maliyetli bir çözüm olduğu doğrulandı. Sonuç olarak, bu çalışmanın bulguları, özellikle ön tasarım aşamasında küçük uyduların geliştirilmesinde ve optimal yörünge konfigürasyonlarının belirlenmesinde faydalı olabilir.

Anahtar Kelimeler: Küp uydu, uydu termal analizi, termal modelleme, uzay ısı akısı, alçak Dünya yörüngesi, havacılık ısı transferi, sayısal yöntemler.

CONTENTS

Ph.D. THESIS EXAMINATION RESULT FORM ii
ETHICAL DECLARATION iii
ACKNOWLEDGMENTS iv
ABSTRACT v
ÖZ vi
NOMENCLATURE x
LIST OF TABLES xiii
LIST OF FIGURES xiv
CHAPTER 1 - INTRODUCTION 1
1.1 Fundamentals 1
1.1.1 Satellites 1
1.1.2 Satellite Orbits 6
1.1.3 Satellite Thermal Design 9
1.1.4 Thermal Modeling 11
1.1.5 Thermal Analysis 12
1.1.6 Thermal Control Systems 14
1.1.7 Thermal Testing 17
1.2 Literature Review 21
1.3 Aim of the Study 29
1.4 Original Contributions 29
CHAPTER 2 - SPACE THERMAL ENVIRONMENT 31
2.1 Orbital Parameters 31
2.2 Heat Fluxes for a Satellite in Space 32
2.2.1 Solar Radiation 33
2.2.2 Albedo Radiation 34
2.2.3 Planet Infrared Radiation 35
2.2.4 Internal Heat Dissipation 35
2.2.5 Heat Rejection 36
2.3 Heat Transfer Mechanisms 36
2.3.1 Conduction 37
2.3.2 Radiation 38
2.4 Balance Equations 42

2.5 Thermal Cases 44
2.5.1 Extreme Hot Case 45
2.5.2 Extreme Cold Case 45
2.6 Thermal Mathematical Modeling 45
2.6.1 Thermal Network 46
2.6.2 Nodal Breakdown 47
2.6.3 Simulation Procedure 49
2.6.4 Simulation Software 49
CHAPTER 3 - INVESTIGATION OF EXTERNAL HEATS FOR CUBESATS AT VARIOUS LOW EARTH ORBITS 53
3.1 Introduction 53
3.2 Material and Methods 54
3.3 Orbital Periods 56
3.4 Orbital Altitudes 57
3.5 Panel Directions 59
3.6 Beta Angles 60
3.7 Satellite Sizes 62
3.8 Surface Coatings 63
3.9 Conclusion 65
CHAPTER 4 - INVESTIGATION OF SURFACE TEMPERATURES FOR CUBESATS AT VARIOUS LOW EARTH ORBITS 67
4.1 Introduction 67
4.2 Material and Methods 69
4.3 Orbital Altitudes 71
4.4 Satellite Sizes 75
4.5 Beta Angles 77
4.6 Surface Coatings 78
4.7 Heat Dissipations 79
4.8 Conclusion 80
CHAPTER 5 - INVESTIGATION ON THERMAL INFLUENCE OF SOLAR PANEL DEPLOYMENT ANGLE 81
5.1 Introduction 81
5.2 Material and Methods 83
5.3 Heat Sources 86
5.4 Earth Days 87

5.5 Deployment Angles 89
5.6 Worst-Case Scenario Analysis 91
5.7 Conclusion 92
CHAPTER 6 - DEVELOPMENT OF A SPREADSHEET ANALYSIS TOOL FOR THERMAL TESTING OF CUBESATS 93
6.1 Introduction 93
6.2 Overview of PiriSat – 6U CubeSat 95
6.3 Thermal Testing of PiriSat 97
6.4 TheSpAn - MS Excel Based Analysis Tool 98
6.5 Numerical Background of TheSpAn 101
6.6 Results 104
6.7 Conclusion 111
CHAPTER 7 - DISCUSSION AND CONCLUSION 113
REFERENCES 116
APPENDICES 128
Appendix A – Some Real Examples on Satellite Thermal Issues 129

NOMENCLATURE

Roman Letter Symbols

A	Heat transfer area, m^2
B	Radiative exchange factor
c	Specific heat capacity, J/(kg·K)
C	Thermal capacitance, J/K
F	View factor
GL	Conductive coupling, W/K
GR	Radiative coupling, m^2
k	Thermal conductivity, W/(m·K)
L	Length, m
m	Mass, kg
q	Heat flux, W/m^2
Q	Heat, W
R	Resistance, V/A
R	Thermal resistance, K/W
S	Separation distance, m
t	Time, s
T	Absolute temperature, K

Greek Letter Symbols

α	Absorptivity
β	Beta angle
ε	Emissivity
ϕ	Solar zenith angle
ρ	Density
σ	Stefan-Boltzmann constant, 5.67×10^{-8} $W/(m^2\cdot K^4)$
θ	Solar ray angle
θ	Variable-weighted implicit factor

Subscripts

c	Cold
h	Hot
i	Specified node number

in	Inlet
IR	Infrared radiation
j	Specified node number
k	Specified node number
m	Mean
max	Maximum
min	Minimum
n	Node number
out	Outlet
p	Isobaric
p	Projected
rad	Radiation
s	Surface
$1, 2$	Any sides (hot or cold side)
x	x-direction
y	y-direction
z	z-direction

Acronyms

AIS	Automatic Identification System
AU	Astronomical Unit
CAD	Computer-Aided Drawing
CTE	Coefficient of Thermal Expansion
FEM	Finite Element Analysis
FSM	First Surface Mirror
GEO	Geostationary Earth Orbit
GMM	Geometrical Mathematical Model
GPS	Global Positioning System
HEO	High Earth Orbit
HEO	Highly Eccentric Orbit
IR	Infrared Radiation
LEO	Low Earth Orbit
MEO	Medium Earth Orbit
MLI	Multi-Layer Insulation

MS	Microsoft
OSR	Optical Solar Reflector
PCM	Phase-Change Material
REF	Radiative Exchange Factor
SC	Spacecraft
SSM	Second Surface Mirror
TBT	Thermal Balance Test
TCT	Thermal Cycle Test
TMM	Thermal Mathematical Model
TT&C	Telemetry, Tracking and Command
TVCT	Thermal Vacuum Cycling Test

LIST OF TABLES

Table 1.1 Categorization of satellites by weights 3
Table 1.2 Classification of CubeSats regarding the size and mass 3
Table 1.3 Evaluating various methods for simulating heat flux in TBT..... 19
Table 2.1 Thermal data example for extreme cases 44
Table 2.2 Equivalent components in electrical and thermal systems..... 46
Table 3.1 Durations in illuminated and shadow for varying beta angles..... 61
Table 3.2 Solar absorptivity and IR emissivity of surface coatings..... 63
Table 4.1 Solar absorptivity and IR emissivity values for coating types..... 70
Table 5.1 Earth days..... 84
Table 5.2 Albedo coefficients and earth surface temperatures 85
Table 5.3 Solar fluxes for different earth days..... 88
Table 5.4 Total absorbed heat by the satellite for different earth days 88
Table 5.5 Total heat absorbed by the satellite for different deployment angles 90
Table 5.6 Worst-Case scenario analysis..... 91
Table 6.1 Technical specifications of PiriSat..... 96
Table 6.2 Significance values of 2-tailed test for satellite panels 108
Table 6.3 Significance values of 2-tailed test for satellite equipment 110

LIST OF FIGURES

Figure 1.1 PICASSO CubeSat 2
Figure 1.2 Standard sizes of CubeSats 4
Figure 1.3 A typical illustration for the bus and the payload of a satellite 5
Figure 1.4 Orbital inclination 7
Figure 1.5 Orbital eccentricity 7
Figure 1.6 Orbital distances 8
Figure 1.7 Iterative process illustration of satellite thermal design 10
Figure 1.8 A general process of thermal modeling 11
Figure 1.9 Basic illustrations of FSM and SSM 15
Figure 1.10 Temperature curve with respect to time for a standard TVCT 21
Figure 2.1 Shadow passages of a satellite orbiting around the Earth 32
Figure 2.2 Space thermal environment for a satellite 33
Figure 2.3 Geometrical definition of view factor 39
Figure 2.4 Nodal illustration of satellite thermal system 44
Figure 2.5 Thermal network for (a) conduction and (b) radiation 47
Figure 2.6 Nodal representation of the model 48
Figure 2.7 Basic workflow demonstration of Systema software suite 51
Figure 3.1 CubeSats models having different sizes 55
Figure 3.2 CubeSats orbits having different beta angles 56
Figure 3.3 Durations of period, shadow and illuminated at different orbital altitudes 57
Figure 3.4 Absorbed heat from external sources with respect to the orbital altitudes 58
Figure 3.5 Total absorbed heat inputs with respect to the orbital altitudes 58
Figure 3.6 Total heat absorbed by different panels of 1U CubeSat at 400 km 59
Figure 3.7 Total solar heat absorbed by different panels of 1U CubeSat at 400 km . 60
Figure 3.8 Total absorbed heat for different beat angles of 1U CubeSat at 800 km .. 62
Figure 3.9 Total absorbed heat for different CubeSat sizes at 800 km 63
Figure 3.10 Total absorbed heat for different coatings applied to 1U CubeSat orbiting at 800 km 64
Figure 4.1 Thermal links for CubeSat panels in space 69
Figure 4.2 Changes in distance of the Earth from the Sun 71
Figure 4.3 Total absorbed heat by 1U CubeSat panels 72
Figure 4.4 Absorbed heat by different panels of 1U CubeSat at 1200 km 72

Figure 4.5 Temperature profiles for +X panel of 1U CubeSat at different altitudes . 73
Figure 4.6 Temperature profiles for -X panel of 1U CubeSat at different altitudes .. 73
Figure 4.7 Temperature profiles for +Y panel of 1U CubeSat at different altitudes . 74
Figure 4.8 Temperature profiles for -Y panel of 1U CubeSat at different altitudes .. 74
Figure 4.9 Temperature profiles of for +Z panel of 1U CubeSat at different altitudes 75
Figure 4.10 Temperature profiles for -Z panel of 1U CubeSat at different altitudes. 75
Figure 4.11 Absorbed heat by panels of different sized CubeSats at 1200 km 76
Figure 4.12 Minimum, average and maximum temperature profiles for different CubeSat sizes 77
Figure 4.13 Temperature profiles for different beta angles of 1U CubeSat at 800 km 78
Figure 4.14 Temperature profiles for different coatings of 1U CubeSat at 800 km .. 79
Figure 4.15 Temperature profiles at -Z Panel of 1U CubeSat for different heat dissipations 79
Figure 5.1 Panel directions of 3U CubeSat 83
Figure 5.2 Kinematics of 3U CubeSat 84
Figure 5.3 Solar panel deployment angle 85
Figure 5.4 Heat absorbed by the satellite per orbit on January 3rd 86
Figure 5.5 Heat absorbed by CubeSat panels per orbit on January 3rd 87
Figure 5.6 Heat absorbed by solar panels per orbit on January 3rd 87
Figure 5.7 Total absorbed heat by the satellite for different deployment angles 89
Figure 6.1 An exterior illustration of PiriSat 95
Figure 6.2 Interior demonstration of PiriSat 97
Figure 6.3 Home sheet of TheSpAn 98
Figure 6.4 GL sheet of TheSpAn 99
Figure 6.5 GR sheet of TheSpAn 99
Figure 6.6 Results sheet of TheSpAn 100
Figure 6.7 Graph sheet of TheSpAn 101
Figure 6.8 Discretization of space and time within a finite difference grid 102
Figure 6.9 Temperature profiles of +X Panel, obtained by SINDA and TheSpAn . 105
Figure 6.10 Temperature profiles of EQ8, obtained by SINDA and TheSpAn 105
Figure 6.11 Temperature profiles of +X Panel, obtained by TVC test and TheSpAn 106
Figure 6.12 Temperature profiles of +Y Panel, obtained by TVC test and TheSpAn 107

Figure 6.13 Temperature profiles of +Z Panel, obtained by TVC test and TheSpAn 108

Figure 6.14 Temperature profiles of AIS, obtained by TVC test and TheSpAn 109

Figure 6.15 Temperature profiles of Power Battery, obtained by TVC test and TheSpAn 109

Figure 6.16 Temperature profiles of Langmuir Board, obtained by TVC test and TheSpAn 110

CHAPTER 1

INTRODUCTION

Space studies have been in the center of interest areas of humankind and spacecraft is one of the most important parts of them. Scientists have dedicated extensive efforts over the years to create innovative concepts, designs, and technologies in the spacecraft industry. Satellites are artificial spacecraft intentionally placed into orbits and they have important duties of communication, broadcasting, navigation, weather forecasting, scientific research, military, and civilian surveillance activities. Designing and developing satellites to provide more reliable and efficient systems requires challenging engineering phases. Both mechanical and thermal strength must be obtained for them to service in harsh space environment.

1.1 Fundamentals

The fundamentals required for providing full understanding of this study are presented under this section. For this purpose, satellite basics including types and orbits are briefly explained. Then, the essentials about satellite thermal design and control are described. Moreover, the approaches for satellite thermal modeling and analysis are introduced. Thus, it is aimed that even people not specialized in this field may also understand the study.

1.1.1 Satellites

The quantity of satellites in space has been increasing every other day and the interest on small satellites has also been growing lately. Satellites are artificial objects intentionally launched and placed into orbits to perform specified missions in space with required equipment. Each satellite is designed for a specific mission and equipped with necessary instrumentation to serve for that purpose in space conditions. Satellites based on their services can be classified as communication, weather forecasting, earth observation, navigation, and military satellites. Communication satellites are engineered satellites to facilitate the transmission of telecommunications signals,

enabling global communication, internet access, television broadcasting, and all other forms of data exchange across vast distances on Earth. Weather forecasting satellites are designed to collect and transmit meteorological data from space to aid in the prediction and monitoring of weather patterns and conditions on Earth. Earth observation satellites are manufactured to capture data and imagery of the Earth surface, atmosphere, and environment for various purposes, including scientific research, environmental monitoring, and remote sensing applications. Navigation satellites are crafted to broadcast signals and deliver highly accurate positioning, navigation, and timing data on a global scale, thereby enabling services like GPS (Global Positioning System) and precise location-based applications. Military satellites, on the other hand, are designed for a range of objectives, including communication, surveillance, reconnaissance, and navigation, to support military operations and national security [1].

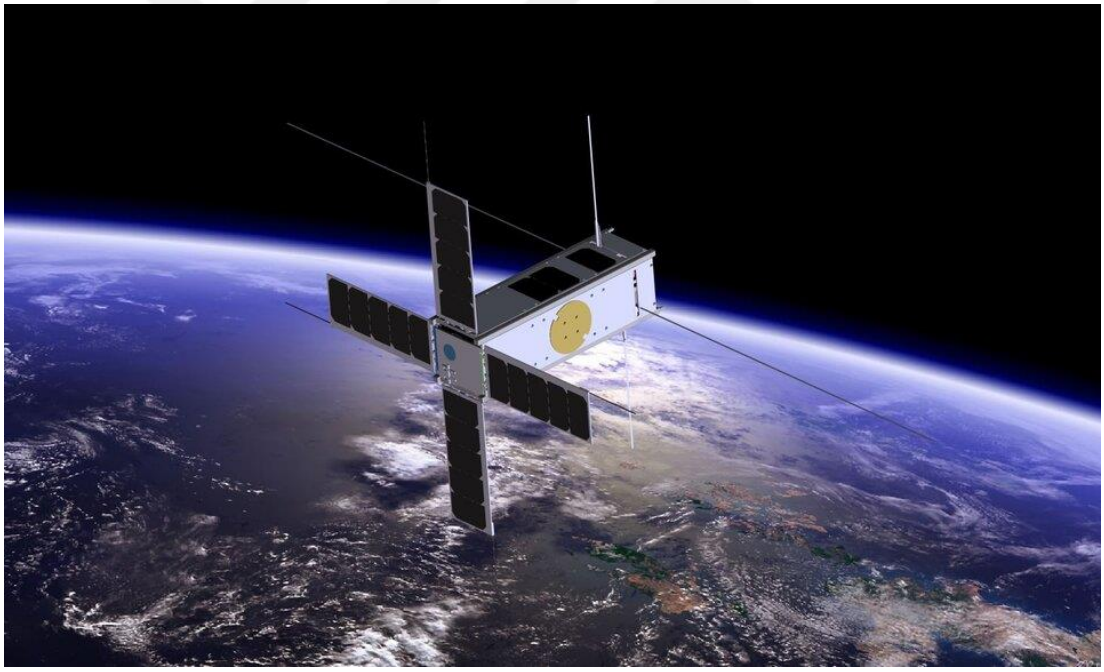

Figure 1.1 PICASSO CubeSat [4]

Satellites, which operate at different altitudes along various trajectories with varying velocities, can exhibit a diverse range of sizes and configurations. Their manufacturing scales have evolved in response to advancements in space technology. Consequently, they can be categorized based on their weight, as illustrated in Table 1.1.

Table 1.1 Categorization of satellites by weights

Satellite Category	Mass
Large satellite	>1000 kg
Medium satellite	500 to 1000 kg
Mini satellite	100 to 500 kg
Micro satellite	10 to 100 kg
Nano satellite	1 to 10 kg
Pico satellite	0.01 to 1 kg
Femto satellite	<0.01 kg

Small satellites, sometimes referred to as miniaturized satellites, are satellites weigh less than 100 kg. Despite having smaller volumes and lighter masses, they perform many different tasks, from military operation, surveillance to communications and broadcasting. This study is concentrated on CubeSats having different sizes and different orbits.

1.1.1.1 CubeSats

CubeSats are small satellites with standard sizes and forms, and they are called by their volumes. The standardized size called 1 Unit, 1U, corresponding 10x10x10 cm^3 is used to classify CubeSats [2] and that size can be extended to define larger CubeSat sizes, as shown in Table 1.2 [3]. An example of 3U sized CubeSat, PICASSO, is illustrated in Figure 1.1 [4].

Table 1.2 Classification of CubeSats regarding the size and mass [3]

CubeSat Designation	Size (max)	Mass (max)
1U	10 cm × 10 cm × 10 cm	1 kg
2U	10 cm × 10 cm × 20 cm	2 kg
3U	10 cm × 10 cm × 30 cm	3 kg
6U	10 cm × 20 cm × 30 cm	6 kg
12U	20 cm × 20 cm × 30 cm	12 kg

The CubeSats in different sizes are illustrated in Figure 1.2 [5] and each box there represents 1U standard volume.

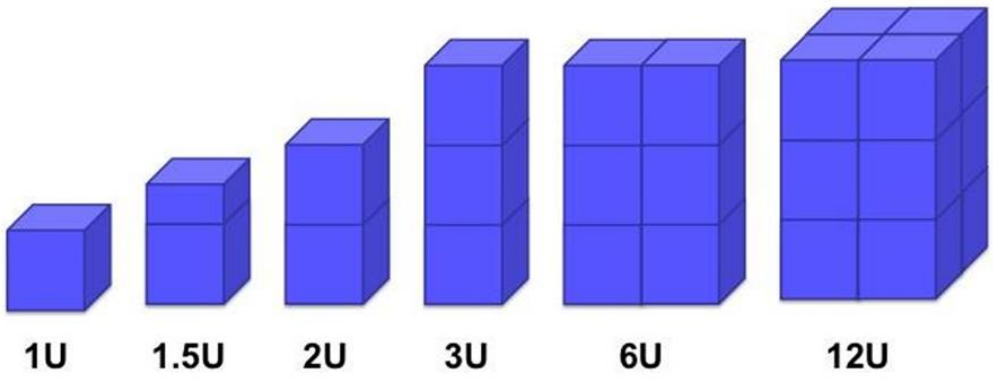

Figure 1.2 Standard sizes of CubeSats [5]

1.1.1.2 Anatomy

Satellites are complex space vehicles by their nature, and they may have varying sizes, shapes, and designs according to their space missions. Their typical anatomy, however, includes basically two main modules that are service or bus module and the payload. These modules are designed and manufactured to meet the requirements of the tasks. A typical illustration for the bus and the payload of a satellite is presented in Figure 1.3 [6].

The service module holding everything together in space is made of a composite or metal frame or body and that provides enough strength to endure all mechanical and thermal loads of launching and serving. This module includes five subsystems that are 1) structural, 2) thermal control, 3) electrical power, 4) altitude control, and 5) telemetry, tracking and commanding [6].

The structural subsystems are mechanical bases with the functions of enclosing, protecting, and supporting of all other systems. Mechanical interfaces with launch vehicles are provided through these subsystems. They are exposed to great g-forces, noises, and vibrations during launches and the loads effecting on satellites are greatly reduced once satellites are settled in their orbits due to the zero-gravity medium.

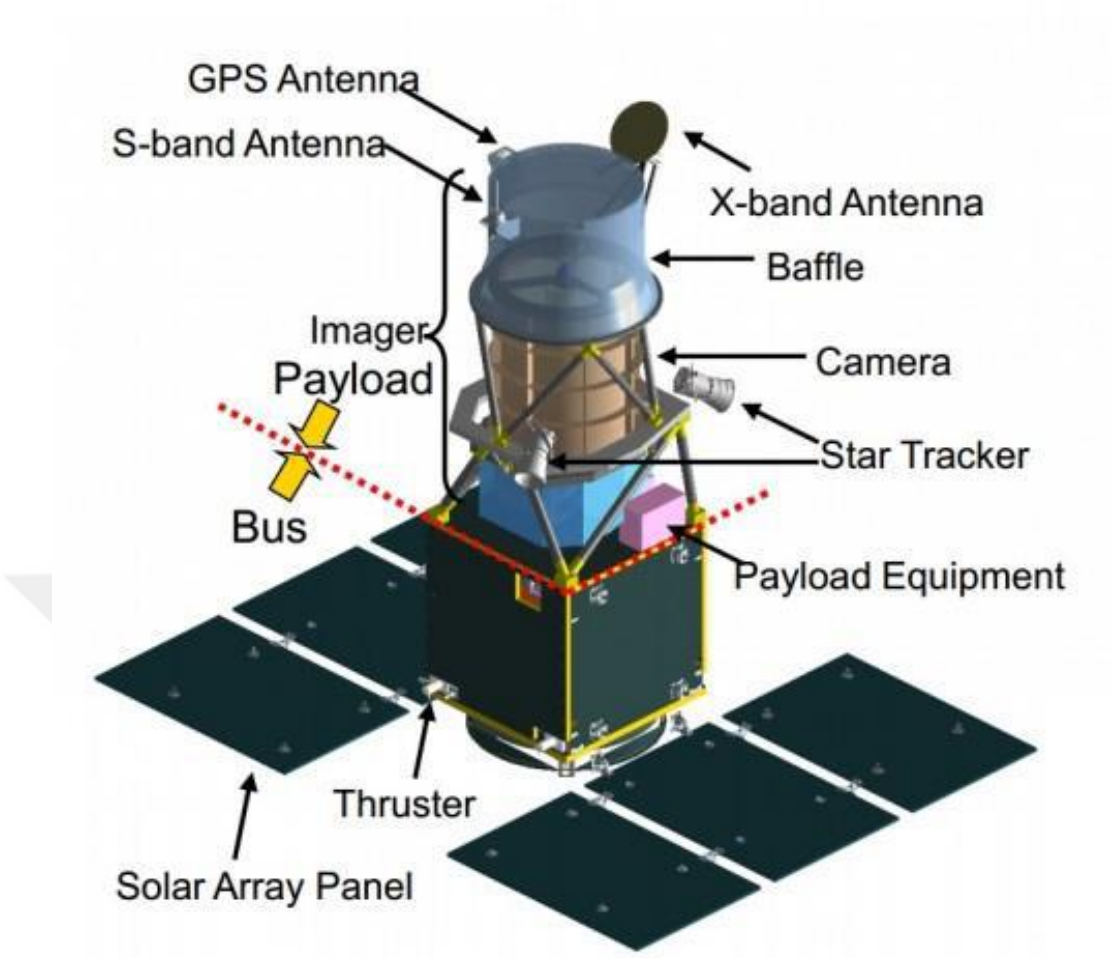

Figure 1.3 A typical illustration for the bus and the payload of a satellite [6]

The thermal control subsystems are necessary to regulate the temperature on board. These subsystems help to maintain the equipment temperatures within the limits of operating temperatures by using every practical means available. Satellites are under the influence of internal and external heat loads. It is quite important to balance structural and thermal requirements in order to achieve the optimum satellite configuration for the desired mission.

The electrical power subsystems include mainly energy sources, energy converting devices and energy storing devices. The energy source is generally solar radiation for Earth-orbiting satellites while nuclear-powered radioactive isotope generators is also used for satellites orbit in places where the solar radiation levels are low. The batteries storing the energy are essential to power satellites continuously.

The altitude control subsystems enable satellites to achieve and sustain desired orbital positions and orientations. They have three components that are navigation sensors, guidance section and control section.

The telemetry, tracking and commanding (TT&C) subsystems provide three important functions that are tracking the satellite position, monitoring the satellite health and status, and processing the received and transmitted data.

The mission payload, on the other hand, is the second major module that is characterized by the specifications of the flight and the mission. That generally includes transponders that can receive uplinked radio signals, amplifying them, sorting those signals, and directing them to the proper downlink antennas for retransmission to the Earth.

1.1.2 Satellite Orbits

A regular cyclic path that an object in space travels periodically around another celestial body is called as orbit. The orbits are formed owing to the gravitational attractions of nearby space objects. Orbits for satellites can be categorized based on their inclinations, eccentricities, and distances from the earth [1].

1.1.2.1 Inclination

Satellites may have orbital planes with different orientations regarding the equatorial plane. Orbital inclination is defined as the angle between these two planes. According to the orbital inclination, orbits can be categorized in three groups as equatorial, inclined, and polar orbits, as illustrated in Figure 1.4.

In the case of a satellite in equatorial orbit, the orbital inclination is 0 degrees because the orbital plane of the satellite aligns perfectly with the equatorial plane of the Earth. Orbits with inclinations greater than 0 degree and less than 180 degrees are called inclined orbits. The orbit, on the other hand, is called as polar orbit if an angle of orbital inclination equals to 90 degrees.

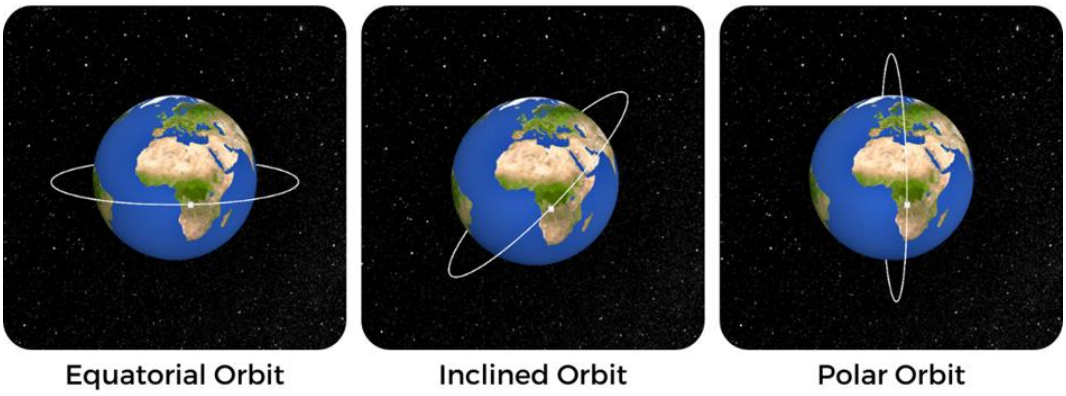

Figure 1.4 Orbital inclination

Satellites travel in the same rotational direction with the Earth for inclinations varying from 0 degree to 90 degrees while they travel in the opposite direction for inclinations varying from 90 degrees to 180 degrees [1].

1.1.2.2 Eccentricity

Orbital eccentricity is the term describing the measure of deviation from a perfectly circular path, and orbits can be defined as elliptical or circular based on their eccentricities, as in Figure 1.5. It equals to 0 for a circular orbit. The orbit is circular when its eccentricity equals to 0, and it is elliptical when its eccentricity is greater than 0 and less than 1 [1].

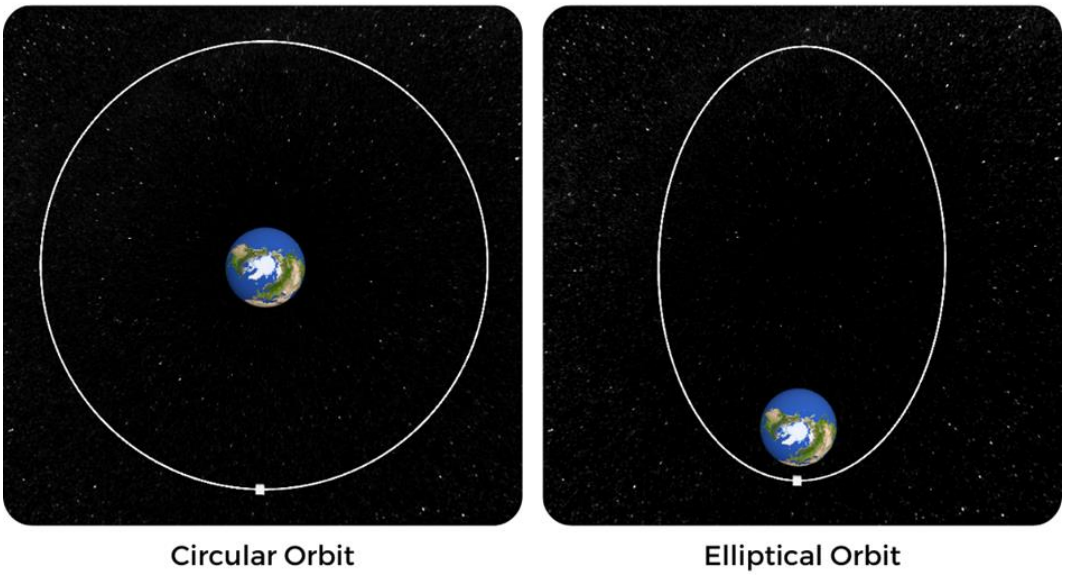

Figure 1.5 Orbital eccentricity

1.1.2.3 Distance

Satellites can orbit at various altitudes and their orbits can be classified into different categories based on their distance above the surface of the Earth as low Earth orbit (LEO), medium Earth orbit (MEO), geostationary Earth orbit (GEO), and high Earth orbit (HEO) [7]. According to their distances, the orbits are shown in Figure 1.6.

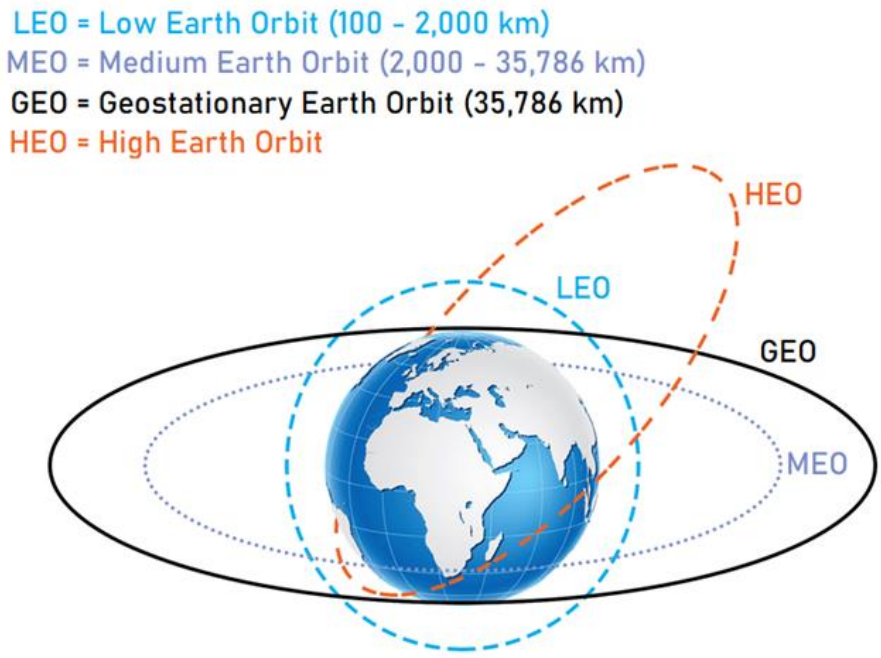

Figure 1.6 Orbital distances

Satellites in the LEO operate at a distance of 100 to 2000 km away from the Earth surface. The orbital periods of LEO satellites range from about 84 and 127 minutes. They have not only shorter orbital periods but also smaller signal propagation delays. Besides providing high bandwidth and low communication latency makes satellites in LEO highly suitable for communication applications.

MEO satellites typically deployed at altitudes above 2000 km and below 35786 km. They have orbital periods that vary between 2 to almost 24 hours. They stay in sight for longer periods of time over a specific region of Earth. These orbits are mostly used for navigation and communication purposes.

GEO satellites fly at a distance of 35786 km away from the Earth surface. They maintain an orbital velocity of approximately 3.07 kilometers per second, and their orbital periods match the rotation period of the Earth, which is approximately 23 hours, 56 minutes, and 4 seconds. Hence, they have stationary footprints on the ground. Most of the communications satellites and weather satellites are launched into GEOs [1].

HEO is characterized by altitudes exceeding 35786 km, and the orbital periods are greater than 24 hours. Since Earth rotates at a faster speed, satellites in HEO appear to be moving in the opposite direction. HEO satellites are suitable to study magnetosphere and perform astronomical observations as well as scientific explorations and military purposes.

1.1.3 Satellite Thermal Design

Satellites undergo thermal cycles with significant temperature fluctuations affecting both their structures and equipment throughout their lifespans, especially during eclipse intervals. One side of the satellite, exposed to the sun, experiences extremely elevated temperatures, while the other side, facing the frigid expanse of space, encounters exceptionally low temperatures. Furthermore, the sun-facing side of the satellite alters periodically as the satellite orbits in its path around celestial bodies. Consequently, this dynamic thermal environment must be considered during the satellite thermal design phase, guiding the selection of materials, equipment, and orbital configurations to ensure effective thermal regulation.

Thermal design, which involves creating a thermal model, assessing the model under various operating conditions, and formulating thermal control strategies, is an iterative process and this process can be demonstrated as in Figure 1.7.

In this process, the inputs basically include physical design specifications, material properties, optical characteristics, orbital configurations, mission parameters, mission modes, payload requirements, and mission duration. On the other hand, the outputs consist of the minimum and maximum temperature values for satellite components, temperature profiles, and the necessary thermal control specifications. Thermal modeling refers to the transformation of the physical geometry of the satellite into a

thermal model that represents its thermal characteristics. This model includes representative thermal surfaces and can be simulated and analyzed to assess how heat is distributed and managed within the satellite.

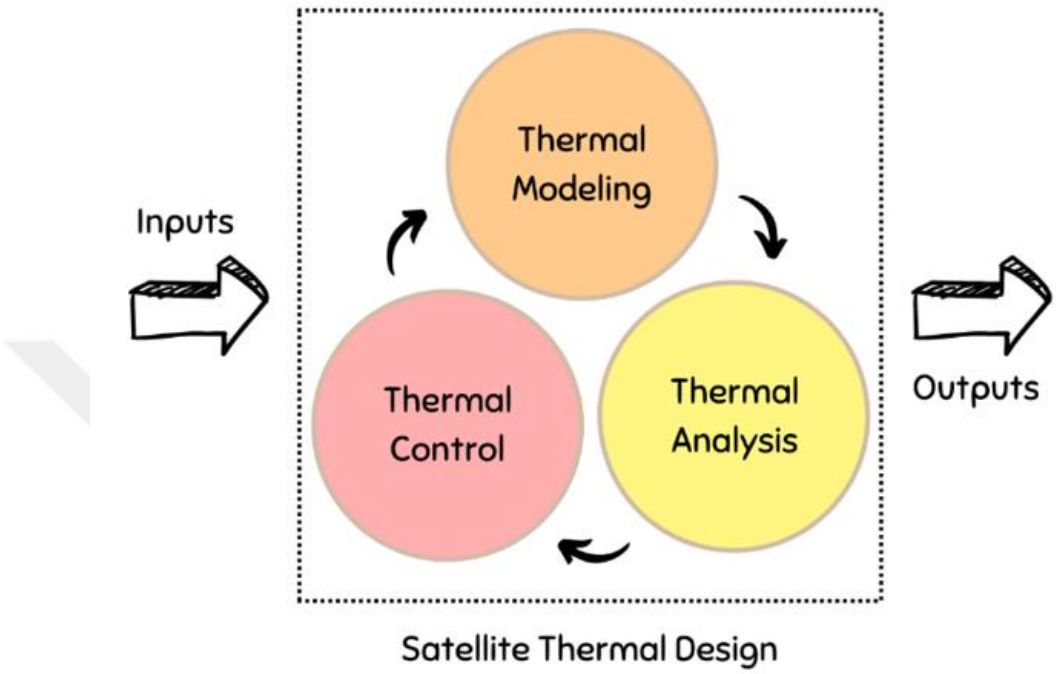

Figure 1.7 Iterative process illustration of satellite thermal design

Thermal analysis is the procedure of simulating and examining a thermal model. During this process, the thermal model is subjected to various conditions, and the analysis produces valuable insights such as predictions of on-orbit temperatures. These findings are essential for making informed decisions regarding the selection of thermal control components and methods.

Thermal control involves the selection of suitable thermal control hardware and its integration into the spacecraft to effectively regulate and manage the temperature of its components and systems. These three processes are frequently executed in conjunction and in iterative cycles. This means that they are often carried out together, with feedback from one informing and influencing the others, to achieve the desired thermal management for a spacecraft [8].

1.1.4 Thermal Modeling

Satellite thermal modeling entails simulating and evaluating how a satellite or spacecraft behaves in the space environment from a thermal perspective. This process revolves around the development of a mathematical or computational representation that mirrors the thermal properties of a satellite, encompassing its heat absorption, conduction, and radiation characteristics. The complexity of thermal models can vary, ranging from simple one-node representations to more intricate three-dimensional models, depending on the level of precision and detail required. The main objectives contain maintaining desired temperatures for the satellite components, understanding how the satellite reacts thermally to various conditions, optimizing the thermal design with control measures, and ensuring mission success by preventing overheating or temperature-related failures.

The thermal modeling process involves several steps and a general process flow of thermal modeling is summarized in Figure 1.8 [9].

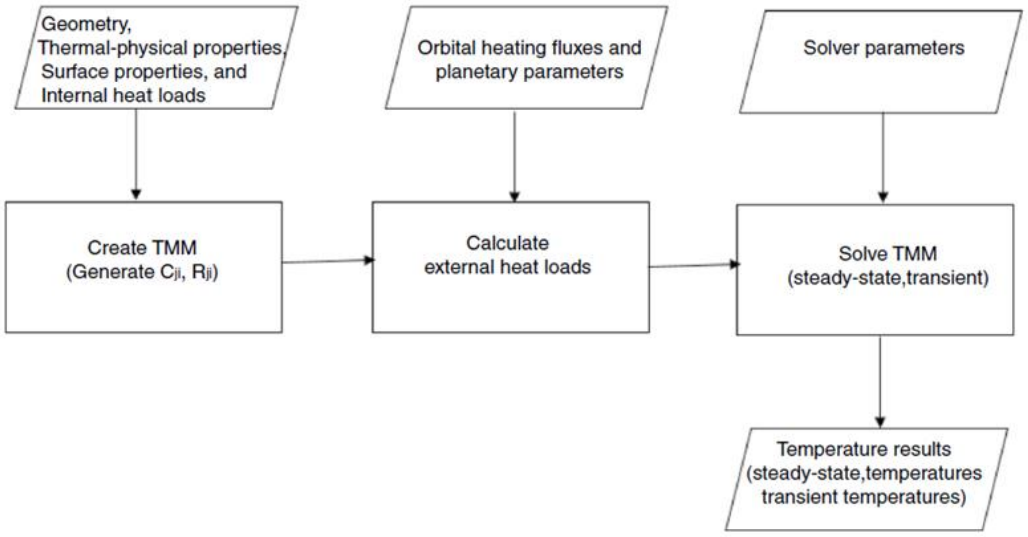

Figure 1.8 A general process of thermal modeling [9]

Firstly, the real geometry of the satellite system is simplified and depicted using a series of shells with the appropriate geometry and thickness. Then, a geometrical mathematical model (GMM) is created to compute the temperature distribution. The

GMM is discretized into a network of nodal points, which are connected by conductive and radiative couplings. External thermal loads and internal power dissipation are imposed to the nodal points, and the ensuing set of equations is solved using approximate linearization and iterative techniques. Finally, the results of the thermal calculations are analyzed to determine the temperature distribution and other relevant thermal parameters. However, it is important to consider several sources of uncertainty and error, such as the simplification of the geometry and the thermo-optical and bulk properties of the materials,

In short, satellite thermal modeling process, which is essential for ensuring the effective design, construction, and operation of spacecraft in the challenging and variable thermal conditions of space, involves the simplifying the geometry of the satellite system, creating a geometrical mathematical model, discretizing it into nodes, accounting for thermal loads, calculating couplings, solving equations, and conducting analyses. Furthermore, it empowers engineers to make informed decisions and adjustments to ensure the satellite functions as intended and can endure the extreme temperature variations it may experience during its mission.

1.1.5 Thermal Analysis

Thermal analysis involves employing mathematical models, numerical simulations, and software tools to predict and evaluate the thermal performance of a satellite in the space environment. This process considers various factors such as the orbit, orientation, materials of the satellite, and the characteristics of the space environment. The objectives of this analysis include predicting satellite temperatures, assessing the margin between predicted temperatures and limits, and ensuring compliance with requirements of thermal control system. Moreover, efficiency is essential in thermal analysis to draw meaningful conclusions and facilitate decision-making, as excessive data interrogation can impede progress in the design process.

Simulations typically produce results that represent temperature changes over time. Within the thermal model, each component has its unique temperature profile. However, analyzing every individual component in the model is often not feasible, so the data must be consolidated. The main findings to extract encompass the lowest and

highest temperatures, temperature gradients, thermal margins, and power requirements for the thermal control system. Furthermore, it is essential to graphically depict and compare these results with basic computations.

Regarding the highest and lowest temperatures, it is necessary to identify these extremes for every component throughout an orbital cycle in each thermal scenario. These values should then be assessed against both operational and survivable boundaries. Certain components may require more thorough scrutiny, demanding the determination of minimum and maximum temperature values for critical sub-parts.

Temperature gradients are particularly important for sensitive components like optics and scientific instruments. In such instances, it is essential to determine both the highest and lowest temperatures encountered by the component and then calculate the temperature difference, or gradient, between these two extremes. This data is essential for maintaining temperature stability within the component and ensuring it stays within acceptable operating limits.

When it comes to thermal margins, it is vital to calculate them for each component in different scenarios. A thermal margin represents the difference between the lowest or highest temperature a component reaches, and the operational or survivable temperature limit it should not exceed. Components with thermal margins falling below a specific threshold should be documented. It is important to highlight that acceptable thermal tolerances may vary as the thermal model undergoes further refinement and improvement.

To effectively analyze the power budget of the thermal control system, power consumption of the heater and other components should be calculated, especially the maximum power used. Each power-consuming component within the thermal control system must have a designated power usage in the power budget, and the requirements of this system typically limit overall power usage as well. Hence, analyzing their power consumption during each thermal case is crucial to ensure that the system performs optimally, meets all requirements, and minimizes energy needs.

Plotting simulation results is a valuable technique for uncovering hidden trends in data. It allows for the visualization of temperature changes in nodes or components over time, aiding in the observation of trends. Additionally, mapping temperatures onto the model provides insights into temperature gradients, heat flow patterns, and model debugging through visual inspection.

In summary, a robust thermal model and accurate thermal analysis are essential for the successful design and operation of satellites. The thermal model should precisely depict the thermal attributes of the satellite, and the thermal analysis should precisely forecast the spectrum of temperatures that its components will encounter. This information is necessary to select the appropriate thermal control system and to develop mission plans that avoid operational problems [8].

1.1.6 Thermal Control Systems

Thermal control systems are integral components of a satellite, specifically engineered to manage and regulate its thermal environment [10]. They have a crucial function in maintaining the temperature within the specified limits to ensure the effective operation and durability of the satellite. Thermal control measures must be chosen in a way that aligns with mission requirements, encompassing considerations like mass and power budget constraints. They can be categorized as either passive or active.

1.1.6.1 Passive Measures

Passive control systems manage thermal balance by regulating both conductive and radiative pathways, all without requiring any power input or moving parts. They primarily encompass radiators, surface coatings, reflective mirrors, multi-layer insulation (MLI), heat pipes, heat sinks, phase-change materials, and thermal filler, all of which depend on the geometry and the structure of a satellite [11].

Most satellites utilize radiators as a straightforward and effective method for dissipating excess heat. These radiators are designed to face deep space to prevent the absorption of unwanted heat fluxes, and in some instances. They are actively controlled to expand their surface area for enhanced heat radiation.

Surface coatings play a vital role in thermal control system design, offering the ability to alter node temperatures significantly and predictably by modifying coatings on satellite surfaces [12]. This cost-effective approach can yield substantial benefits in temperature management.

Reflective mirrors are frequently used in satellites for thermal control. One common type is the Optical Solar Reflector (OSR), featuring a dual-layer design with an inner mirror layer and an outer quartz layer. OSRs allow solar light transmission while emitting effective infrared radiation, making them suitable for radiators. Other types are the First Surface Mirror (FSM) and the Second Surface Mirror (SSM). As exhibited in Figure 1.9, FSM has a single metallic coating layer on the front surface, while SSM utilizes the substrate for high emittance and a back-surface metallic coating with low absorptance. Both FSMs and SSMs offer high reflectivity and low light absorption, with their distinction lying in the coating location. The choice depends on specific application needs, including considerations of double reflections and precise temperature control.

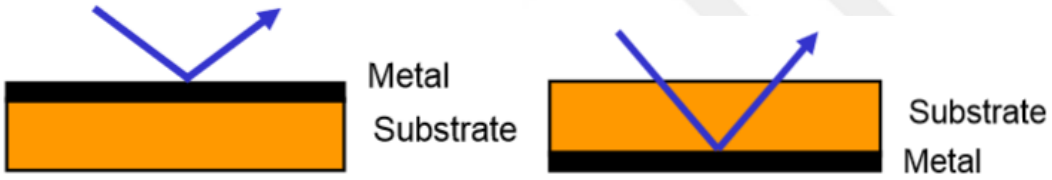

Figure 1.9 Basic illustrations of FSM and SSM

Multi-layer insulation is another passive measure widely used in satellites. It employs multiple layers of insulation stacked together to minimize heat loss due to internal radiation and applied across various satellite components, including exterior solar-facing panels, interior surfaces, and fuel tanks.

Heat pipes are becoming increasingly valuable as a passive control method, especially when combined with thermal radiators. They possess several advantageous properties: they efficiently transport heat over significant distances, even in micro-gravity conditions, require no external power source, and maintain nearly uniform temperature distribution. Using heat pipes, especially in situations where heat needs to be

transferred from hot electronic components to radiators, offers a cost-efficient option as compared to employing more intricate active control techniques.

Heat sinks provide substantial thermal capacity for effective temperature regulation. They are positioned in direct contact with the components needing temperature control. As these components generate heat, the heat is conducted into the heat sink and subsequently transferred to nearby areas through conduction and radiation.

Phase-change materials (PCMs) are valuable for managing thermal conditions in spacecraft when there are rapid fluctuations in incident orbital heat or internal heat dissipation. These materials typically involve a container filled with substances that can undergo a chemical phase change [13]. When spacecraft surfaces heat up, the PCM absorbs excess heat by melting, and it releases the stored heat and solidifies when temperatures decrease.

A thermal filler, also called a gasket, is a material placed between other materials to alter their heat conduction properties. The purpose of using this filling element is to significantly modify the thermal conductivity between the two distinct components, with the choice of a soft material tailored for each particular situation.

1.1.6.2 Active Measures

Active control systems, on the other hand, requires power and the use of mechanical systems to dynamically control temperature. The typical components of this approach are heaters, cryogenic coolers, mechanical refrigerators, Peltier element, and thermal louvers [14].

Heaters are compact electrical circuits designed to generate localized heat in specific areas. Ideally, satellites would rely solely on passive thermal control methods; however, extreme thermal conditions in space often necessitate additional measures. They are frequently used to maintain the desired temperature ranges for sensitive components and represent the most used form owing to their relative simplicity compared to other active methods.

Cryogenic coolers, known as cryocoolers, are specialized cooling systems designed to lower temperatures. They are primarily used to cool satellite instruments to their optimal working temperature range. However, their use in satellite thermal design requires careful consideration due to their high-power consumption and relatively heavy weight compared to other thermal control systems.

Peltier Elements, also referred to as Thermoelectric Heat Pumps, are active devices that use electrical energy to move heat from one side to another. They are preferred for satellite thermal control applications due to their lack of moving parts, long lifespans, small sizes, and resistance to leaks although their electrical efficiency is relatively lower.

Thermal Louvres are movable mechanical panels that can be operated actively to regulate the amount of surface area available for radiating heat into space. They typically enable approximately six times greater heat rejection in their fully open position compared to fully closed position. They usually place above external radiators of satellites and are operated by actuators to control heat release rate. Moreover, they are primarily selected as thermal control measure where notable fluctuations in internal heat dissipation present resulted by equipment in service.

1.1.7 Thermal Testing

Crafting satellites is a multifaceted endeavor that involves the design, manufacturing, assembly, integration, and rigorous testing of highly intricate hardware and software components. To secure a successful outcome, a meticulous prelaunch validation process is imperative, as the cost of addressing failures and making repairs escalates progressively during development and becomes practically insurmountable once the system is in space. Subsequently, it is very crucial to develop a well-constructed validation plan that outlines the methods employed to validate the specified requirements. Common validation techniques include inspection, analysis, similarity assessments, testing, or simulation. Typically, testing serves the purpose of confirming both the design and manufacturing aspects through qualification tests, as well as ensuring the quality of the product through acceptance tests [15].

Thermal testing is highly significant in the validation and qualification of the satellite capability to endure the extreme conditions encountered during its service in space, and these conditions include severe temperature fluctuations and the near-vacuum pressures of space [16]. Common thermal tests, applicable to components, subsystems, and system levels, comprise the Bake-out test, Thermal Balance Test (TBT), Thermal Cycle Test (TCT), and Thermal Vacuum Cycling Test (TVCT).

The Bake-out test, which can be conducted at either subsystem or system levels, involves exposing a satellite test article to high temperatures in a high vacuum environment for a specified duration. They play vital role in hardware testing by eliminating excessive contaminants that could potentially harm the launch vehicle or primary payload. In the case of CubeSats, the Bake-out test is crucial to meet launch requirements, ensuring the fitness-for-launch of the satellite. To accomplish these objectives, all subsystems undergo an outgassing process, with a strict requirement that no more than 1% of the total satellite mass should be released. It is typically performed inside thermal vacuum chambers and importantly, the satellite remains in a non-operational state throughout this procedure.

TBT necessitates achieving thermal steady-state conditions for the test article, enabling a comparison between equilibrium temperatures and temperature predictions derived from the thermal model. Several approaches are used to simulate heat flux and the details on the pros and cons of these methods are provided in Table 1.3 [15]. It has two main objectives of verifying design and gathering data for development. It validates the performance of thermal control subsystem within operational limits and assesses the viability of the design approach [17]. This testing can occur at either the subsystem or spacecraft level. Subsystem testing offers in-depth insights into individual components, high-quality testing at a lower cost, but does not reveal interactions between subsystems. Conversely, spacecraft-level thermal balance testing can involve the flight spacecraft, a prototype, or a thermal-structural model. Prototypes and models provide more testing flexibility, better instrumentation, easier design adjustments, and a broader temperature range for comprehensive baseline thermal data compared to the flight model.

This test also validates the thermal mathematical model, confirms design suitability, verifies hardware performance, and assesses design sensitivity to parameter changes. It typically includes two steady-state cases (cold and hot worst cases) and a transient case for dynamic items. Test success depends on meeting conditions, verifying predicted parameters, and resource adherence. Correlations ensure that deviations between measured and predicted values meet specifications. Coordination with the system thermal vacuum test is essential, often conducted sequentially in the same vacuum chamber at the spacecraft level.

Table 1.3 Evaluating various methods for simulating heat flux in TBT [15]

Method	Pros	Cons
Heater sinks	Possible to simulate spatial and temperature fluctuations of absorbed heat flux	Difficulties in verifying the energy received by the test sample due to the complexity of the test support equipment
Quartz lamps	Achievable high rates of heat flux	Uneven distribution of spectral simulation and heat flux
Solar simulation	Most closely resembling the actual environment	Costly
Test chamber wall	The most cost-effective simulation method	Evenly distributed incident heat flux across the test specimen

The thermal balance test includes specific limit values, with a 5 K deviation allowance for internal units and a 10 K allowance for external units. Additionally, the temperature mean deviation must fall within ±2 K, and the temperature standard deviation should not exceed 3 K. Coordination between the thermal balance test and the system thermal

vacuum test is crucial and often involves sequential testing within the same vacuum chamber at the spacecraft level.

TCT is typically conducted at ambient pressure within environmental chambers, primarily at the subsystem or system level. During this test, the test article undergoes a repeated sequence of hot and cold temperature cycles. These thermal fluctuations create environmental stress within the test article, which helps identify any potential material and workmanship defects.

The primary goal of the thermal cycle test is to demonstrate the spacecraft's ability to endure the stress levels associated with the thermal cycling encountered during flight vehicle thermal cycle acceptance testing. This involves establishing a qualification margin for temperature range and the maximum number of cycles. In some cases, the thermal cycle test, when combined with a reduced cycle thermal vacuum test, can serve as an alternative to the full thermal vacuum test, providing an efficient means of assessing the spacecraft's thermal resilience [18].

TVCT involves exposing the test article to a series of hot and cold temperature cycles within a high vacuum environment. This test is typically conducted at the subsystem or system level and takes place within space simulation chambers or thermal vacuum chambers. As part of the TVCT development process, functional tests are conducted to verify the performance of the subsystem or system.

A typical order of steps in a temperature cycling test under vacuum conditions for qualification purposes is illustrated in Figure 1.10 [15], where T_a is ambient temperature, T_1 is minimum mission temperature, T_2 maximum mission temperature, ΔT is temperature margin corresponding 10℃, t is test time, $A-B$ and $C-D$ are functional tests. The test includes stages of pump-down, hot balance, cold balance, cold survival balance, and hot cycling to assess the performance and the functionality of the satellite in various thermal conditions.

In essence, TVCT is designed to assess how well the test article can withstand the temperature fluctuations and vacuum conditions representative of space environments.

It serves as a critical evaluation method for subsystems and systems, with a focus on performance verification during the development phase.

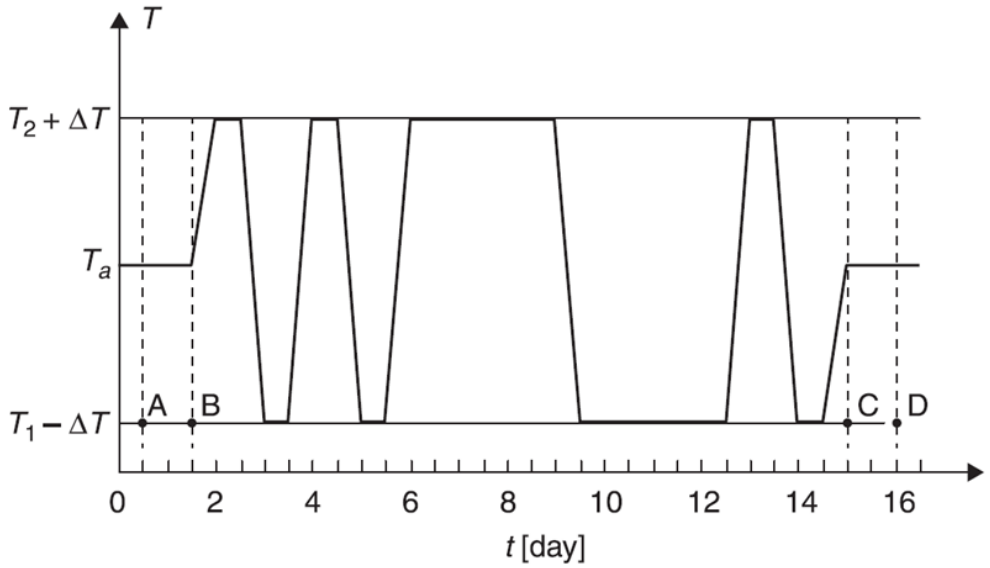

Figure 1.10 Temperature curve with respect to time for a standard TVCT [15]

Both the TBT and TVCT play crucial roles in demonstrating the capability of a subsystem or a system to endure continuous thermal cycling during space missions. The number of thermal cycles administered during TBT and TVCT varies depending on the chosen test level, with these tests serving as vital assessments for space operations.

1.2 Literature Review

Performing thermal analyses for space vehicles has been one of the most important steps towards the successful space missions for years. Spacecraft thermal design is a complete process including thermal modeling, analyzing results obtained through mathematical models and tests, manufacturing, and improving the structure for defined purposes and services. In order to conduct detailed evaluations in satellite analysis, some basic approaches are needed and these are essentially analytical and numerical ones [19].

Several mathematical techniques are applied to analytically solve the heat balance equations for a satellite system. Analytical methods in general include one-nodal, two-nodal, and multi-nodal models. The most basic approach is one-node linear model that considers energy transfer only between the environment and itself. The only node in this approach represents the spacecraft. Although it may be useful for rough prediction in preliminary phases, it leads to extremely poor accuracy in terms of satellite thermal analysis. This model is improved by adding another node to evaluate energy transfer between parts and that is called two-nodal model. The nodes may represent two parts of the spacecraft at varying temperatures such as the main body and the equipment. However, more realistic approaches are needed for more accurate predictions in space thermal modeling. Therefore, the multi-nodal model with more than two nodes is introduced. This approach requires numerical computations because it is not easy to deal with multiple nodes by hand.

The one-nodal analytical approach was used by Oshima and Oshima [20] to confront the thermal design for a spacecraft but their results were far from the reality since the model was too simple and hypothetical. Through linearized methods, a new technique was proposed by Arduini et al. [21] to calculate inverse problem for a basic cylindrical structure that represent the satellite with three nodes. It was stated in their study that pseudo-inverse expression might be suitable to exhibit better thermal estimations by correcting conduction and radiation coefficients. Yet, they did not present a comparative study between the model they offered and other conventional techniques.

Essential technologies of space thermal control were presented by Gilmore [22] and space thermal environments, thermal design and thermal control applications for spacecraft were explained. Not only were examples of thermal design for satellite parts covered but also handy tables for values of Albedo radiation and planetary-infrared radiation were introduced in his handbook. The computational methods for thermal analysis of spacecraft including finite-difference method and finite-element method were explained.

Basic analytical methods in satellite thermal control were reviewed by Tsai [23] and a system of equations by using Taylor series approximation were constructed for a numeric thermal model. The finite-difference schemes of explicit, implicit Crank-

Nicolson, and Dufort-Frankel were compared. The outcome in that study was that methods in spacecraft thermal analysis were equally important because one method could provide more accurate solutions while other could offer faster calculations.

The traditional method used in the initial stages involved simulating spacecraft using basic geometric shapes. As the importance of the geometric arrangement of satellites became more pronounced in thermal analysis, research shifted towards investigating various types of structures. Ziebart et al. [24] provided a comprehensive overview of systematic approaches to address challenges related to non-conservative thermal forces and the sophisticated nature of radiation fluxes in complex satellite shapes. Several models for solar radiation pressure, anisotropic thermal re-radiation forces, and Albedo/Earthshine forces were utilized to tackle intricate satellite structures. However, the research primarily concentrated on orbit determination rather than thermal modeling.

Analyzing the thermal properties of satellites in motion has been a distinct field of research, and among the various scenarios, spinning satellites have garnered the attention. Simulating rotational conditions held significance as it had the potential to mitigate temperature peaks through the effects of spinning motion. The prediction of temperature distribution in a thick-walled cylindrical space vehicle that rotates in space with a constant angular velocity and experiences uniform solar radiation in the deep space environment was investigated by Gadalla [25] using an analytical approximation method. By employing the complex form the Fourier series, the temperature distribution in surfaces of the spacecraft was ascertained taking both radiative and conductive heat exchanges through the walls of it into account. The findings indicated that the previously observed symmetry in the surface temperature distribution faded, resulting in a shift of peak temperature positions along the angular position of the spacecraft due to its rotation. In the study conducted by Prajapati et al. [26], the change in temperatures of a spinning satellite was investigated through the utilization of a fractional calculus approach. The Caputo fractional model was computed through the application of Laplace transformation, leading to the derivation of a non-dimensional representation of temperature variation concerning the spin rate. Utilizing the dual equivalent linearization method, a small satellite was simulated by Chung et al. [27]

with two-node model. It was proposed that the model could be suited for small and compact spinning satellites while the study could be further studied by increasing the nodes to evaluate the effectiveness and the precision. The thermal performance of a satellite spinning in sun-synchronous orbits around the Earth were analyzed by Farrahi and Perez-Grande [28] applying a simple analytical method suggested by them as a handy tool for initial design phase.

The presence of solar panels on a spacecraft significantly impacts its thermal design. Hence, comprehending the thermal mechanisms associated with a satellite that is equipped with solar panels has held substantial importance. To examine temperature fluctuations and thermal stability in small, compact satellites incorporating mounted solar panels, a simplified analytical model was used by Perez-Grande et al. [29] and that was mainly a Fourier analysis with a strategy integrating the balance equations of the reduced two-node thermal model. By means of simple computational models employing non-linear approaches, the thermal variations of a satellite over time were studied by Gaite et al. [30], assuming it to be isothermal. Taking two-node models into account, another thermal analysis with non-linear analytical methods was conducted by Gaite [31] as well.

Satellite sizes have been progressively decreasing to lower launch expenses, expedite development timelines, and offer increased ease and adaptability. However, small satellites have been encountering significant structural obstacles due to limitations in thermal management and power availability. Given the constrained mass and volume of small satellites, thermal modeling becomes a crucial tool to ensure the safety and success of space missions. Overarching concepts of thermal control and its components in micro-satellites were outlined by Baturkin [32] and the insights about thermal hardware, along with discussions on the ground testing of thermal control systems were also provided. An analysis on a cubic micro-satellite equipped with deployable solar panels were conducted by Das et al. [33] and it was aimed to get its optical properties through two- and three-nodal parametric studies. The study carried out by Bulut and Sözbir [34] involved an analytical examination of a nanosatellite operating in LEO with the goal of comprehending its thermal behavior, considering

various panel combinations. A finding of their study was the need of heaters to elevate the battery temperature in the worst-case scenario.

Conducting thermal analysis for spacecraft and space structures demands distinct skills due to the inherent presence of non-linearity and complexity. In recent times, specialized software tools have emerged to address the heat balance equations, particularly for intricate and detailed structures. These tools offer more dependable and efficient solutions for highly detailed calculations, allowing the simulation of spacecraft under various designs and operational circumstances.

A summary of numerical methods applicable to solving ordinary differential equations within spacecraft thermal problems was provided by Krishnaprakas [35], along with the commonly used lumped-mass formulation. A set of coupled, non-linear, first-order ordinary differential equations to express the energy balance within the context of spacecraft thermal analysis was given with various solution methods for them. Based on the comparison of methods, Crank-Nicolson was found to be efficient in solving the equations of thermal mathematical model of the satellite based on lumped-parameter network. In addition, computer codes for examining heat transfer problems specific to spacecraft by solving these equations were provided.

A satellite thermal model using Simulink, a graphical programming environment within MATLAB, has been developed by Lyon et al. [36] to study the operational performance of FalconSat-2. Their objective was to determine whether any components of the satellite exceeded temperature thresholds during on-orbit scenarios and to mitigate temperature fluctuations across all components. These thermal simulations were carried out for various attitude and subsystem operation modes, encompassing both typical on-orbit conditions and extreme cases. Thermal vacuum tests on FASTRAC, a small satellite, and computational thermal analysis using MATLAB and ABAQUS were conducted by Diaz-Aguado et al. [37] for altitudes between 300 km and 500 km with aiming to assess its fitness for spaceflight. The affecting environmental heat fluxes were approximated by MATLAB while satellite temperatures were estimated by ABAQUS. The offered model was tried to be verified by the thermal vacuum test data; however, it was found that they did not accurately match. Additional research concerning the thermal design and on-orbit thermal

performance of HAMSAT, a cuboid micro-satellite providing satellite-based amateur radio services in a sun-synchronous orbit, was conducted by Narayana and Reddy [38]. The isothermal node concept served as the basis for the utilized thermal model, and the mathematical model was generated through the application of NX I-deas TMG Thermal Analysis software. An assessment of the satellite's thermal control system was conducted to determine its suitability for operational conditions. The findings indicated that all subsystems consistently maintained temperatures within the specified limits for the entire mission duration. Thermal simulations were carried out on the Turkish communication satellite TUSAT, positioned in GEO, utilizing the ThermXL software by Sözbir et al. [39] in their research. The objective was to gain insights into the efficiency of the satellite's thermal control subsystem. Essentially, the study outlined the thermal design process during the preliminary design review stage. The effectiveness of both active and passive thermal control measures was scrutinized to ensure that the satellite remained within the desired temperature boundaries throughout its operational lifespan. A nanosatellite in LEOs was simulated using ThermXL software by Bulut et al. [40], who employed a simplified model for quick solution generation. The satellite was equipped with solar panels on all sides in their simulation. The results indicated that the surface facing the sun reached the highest temperatures, while the side exposed to the cold vacuum of space reached the lowest temperatures. Remarkably, temperatures on both the solar cells and the structures of the satellite were found to be almost identical. Their future intentions included verifying and comparing these findings through a more comprehensive analysis using ESATAN software. The thermal performance of a nanosatellite was investigated by Dinh [41] for the altitudes of 300 km and 400 km. Simulations were carried out using a 3-D model of the Pumpkin CubeSat in Thermal Desktop for external analysis and ANSYS Icepack for internal component analysis. It was concluded that the optimal design could be attained by continually updating the thermal model as design modifications were made. The thermal environment for OSIRIS-3U under worst-case orbital scenarios was modeled in the study conducted by Garzon [42] using COMSOL Multiphysics software. The need of future works including more detailed models and simulations to ensure thermal design was concluded. Stress and thermal simulations were conducted on a CubeSat by Athirah et al. [43] using ANSYS software. Their objective was to evaluate safety

factors, weight, and battery discharge rates. Two structural configurations were analyzed, one with a beam and one without. In their study, thermal simulations were employed to assess the battery discharge rate during periods when the satellite was in eclipse conditions. Their results demonstrated that as the discharge duration increased, the internal temperature of the satellite decreased. To manage eclipse periods lasting longer than one hour, they suggested the implementation of a heater as a thermal control system. The thermal control design and analysis for the Brazilian remote sensing satellite Amazonia-1 were presented by Silva et al. [44] by employing passive methods and heaters. Their thermal model was constructed using a lumped parameter technique, assuming isothermal nodes, and simulations were executed using Thermal Desktop, RadCAD, and SINDA/FLUINT. Their primary investigation centered on temperature variations and heater power consumption during critical scenarios. Thermal modeling for a 1U pico-satellite in LEO was conducted by Wachche et al. [45] using NX Space Systems Thermal software. Various thermal insulation combinations suggested to guarantee the safety of satellite components were analyzed. Thermal simulations for the PICSAT and CIRCUS nanosatellites were conducted by Flecht [46] using Systema Thermica software. Initially, an analysis of PICSAT was conducted, focusing on extreme conditions and potential failure modes, which encompassed assessing malfunctions in the attitude control system and deployable solar panels. Various deployable solar panel setups for CIRCUS were studied by modifying the thermal model of PICSAT. This modification allowed for initial estimations of the satellite thermal behavior during the preliminary design phase. Other thermal simulations using Systema Thermica was conducted by Chandrashekar [47] to assess the MIST CubeSat. During the development stage, the thermal behaviors of the satellite in various scenarios, including operational and non-operational cold cases, were investigated. The thermal control system of the TURKSAT 3U nanosatellite was examined by Bulut et al. [48] to secure the operation of all satellite components within their specified temperature ranges. They proposed the use of a coating during the initial design stages and the employment of heaters to maintain the cube satellite's warmth during cold-case conditions. Simulations utilizing Systema Thermica were performed by Still [49] to assess a satellite sun-synchronously orbiting the Earth. The study primarily examined the thermal performance of the radiators and heaters mounted on

the satellite. Numerical simulations in ANSYS were conducted by Bonnici et al. [50] to examine the on-orbit thermal behavior of the pico-satellite UoMBSat-1. The conclusion was that passive measures proved effective in regulating maximum temperatures. However, mitigating minimum temperatures posed a considerable challenge due to the constrained space capacity, essentially rendering the implementation of active thermal control measures almost unfeasible. The ESEO satellite, characterized by a cuboid shape composed of six structural panels and three solar panels, was subjected to modeling and simulations by Ahmed and Ahmed [51] using Thermal Desktop software. Temperature variations of both components and solar panels were examined. The verification of the thermal model was achieved by altering design variables and confirming the resulting temperatures. The study on thermal analysis of a 3U-scaled CubeSat named Pakal, addressing the design criteria and the proposed thermal control measures was performed by Salazar-Salinas et al. [52], utilizing the lumped parameter approach, and Thermal Desktop for verifying the model. It was aimed to analyze temperature ranges of satellite parts in critical orbit scenarios, leading to the design of a thermal control model by means of coatings. The outcome of the study was that safe operating temperatures could be maintained by implementing coatings on different surfaces of the satellite to optimize heat transfer between them and space thermal environment. Another study [53] focused on assessing the thermal performance of coatings applied to small satellites at LEOs, through the analysis of external radiation loads in space and the heat dissipation, using finite element approach. A case study [54] employing numerical simulations through COMSOL, commercial software, on the university class 3U CubeSat was conducted to reveal he significance of passive thermal control techniques. It was concluded in the study that use of coatings decreased temperatures for some internal component to maintain safe operational temperature range throughout the lifespan of the satellite. A recent study [55] covered efforts of a code development on MATLAB environment to estimate external thermal loads. The results of the code were compared to those obtained from the STK software, revealing an error margin of 9.32%. The thermal performance of AlAinSat-1 was studied in a study [56] under extreme condition, utilizing NX Space Systems Thermal. One of the outcomes in this research was the need of validation through actual experimental testing to mitigate the risk of potential

in-orbit failures. Various other studies [57, 58] presented thermal analyses for 3U CubeSats, covering the thermal design requirements and outline schemes for thermal control design, including simulations. The studies on thermal modeling, design, and analysis of satellites will maintain to be an important research area in the future with regards to the technological developments.

1.3 Aim of the Study

This research demonstrates the available concepts in thermal modeling and analysis of small satellites and explains the recent trends in thermal design of them. The aims of the dissertation, on the other hand, can be mainly listed as follows:

- to exhibit relations between external heat loads and orbit characteristics
- to provide detailed study investigating and comparing thermal influences of different satellite design parameters and orbital configurations
- to reveal relationships between panel temperature distributions of small satellites and design parameters, and orbital configurations
- to present useful data for thermal modeling and analysis of small satellites under space conditions
- to analyze the influences of deployable solar panels on external heat and surface temperature distributions
- to develop an in-house spreadsheet for thermal vacuum chamber tests of CubeSats with an acceptable accuracy for preliminary satellite design phases
- to compare the developed spreadsheet with the real thermal vacuum chamber test results for a real small satellite

1.4 Original Contributions

This study contributes originally to the literature as stated below:

A review paper has been published in the Gazi University Journal of Science [19]. A brief background about the space thermal environment and the basics of heat transfer mechanisms is presented in the study. The present concepts of satellite thermal modeling and analysis are introduced while the recent trends in thermal design of small

satellites improving day-after-day are also covered. Besides, thermal simulation software tools and procedures for modeling satellites are discussed in detail. This article has also been cited by other international studies [59-62].

A conference presentation has been delivered in the 2nd International Congress on Multidisciplinary Natural Sciences and Engineering [63]. The influences of solar panel deployment angles on heat amounts received to the satellite from external thermal sources of space are analyzed for various conditions. The absorbed heat by CubeSat panels and its solar panels are compared.

An original research paper has been published in the Pamukkale University Journal of Engineering Sciences [3]. Under different orbital and satellite design parameters, the impact of space thermal environment on CubeSat is demonstrated. The rates of heat transferred from external thermal sources to the satellite panels are comprehensively investigated.

Another original research paper has been published in ASME Journal of Thermal Science and Engineering Applications [64]. The thermal effects are studied for various CubeSat design parameters and orbital configurations. Analytical investigations are performed to determine the thermal behaviors of CubeSat panels under harsh conditions at low earth orbits.

CHAPTER 2

SPACE THERMAL ENVIRONMENT

Satellites orbiting in space encounter various heat loads over their service periods. Not only the lifetimes but also the performances of satellites in service are greatly affected by the harsh space thermal environment [19]. The periodical changes in this thermal environment, depending on orbital parameters, have extreme impacts on satellites [48]. Therefore, conducting thermal analysis of a satellite relies on an accurate definition of the space thermal environment that it is exposed to. There are three main heat sources that are direct solar radiation, Albedo radiation and Earth IR in this environment. These sources are determined by the satellites' specific orbits, orientations, surface properties and sizes [34]. In addition, between the satellite and the outer space the heat is transferred via the radiation mechanism while it is exchanged via the conduction mechanism through the satellite materials. Convection and aerodynamic heating, however, can be negligible owing to the vacuum state existed in space.

This chapter presents the elements of the space thermal environment. First, orbital parameters effecting the space thermal environment are introduced. Then, both internal and external heat sources of satellites are discussed in detail for service conditions in space and the heat transfer mechanisms in space are explained. To perform satellite thermal analysis, the heat balance equations are derived. Finally, the thermal cases that a satellite may experience are described by considering extreme probabilities.

2.1 Orbital Parameters

The orbital parameters influencing the periodical external heat fluxes in space should be specified and examined to conduct satellite thermal analysis. The heat fluxes available in space thermal environment are influenced by the position of satellites according to the celestial bodies [50]. In the altitude range of 160 km to 2000 km corresponding to low earth orbits, most satellites fly at almost circular orbits while some fly at elliptical orbits with limited eccentricity. The external heats for a satellite change depending on its altitude [3].

In addition, the periods of illuminated and shadow passages greatly affect the satellite thermal environment. The intervals of penumbra, that is partial shadow, and umbra, that is total shadow, are mainly determined by orbital parameters, as shown in Figure 2.1, and these are basically orbital period, orbital height, and beta angle that a satellite has. They influence scales of external heat fluxes. In this context, satellites staying more in eclipse eventually receive less heat. To put it other way, satellites having less durations of penumbra and umbra receive greater heat amounts. Consequently, evaluating the eclipse intervals is very significant in terms of maintaining proper thermal control for satellites [3].

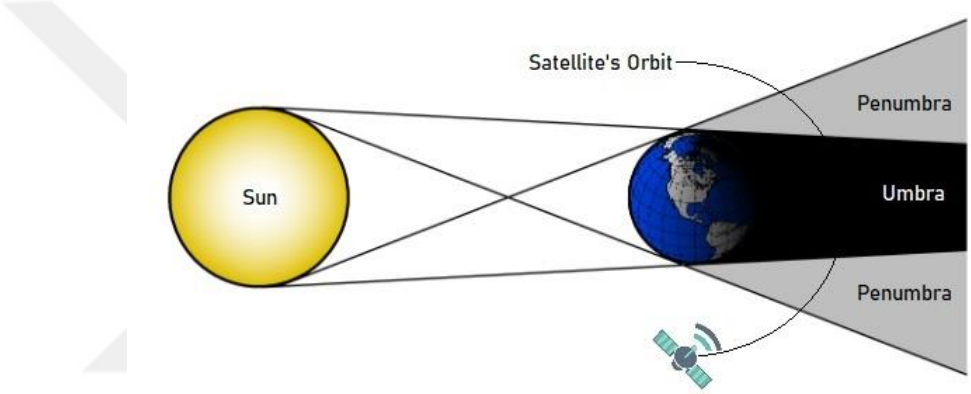

Figure 2.1 Shadow passages of a satellite orbiting around the Earth

The beta angle, on the other hand, is another influential parameter and it is defined as the minimum angle between the orbital plane and the solar vector. It can vary in the range -90 to + 90 degrees. While satellites have the longest eclipse durations at the beta angle of 0 degree as they fly over the subsolar point, they have no eclipse at the beta angle of 90 degrees as they fly near the terminator. Thus, the lower the beta angles are the more the orbit-averaged solar heats are.

2.2 Heat Fluxes for a Satellite in Space

The heat transferring between the outer space and the satellite takes place through the radiation mechanism due to the presence of vacuum condition in space. The heat sources for a satellite at low earth orbit are mainly direct solar radiation (1), albedo

radiation (2), and Earth infrared-radiation (3), that are called external heat sources [16]. Thermal conditions in space are not constant and change periodically throughout the service period. Not only orbital parameters, but also material properties of satellites alter the magnitudes of heats exchanged from these sources [9].

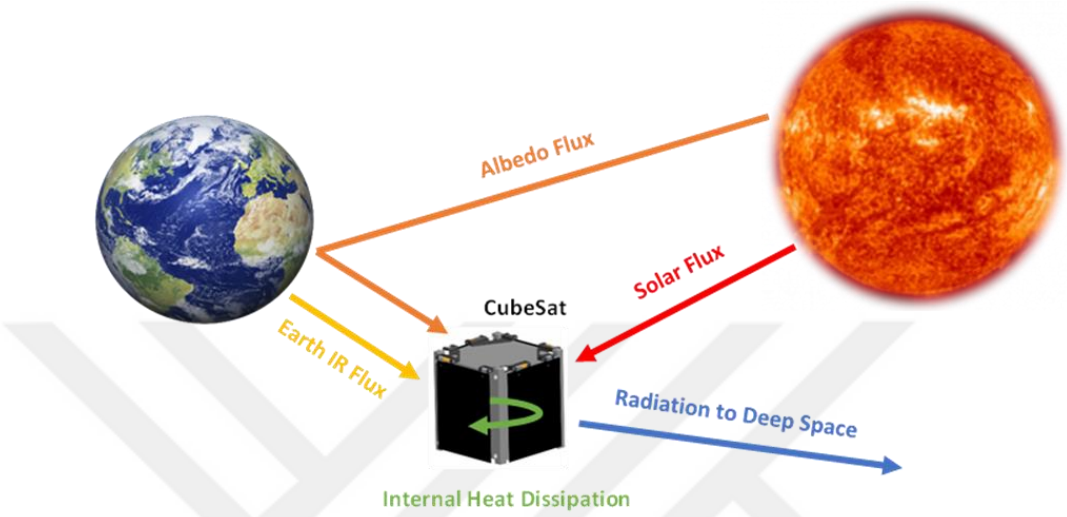

Figure 2.2 Space thermal environment for a satellite

Moreover, the heat dissipated from electronics placed on satellites is another heat source and that is called as the internal heat source. A simplified illustration of heat sources for a satellite is given in Figure 2.2.

2.2.1 Solar Radiation

The direct solar radiation is by far the most intense heat load for satellites in space. The direct solar flux received on the unit area of a surface normal to the solar rays is called solar irradiance or solar constant. The solar constant varies with respect to the distance from the sun. It averagely equals to 1367 W/m^2 at the distance of 1 Astronomical Unit (AU) that is 149.5 Mkm and can be estimated as a function of the distance as given in Equation 2.1 [65].

$$q_{Solar} = \left(1367.5\ {}^{W}/_{m^2}\right) \cdot \frac{1}{(distance\ AU)^2} \tag{2.1}$$

The solar constant fluctuates owing to the change in distance between the earth and the sun. Due to the orbit eccentricity of the earth, it varies during the year period. It

ranges between the minimum flux of 1322 W/m^2 occurred at summer solstice and the maximum flux of 1414 W/m^2 occurred at winter solstice according to the time of the year and the position of the earth with respect to the sun accordingly.

The heat received by a satellite through the solar radiation can be written as in Equation 2.2,

$$Q_{Solar} = q_{Solar} \cdot \alpha_s \cdot A_p \quad \textbf{(2.2)}$$

where q_{Solar} is the solar constant, α_s is the solar absorptivity of surfaces, and A_p is the projected area of the surface viewing the sun. Hence, available heat to be transferred via direct solar radiation is dependent on orientations, surface properties and surface sizes of satellites.

2.2.2 Albedo Radiation

The solar energy resulted due to the reflection of solar radiation from the illuminated part of the earth is called albedo radiation. The albedo heat can be expressed as given in Equation 2.3,

$$Q_{Albedo} = \left(A_p \cdot F_{s-Earth}\right) \cdot \alpha_s \cdot a \cdot q_{Solar} \cdot cos\,\theta \quad \textbf{(2.3)}$$

where a is the albedo coefficient, $F_{s-Earth}$ is the view factor of the satellite surface to the earth, and θ is the angle between the position of the satellite and the solar vector.

Albedo radiation is usually defined by a percentage or a fraction that is called albedo coefficient [66]. It is a geometric heating property and thus it varies considerably depending on the orbital height and the position of satellites. The impact of albedo increases as the satellite flies closer to the earth and it becomes more significant at low earth orbits. The albedo coefficient can vary between 0.25 and 0.55 based on the properties of the reflection surface at the earth because the reflectance characteristics of clouds, oceans, snows, forests, and lands are not the same. Cloud covers increases the reflectivity, and the albedo coefficient is typically around 0.8 for clouds. On the other hand, forests and oceans decrease that coefficient because they absorb most of the solar irradiance.

2.2.3 Planet Infrared Radiation

Some portion of the radiation received by the planet transmit back to the space through longwave infrared rays owing to the temperature of the Earth and that radiation emitted back is called planet infrared radiation. Depends on the thermo-optical characteristics of planet surface [67], the planet infrared radiation is highly varying at each point on the planet [64]. The magnitude of this radiation type is determined by the emissivity and the temperature of the surface. This type may also be referred to by the name of the planet. The Earth infrared radiation is an important source of heat for satellites serving at low Earth orbits and it can be calculated by Equation 2.4,

$$Q_{EarthIR} = \left(A_p \cdot F_{s-Earth}\right) \cdot \varepsilon_{IR} \cdot q_{Earth} \quad \textbf{(2.4)}$$

where q_{Earth} is the flux of the Earth radiation and ε_{IR} is the IR emissivity of external surfaces of the satellite. To estimate the Earth infrared radiation, it can be assumed that the Earth is an equivalent blackbody transmitting a flux of 237 W/m^2 heat at a mean temperature of 255 K. The average heat flux of Earth infrared radiation is higher for deserts while it is less for areas in the poles. Besides, cloud coverages affect the heat transfer since outgoing radiations from the Earth are blocked by them. In addition, the Earth infrared radiation changes slightly due to the variations at season, latitude, and nighttime.

2.2.4 Internal Heat Dissipation

Electronics mounted on satellites may lead generating heat because of the irreversibility according to the thermodynamic laws. The electrical power available for electronics is completely converted into heat for satellites having no moving parts. The amount of dissipated heat depends on the power consumption on this case. The lower efficiencies of electronics lead to higher internal heat generation as well. Besides, heat dissipations are not constant during the service period and may alter according to the mission requirements. Hence, the internal heat generation should be considered in satellite thermal analysis. It considerably influences the thermal budget and the thermal performance of a satellite serving in space conditions. Therefore, it is very important to manage this source in order to keep electronics operationally safe and reliable.

2.2.5 Heat Rejection

All surfaces of a satellite facing out transfer heat away towards the outer space via radiation. The average temperature of the deep space can be considered as 2.7 K while satellite surface temperatures may range to 400 K. Hence, the outer space behaves as a heat sink and heat naturally radiated away from the hotter satellite surface to the colder space. The amount of rejected heat by the external surfaces of a satellite depends on the surface temperature, surface emissivity and surface area. The heat radiated away can be described as given in Equation 2.5,

$$Q_{Rejected} = \left(A_p \cdot F_{s-space}\right) \cdot \varepsilon_{IR} \cdot \sigma \cdot \left({T_s}^4 - {T_{space}}^4\right) \quad \textbf{(2.5)}$$

where σ is the Stefan-Boltzmann constant, $F_{s-space}$ is the view factor of the satellite surface to space, T_s is the surface temperature and T_{space} is the outer space temperature. It is assumed that the external surfaces face nothing but the outer space and thus the view factor is considered as 1 when estimating heat rejection. Another assumption is that the temperature of the outer space can be taken as 0 since the fourth power of the surface temperature is incomparably greater than the fourth power of the outer space temperature. Hence, the total amount of heat rejected from a satellite can be computed by Equation 2.6,

$$Q_{Rejected} = \sum_{i=1}^{n} A_i \cdot \varepsilon_{IR,i} \cdot \sigma \cdot {T_{s,i}}^4 \quad \textbf{(2.6)}$$

where i denotes the ith surface and its properties, and n is the number of external surfaces of the satellite, radiating heat to outer space [8].

2.3 Heat Transfer Mechanisms

It is highly essential to understand the basics of heat transfer mechanisms when conducting satellite thermal analyses. Heat can be transferred through conduction, convection, and radiation mechanisms. In satellite thermal analyses, on the other hand, the main heat transfer mechanisms are thermal radiation exchange and conduction through the materials of the satellite [19] while convection can be neglected in space due to the presence of the vacuum condition.

Combined heat transfer mechanisms are required to perform thermal analyses and to define the energy budget of a spacecraft.

2.3.1 Conduction

Conduction, a heat transfer form, occurs colliding and diffusing particles of microscopic levels. Materials conduct heat but the thermal conductivity changes from one material to another. Heat is mostly transferred via conduction among satellite elements. Thermal design in spacecrafts can be manipulated by changing the material and material properties so that the heat can be diverted or insulated as desired.

Conduction is governed by Fourier's Law, in which heat transfer is proportional to the measured area normal to the heat flow direction and the temperature gradient in that direction. Fourier's Law for conduction can be written in the differential form as presented in Equation 2.7.

$$\vec{q} = -k\nabla T \tag{2.7}$$

Thus, the amount of heat transferred through conduction can be written as in Equation 2.8.

$$Q_{con} = \frac{A}{L}\, k\, (T_h - T_c) \tag{2.8}$$

The equation of three-dimensional conduction can be written as given in Equation 2.9.

$$\rho c \frac{\partial T}{\partial t} = \frac{\partial}{\partial x}\left(k_x \frac{\partial T}{\partial x}\right) + \frac{\partial}{\partial y}\left(k_y \frac{\partial T}{\partial y}\right) + \frac{\partial}{\partial z}\left(k_z \frac{\partial T}{\partial z}\right) \tag{2.9}$$

The temperature distribution in three-dimensions can be obtained as a function of time by solving this heat equation.

2.3.1.1 Thermal Resistance

Thermal resistance, R, is a measure of the ability of a material to resist the heat flow. A higher thermal resistance value signifies better insulation and a stronger resistance to heat flow. Conversely, lower thermal resistance values indicate more efficient heat conduction within the material or structure. It quantifies how effectively a material

insulates against the transfer of thermal energy due to a temperature difference. It can be expressed as given in Equation 2.10.

$$R = \frac{\Delta T}{Q} \tag{2.10}$$

Thermal resistance is a critical factor in applications like designing insulation systems, evaluating the effectiveness of thermal barriers, and assessing the heat dissipation capabilities of electronic components.

2.3.1.2 Linear Coupling

Conductive coupling, often referred to as linear coupling, is the conductance between node points in a system. This can be mathematically expressed for node i and j as in Equation 2.11, where k is the thermal conductivity, A is the heat-flow area, and L is the distance between the nodes.

$$GL_{ij} = \frac{k_{ij}A_{ij}}{L_{ij}} \tag{2.11}$$

This parameter is essential for quantifying how heat is conducted between nodes or regions in a thermal system.

2.3.2 Radiation

Radiation is another type of heat transfer occurs by means of electromagnetic waves or traveling particles. Satellites encounter three external sources of radiation that are direct solar radiation, albedo radiation and earth infrared radiation while orbiting in deep space. At the same time, through radiation, they not only exchange heat among internal surfaces and equipment inside, but also reject heat towards outer space. Therefore, it is important to understand the radiation mechanism.

Heat exchange through radiation is governed by Stefan-Boltzmann Law stating that black-body irradiance is proportional to the fourth power of its temperature [68]. The governing equation of radiating heat can be written as given in Equation 2.12.

$$Q_{rad} = \varepsilon\sigma A \left({T_1}^4 - {T_2}^4\right) \tag{2.12}$$

Direct solar irradiances in terms of radiative heat transfer have the highest energy contribution for a satellite. The total heat fluxes radiated vary with respect to the distance between a satellite and the sun, the direction of the satellite according to the sun, and the ratio of solar absorptivity to infrared emissivity. As the temperature difference between two bodies exchanging heat is increased, the amount of radiated heat is also increased.

2.3.2.1 View Factor

The view factor, also known as configuration factor or shape factor, is a fundamental concept in heat transfer through radiation. That represents the fraction of radiation leaving one surface (surface i) that directly arrives at and interacts with another surface (surface j). In another words, it quantifies the thermal radiation emitted by or reflected from one object is received by another one. Simply, the view factor assesses the extent to which one surface can observe another surface.

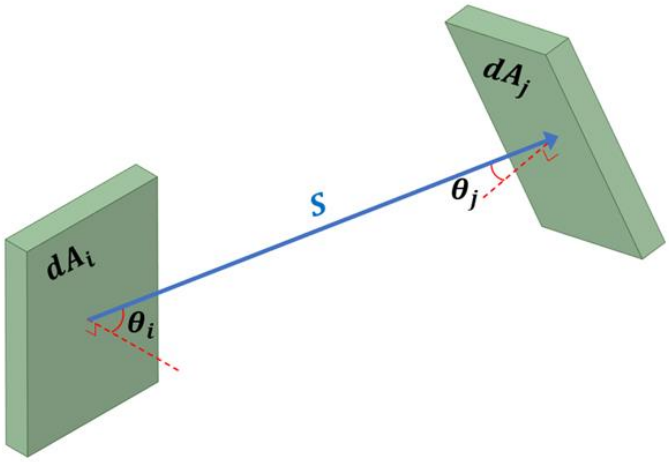

Figure 2.3 Geometrical definition of view factor

The view factors are exclusively dictated by the geometric features and can be calculated by considering the surface area, distance and angles between the surface normal vectors while remaining unaffected by the physical attributes or temperature of the surfaces involved.

The view factor from surface i to surface j for two infinitesimal surfaces i and j with differential areas dA_i and dA_j, as shown in Figure 2.3 can be calculated through the Equation 2.13.

$$F_{ij} = \frac{1}{A_i} \int_{A_i} \int_{A_j} \frac{\cos\theta_i \cos\theta_j}{\pi S^2} dA_j \, dA_i \quad \textbf{(2.13)}$$

The law of reciprocity for radiative heat transfer given in Equation 2.14 states that the view factor from one surface to another is equal to the view factor from the second surface back to the first surface. This principle is essential for making sure that heat exchange between surfaces works both ways and keeps energy balanced in thermal systems.

$$F_{ij} A_i = F_{ji} A_j \quad \textbf{(2.14)}$$

In a closed system, the summation rule declares that the sum of all view factors from a given surface to all other surfaces within the system will always equal 1, as mathematically expressed in Equation 2.15.

$$\sum_j^n F_{ij} = 1 \quad \textbf{(2.15)}$$

Estimating view factors can be challenging, especially for complex geometries. There are two main methods for calculating view factors: analytical and numerical. Analytical methods work well for simple cases but can be complex for more complicated geometries. Numerical methods, like the Monte Carlo method, are versatile and handle complex situations effectively, making them especially useful when dealing with intricate geometries or when analytical solutions are unavailable.

2.3.2.2 Radiative Exchange Factor

Unless all surfaces are perfect black bodies, the view-factor matrix is insufficient for representing the necessary radiative couplings to maintain energy balance. To overcome this limitation, the radiative exchange factors (REF), also known as Gebhart factors are employed. This factor signifies the portion of energy emitted by one surface (surface i) that eventually gets absorbed by another surface (surface j). This factor is crucial for understanding the transfer of thermal energy between these surfaces

through radiation, considering both emission and absorption processes in a given system.

The radiative exchange factor, B, can be estimated through an iterative calculation as presented in Equation 2.16, where F is the view factor. The calculation considers the contributions from all intermediate surfaces (denoted as k in Equation 2.16) within the system.

$$B_{ij} = \varepsilon_j \cdot F_{ij} + \sum_k \left((1 - \varepsilon_k) \cdot F_{ik} \cdot B_{kj} \right) \quad \textbf{(2.16)}$$

The values of radiative exchange factors are influenced by both the geometric configuration of the model and the thermal and optical characteristics of the surfaces involved.

2.3.2.3 Radiative Coupling

Radiative coupling quantifies how much thermal radiation is transferred between these elements due to their relative positions and temperatures. The radiative coupling can be calculated as the product of the view factor and the surface area between node points, as given in Equation 2.17, in case of all nodes being blackbodies.

$$GR_{ij} = A_i F_{ij} \quad \textbf{(2.17)}$$

It is a key aspect of modeling radiative heat transfer in complex systems and plays a crucial role in determining the overall heat transfer rates within the network.

2.3.2.4 Monte Carlo Ray Tracing

Monte Carlo ray tracing is a potent computational method for analyzing radiative heat transfer. It simulates how thermal radiation behaves when it encounters surfaces and materials within complex systems, making it ideal for intricate, three-dimensional geometries where analytical solutions are challenging. The process involves tracking individual photons as they move through the system, interacting with surfaces and undergoing events like absorption, emission, and scattering. These interactions are determined through random sampling techniques, considering material properties and surface characteristics. Energy transfer between photons and surfaces is computed,

accounting for factors such as view factors, emissivity, and temperature differences. By statistically averaging the results from tracking a large number of photons, Monte Carlo ray tracing provides valuable estimates of radiative heat transfer rates and temperature distributions in the system.

Advantages of Monte Carlo ray tracing in radiative heat transfer analysis include its versatility in handling complex geometries, the ability to model surfaces with varying properties, and its applicability to both steady-state and transient heat transfer problems. However, it can be computationally intensive, especially for large systems, and the accuracy of the results depends on the number of photons tracked.

2.4 Balance Equations

The thermal management of a satellite is a process influenced greatly by the space thermal environment including heat fluxes of direct solar, albedo and earth infrared. Establishing a proper thermal management for a satellite and thereby keeping it safe and operational throughout its lifespan in space requires analyzing spatial and temporal thermal behaviors for all possible orbital conditions. For this aim, the overall thermal balance can be simply achieved for a satellite by balancing the thermal energy emitted to deep space against the energy received from space thermal environment together with the internally dissipated heat. In this context, the energy balance equation can be written as in Equation 2.18.

$$C\frac{dT}{dt} = \dot{Q}_{in} - \dot{Q}_{out} \quad \textbf{(2.18)}$$

A satellite, as described earlier, encounters external heats of direct solar, albedo and earth-infrared, and internal heat dissipated by electronics. These are the energy inlets for a satellite thermal system, as also presented in Equation 2.19.

$$\dot{Q}_{in} = \dot{Q}_{Solar} + \dot{Q}_{Albedo} + \dot{Q}_{EarthIR} + \dot{Q}_{Internal} \quad \textbf{(2.19)}$$

On the other hand, the heat rejected from the satellite is the energy outlet, as in Equation 2.20.

$$\dot{Q}_{out} = \dot{Q}_{rejected} \quad \textbf{(2.20)}$$

Thus, the energy balance equation can be expressed as in Equation 2.21.

$$C\frac{dT}{dt} = \dot{Q}_{Solar} + \dot{Q}_{Albedo} + \dot{Q}_{EarthIR} + \dot{Q}_{Internal} - \dot{Q}_{Rejected} \quad \textbf{(2.21)}$$

For a satellite, a simplified geometry including only required thermal details is defined to represent its physical system and that is called as the geometrical mathematical model. Then, the model is discretized into a network of nodes. A basic illustration is presented in Figure 2.4 for thermal network of nodes. A node is a mathematical representation of an element where exchanges of radiative fluxes through its external surfaces, internal dissipation and capacitive fluxes through its surfaces, and conductive fluxes through its contact surfaces take place. Each nodal point is assumed isothermal and described by its both temperature and thermal capacitance. Lumping continuous parameters of the satellite thermal system into discrete set of nodes are called lumped parameter networks [69].

The energy balance equation can be expressed at each node as in Equation 2.22.

$$C_i\frac{dT_i}{dt} = \dot{Q}_{solar,i} + \dot{Q}_{Albedo,i} + \dot{Q}_{EarthIR,i} + \dot{Q}_{Internal,i} + \sum_{j=1}^{n} GL_{ij}\left(T_j - T_i\right) + \sigma\sum_{j=0}^{n} GR_{ij}\left({T_j}^4 - {T_i}^4\right) \quad \textbf{(2.22)}$$

where GL_{ij} and GR_{ij} are respectively conductive and radiative couplings between node i and node j and the heat loads are given at node i [64]. It should be noted here that $GL_{ij} = GL_{ji}$ and $GR_{ij} = GR_{ji}$. The heat transfer between the nodes through conduction is represented with the term $\sum_{j=1}^{n} GL_{ij}\left(T_j - T_i\right)$ while that through radiation is with the term $\sigma\sum_{j=0}^{n} GR_{ij}\left({T_j}^4 - {T_i}^4\right)$. The radiation term in the equation starts from 0 corresponding the outer space. On the contrary, that is not considered in conduction term since there is no possible heat transfer from outer space to the satellite via conduction [69].

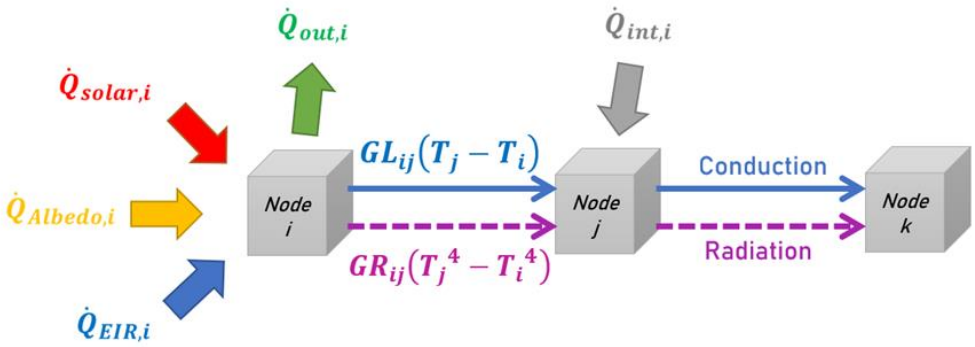

Figure 2.4 Nodal illustration of satellite thermal system

A system of ordinary differential equations is obtained when balance equations are applied to all available nodal points of the satellite thermal model. The solution of this system yields the thermal behavior of a satellite and enables to understand the thermal balance predictions for all phases of a satellite.

2.5 Thermal Cases

Satellites encounter several thermal conditions according to their mission modes, orbits, and requirements of their thermal control systems. Thermal cases of satellites are directly related with orbital altitudes, beta angles, external heat fluxes, internal heat dissipation amounts, and thermal control system requirements, and therefore these must be defined as a minimum.

An example for the extreme thermal cases is given in Table 2.1.

Table 2.1 Thermal data example for extreme cases

	Hot Case	Cold Case
Orbit	Direct sunlight	Total eclipse
Solar Heat Flux	1414 W/m^2	0 W/m^2
Albedo Coefficient	0.35	0.25
Earth Heat Flux	260 W/m^2	220 W/m^2
Internal Heat	5 W	0 W

For satellites, thermal activity in space changes momentarily and the range between the solar maxima and minima usually determines the satellite design and thermal

control requirements. Orbits with minimum and maximum heat loads for a given period of year can be defined as cold and hot orbits, respectively [8].

The extreme case scenarios, on the other hand, correspond the situations where either maximum thermal loads or their minimum are received from both external and internal sources.

A satellite is generally designed not to encounter these worst-case scenarios; however, these scenarios are useful in the early design stage for planning mission modes and performing thermal design iterations.

2.5.1 Extreme Hot Case

The extreme hot case is a term to describe the thermal situation where a satellite receives the greatest amount of solar, albedo and earth infrared radiation fluxes while the internal heat generation is also at its maximum.

2.5.2 Extreme Cold Case

The extreme cold case, in contrast, is a term to describe the thermal situation where a satellite in eclipse receives only minimum amount of earth infrared radiation flux while there is no solar flux, albedo flux or the internal heat available.

2.6 Thermal Mathematical Modeling

Thermal mathematical modeling involves using mathematical equations and computer simulations to describe and predict the behavior of heat transfer and temperature distribution in various systems and materials. This modeling approach is widely used in satellite thermal design to understand and optimize thermal processes [70, 71]. Working with thermal mathematical models necessitates a basic grasp of heat transfer mechanisms and fundamental techniques.

The development of an effective thermal model, especially when crafting a lumped parameter representation of a thermal system, necessitates a blend of knowledge, experience in both real and model systems, and the application of engineering judgment.

2.6.1 Thermal Network

A thermal network is a conceptual model that represents intricate thermal systems, commonly employed in engineering and physics for the purpose of analyzing and solving heat transfer problems. The thermal-electrical system analogy constitutes a conceptual framework wherein comparisons are made between the behavior of heat in physical systems and the behavior of electrical current in corresponding electrical circuits. Two systems, electrical and thermal, serve as analogous systems, as shown in Table 2.2 [72]. This analogy is employed with the aim of comprehending and resolving issues related to heat transfer and thermal systems, primarily in the fields of engineering and physics.

Table 2.2 Equivalent components in electrical and thermal systems

Electrical		Thermal	
Voltage	[V]	Temperature	[K]
Current	[A]	Heat Flux	[W]
Capacitance	[C/V]	Heat Capacity	[J/K]
Conductance	[A/V/m]	Conductivity	[W/K/m]
Resistance	[V/A]	Thermal Resistance	[K/W]

In a thermal network, the components of the system are represented as interconnected nodes and branches, similar to an electrical circuit. Thermal network examples for conduction and radiation mechanisms can be basically illustrated as in Figure 2.5.

Nodes in a thermal network are specific points within the system where temperature values are established, serving as reference points for temperature measurements. Meanwhile, branches in the network symbolize the routes through which heat can transfer between nodes. The attributes of these branches, such as thermal resistance and capacitance, govern the mechanism of heat transfer.

To simplify the process, computer programs for thermal analysis have been developed. These software applications necessitate users to define a thermal network for the system, resembling the design of an electrical circuit. Users input the components of this network system into the computer, after which preprogrammed routines take

charge of performing calculations for both steady-state and transient conditions. This methodology streamlines the analysis and design of thermal systems, enhancing accessibility and efficiency for engineers.

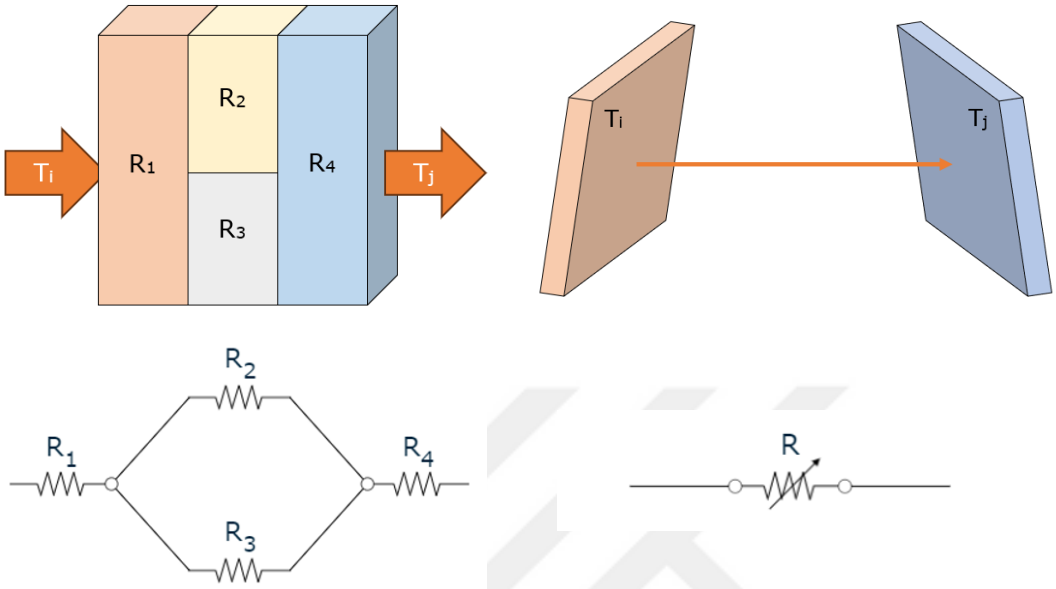

(a) Conduction (b) Radiation

Figure 2.5 Thermal network for (a) conduction and (b) radiation

2.6.2 Nodal Breakdown

In satellite thermal modeling, nodal breakdown is the procedure of partitioning the satellite structure into discrete sections, called as nodes. This serves the purpose of analyzing and simulating thermal behaviors of satellites. Each node corresponds to a particular region or component of the satellite, and the modeling accounts for its thermal properties and interactions with adjacent nodes. This detailed breakdown facilitates an in-depth examination of temperature distribution, heat transfer, and overall thermal performance across the satellite structure. This analysis is vital for ensuring that the satellite functions within its designated temperature constraints and meets its thermal design specifications.

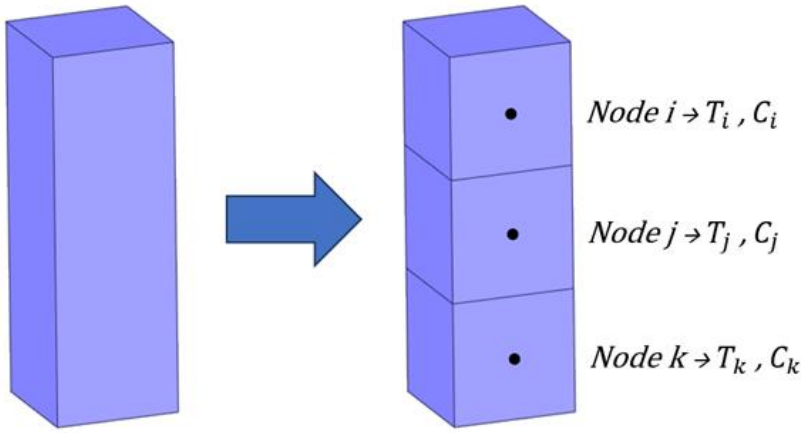

Figure 2.6 Nodal representation of the model

In this context, each node symbolizes two important components within the thermal network as shown in Figure 2.6: a temperature, which represents the thermal potential, and a capacitance, which represents the thermal mass.

There are three node types in thermal modeling; finite capacitance, zero capacitance, and infinite capacitance called diffusion, arithmetic, and boundary, respectively. Diffusion node, defined as in Equation 2.23, represents a region with finite thermal capacitance, and it accounts for thermal mass within the system and allows for heat to be stored and transferred over time.

$$\sum \dot{Q} - \frac{C\Delta T}{t} = 0 \tag{2.23}$$

Arithmetic nodes that can be expressed as in Equation 2.24 have zero thermal capacitance, and they are primarily used to calculate temperature differences and perform mathematical operations within the thermal model.

$$\sum \dot{Q} = 0 \tag{2.24}$$

Boundary nodes, on the other hand, are nodes with infinite thermal capacitance, and they are used to model external boundaries or interfaces where the temperature remains

constant, reflecting a boundary condition. They can be mathematically described as in Equation 2.25.

$$T = constant \tag{2.25}$$

These three node types are essential in creating comprehensive thermal models to analyze and predict the behavior of thermal systems.

2.6.3 Simulation Procedure

The thermal simulation process for a satellite begins by initially generating the geometric model according to its actual design. Afterward, a mathematical model that represents this geometry is developed, and then the geometry is further subdivided into a network of nodes through meshing. Based on the mission specifications and the characteristics of the satellite equipment, external and internal thermal loads at each node are defined. Subsequently, the balance equation is applied to all of these nodes. The equation is individually solved for each node through the application of diverse mathematical techniques, which allows for the computation of the temperature distribution. Additionally, it can be resolved under extreme conditions to establish the upper and lower temperature limits that are pertinent to the space mission [19]. Calculations can be conducted in either steady-state or transient modes. Steady-state simulations serve as a valuable tool for troubleshooting and correlating with test data, but they are not well-suited for mission planning, particularly in the case of small satellites operating in environments with fluctuating thermal conditions during their orbits. Transient simulations, on the other hand, are the primary method employed for thermal analysis. These simulations should be run until a state of oscillating thermal equilibrium is achieved, and this equilibrium can be confirmed by examining temperature plots [8]. Solving the balance equations for both steady-state and transient scenarios can pose challenges when using traditional methods, necessitating the use of simulation software tools to obtain solutions.

2.6.4 Simulation Software

Thermal analysis software plays a crucial role in spacecraft design and development. It accomplishes this by solving the general energy balance equation, which enables the

prediction of temperature distribution and heat flux within the spacecraft system. This information is vital to ensure the spacecraft operates within its specified temperature limits. Solving the energy balance equation analytically can be a challenging and time-consuming task, especially for complex systems like spacecraft. Thermal analysis software addresses this challenge by employing numerical methods to simulate a spacecraft's thermal behavior, based on its geometry and material properties.

Typically, thermal analysis software consists of three key components: a model generator, a solver, and a post-processor. The model generator creates a digital representation of the spacecraft system, while the solver calculates temperature distribution and heat flux. The post-processor displays analysis results, including temperature and heat flux plots.

Some thermal analysis software tools can import computer-aided design files from other programs, simplifying the modeling of intricate systems. Thermal analyzers primarily use one of three numerical methods to solve the energy balance equation: lumped-parameter, finite-difference, or finite-element. Radiation codes, used to model radiative heat transfer within a system, typically rely on the Monte-Carlo approach or the gray-diffuse assumption.

Numerous commercial software tools are available for the satellite industry, each possessing distinct capabilities. These are mainly TRASYS (Thermal Radiation Analyzer System), SINDA/FLUINT (System Improved Numerical Differential Analyzer/Fluid Integrator), TSS (Thermal Synthesizer System), ESATAN-TMS (European Space Agency Thermal Analysis Network-Thermal Modelling Suite), NX Space Systems Thermal, TD (Thermal Desktop), and Systema Thermica.

TRASYS, a NASA-developed software for thermal radiation analysis in the early 1970s, remains operational but has seen a significant decline in adoption over time due to its limited accessibility and the emergence of more sophisticated tools [73].

SINDA/FLUINT is an extensive software tool designed for conducting thermal and fluid analyses of intricate systems. It offers a diverse range of modeling capabilities with its modules of SINAPS for 2D models and Thermal Desktop for 3D models. It

also includes radiation exchange factor estimation through RadCAD and supports the integration of user-defined FORTRAN code and MATLAB.

TSS is a sophisticated solution for thermal analysis software provided by NASA [74]. Its purpose is to replace the older TRASYS software and enhance the performance of outdated codes. It is used to design and analyze spacecraft systems and to optimize their performance for a wide range of operating conditions. It integrates the capabilities of SINDA/FLUINT and radiation analysis into a user-friendly and comprehensible interface.

ESATAN-TMS is a FORTRAN-based software tool developed by European Space Agency to employ a thermal network analysis approach for predicting temperature distributions of spacecraft. It integrates the capabilities of two robust tools, ESATAN and ESARAD [75]. While ESATAN is specialized in thermal network modeling, enabling the prediction of temperature distributions within spacecraft, ESARAD excels in radiation analysis, calculating parameters such as view factors, radiative heat exchange factors, direct heat fluxes, and absorbed heat fluxes [19].

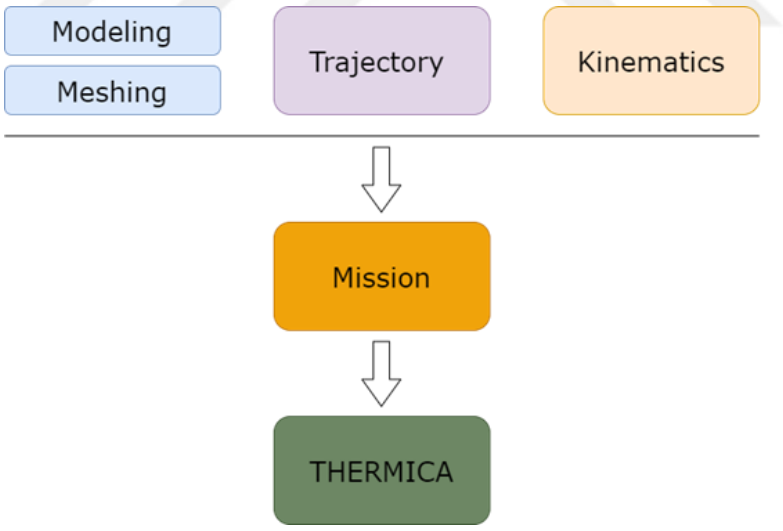

Figure 2.7 Basic workflow demonstration of Systema software suite

NX Space Systems Thermal, a tool widely used in Europe, is programmed in Fortran language based on finite element approach and employs a finite volume solver. It enables to simulate swiftly and precisely nonlinear transient thermal processes as well as thermal couplings [76].

Thermal Desktop is another software widely used for constructing intricate thermal models of satellites and assessing their thermal behavior. It is frequently employed alongside SINDA/FLUINT to enhance the analysis of thermal performance in satellite systems.

Systema Thermica is a versatile thermal design and analysis software suite developed by Airbus Space Systems, commonly used in the aerospace industry for spacecraft, satellites and other complex aerospace vehicles. Its capabilities extend from geometric modeling to mission-specific simulations, making it a valuable tool for engineers working on spacecraft and satellite thermal design, and its basic workflow is demonstrated in Figure 2.7. In this way, it eliminates the necessity to utilize multiple tools by saving time and effort.

In summary, selecting the right software for satellite thermal analysis involves a holistic assessment considering project requirements, user expertise, compatibility, features, accuracy, user-friendliness, cost, support, and updates on available tools. The choice on software greatly affects the efficiency and accuracy of the thermal analyses. In this study, Systema Thermica software is used to perform thermal modeling and analysis of CubeSat systems under various scenarios by considering aforesaid.

CHAPTER 3

INVESTIGATION OF EXTERNAL HEATS FOR CUBESATS AT VARIOUS LOW EARTH ORBITS

Satellites orbiting in space are exposed both extreme temperatures and rapid temperature changes. Therefore, thermal management for CubeSats is not an easy task because of their limited volumes. The limitations on active measures lead to apply passive thermal control measures to maintain safe ranges of operational temperatures and not to exceed mass and power budgets. External heats in space thermal environment and their impacts on CubeSats should be carefully analyzed. Granting safe service conditions in space relies on that. This chapter addresses the changes in the radiative heat loads on CubeSat panels with respect to various orbital and structural configurations. The numerical study of space thermal environment impacted the heat loads on satellite panels under different conditions is presented in detail based on [3].

3.1 Introduction

Research on thermal design and analysis of CubeSats has been increasingly conducting; however, the studies considering effects of space thermal environment on small satellites in particular orbits are very limited in the existing literature.

The nanosatellite orbiting in low earth orbit was evaluated analytically to reveal the thermal performance of the satellite design under the altitudes changing from 500 km to 2000 km and different panel combinations [34]. Three orbit scenarios of oriented-free, sun-oriented, and nadir-oriented were investigated at 700 km sun-synchronous orbit for a 3U CubeSat in terms of the solar energy and energy storage behaviors [77]. It was investigated [28] that how angular velocity effects the temperature distribution on a small satellite by selecting 4 different beta angles at 800 km height for a sun-synchronous orbit. In another study [78], the influence of 3 different satellite orientations for a 2U CubeSat, named EIRSAT-1, was examined to determine the most critical element in terms of satellite thermal management. To analyze heat fluxes on

solar panel and to define the most effective path of heat transfer between the solar panel and the satellite, simulations were performed by means of NX Space Systems Thermal package software for low earth orbits [79]. A review study [80] theoretically discussing the neutral atmosphere, meteoroids, orbital debris, and solar environments of various orbits covering low earth, medium earth, geosynchronous and highly elliptical orbits was presented. Data obtained from the flight test of the Meteor-2 satellite, orbiting at an altitude of 900 km in a circular trajectory, was used to study the impacts of radiative properties of satellite materials [81]. Thermal simulations for an observation satellite in low earth orbit with an altitude of 840 km were performed by using Systema Thermica v4.8 P1 package software in another study [82] to analyze batteries, radiators and heaters under extreme conditions. However, there was no detailed study assessing external heat loads on small satellites at varying orbits for several orbital configurations all together in the literature.

This study concentrated on evaluating the impacts of external heat sources in the space thermal environment on small satellites at various low earth orbits. To this end, the external heat fluxes were examined for varying satellite sizes, orbital beta angles and altitudes. The standard sizes of 1U, 2U, 3U, 5U, 6U and 12U were selected for small satellites while sun-synchronous orbits were used with heights ranging from 400 km to 2000 km and beta angles ranging from 0 to 75 degrees. The purpose of this work was to determine the relationships among external space fluxes, and satellite and orbital parameters, and to deliver useful knowledge for thermal modeling and designing of small satellites for service conditions in space.

3.2 Material and Methods

In order to study the effects of space thermal environment, the orbital and structural parameters were defined for CubeSats. The CubeSats having sizes of 1U, 2U, 3U, 5U, 6U and 12U were modeled as shown in Figure 3.1 by using the material of Al7075 Aluminum alloy with the panel thickness of 1 mm. The Al7075 alloy had a density of 2800 kg/m3, a conductivity of 130 W/mK and a specific heat of 915 J/kgK. The absorptivity and emissivity values of the alloy were taken as 1 for base simulations.

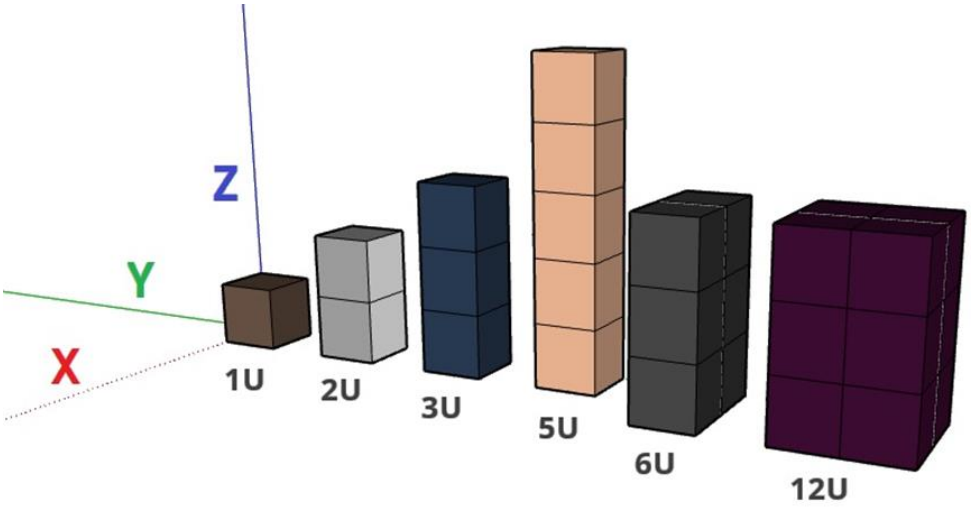

Figure 3.1 CubeSats models having different sizes

The altitudes of sun synchronous orbits were chosen as 400 km, 600 km, 800 km, 1000 km, 1200 km, 1600 km, and 2000 km to cover the range of low earth orbits and they were defined in Systema Thermica. The mean solar time was selected as 12:30:00.000 and the anomaly was taken 0 while Feb. 11, 2021 was chosen for the simulation calendar date. In the performed simulations, it was modeled that the panel oriented towards the -Z axis served as the nadir-pointing (Earth-viewing) surface, and the CubeSat traveled in the direction of the +Y axis.

In order to present a better understanding of the impacts of space thermal environment, the illuminated and shadow durations over periods were studied for various altitudes and beta angles. The beta angles of 0, 15, 30, 45, 60, 75 degrees given in Figure 3.2 were defined to investigate the change in external heat fluxes for 1U-sized CubeSat flying at an altitude of 800 km.

Finally, the influences of surface properties on external heat loads were examined by applying different coatings to CubeSat panels. For that purpose, the coatings of black paint, Kapton, Multi-layer insulation (MLI), Optical Solar Reflector (OSR), solar cells, and white paint were applied to the panels of the 1U CubeSat.

The thermal simulations under different conditions were dynamically conducted by using Systema Thermica v4.9.0 software that is developed by Airbus Defense and

Space SAS. This tool enables to perform a highly accurate complete thermal analysis of space systems by computing all elements accurately to simulate the heat transfer and the temperature. It transforms the geometrical model of a satellite into the mathematical model based on nodal approach. The Monte Carlo Ray Tracing method was used to calculate the heat transfer among radiative couplings for nodal points of a satellite system.

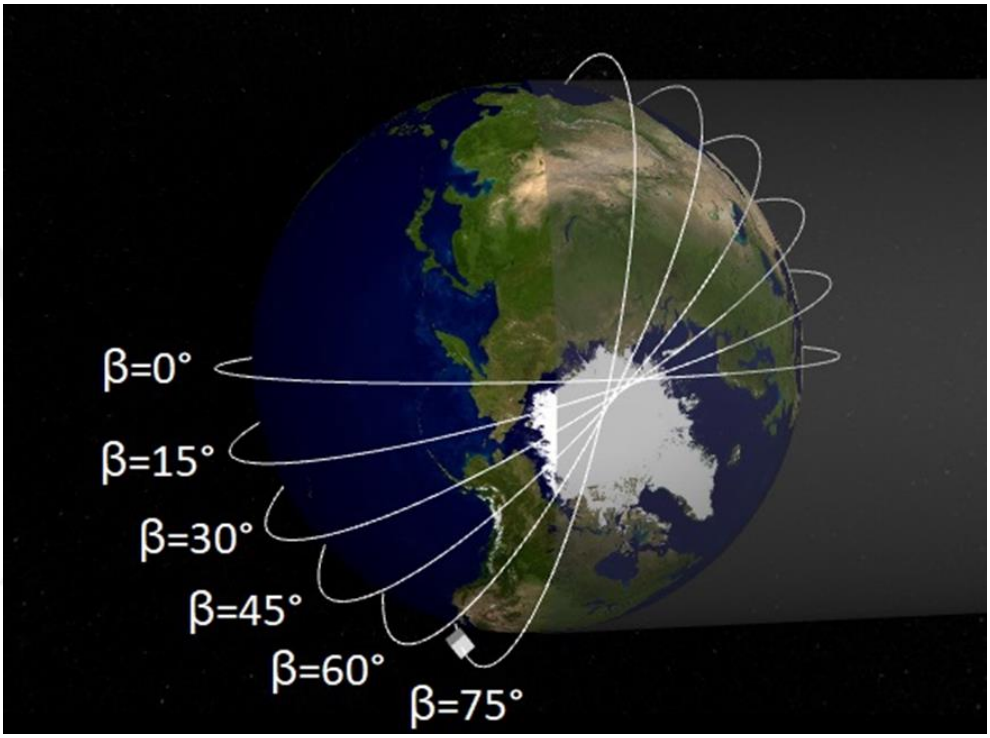

Figure 3.2 CubeSats orbits having different beta angles

Since the purpose of this study was to analyze external heat loads depending on radiative mechanisms for CubeSats at various orbits, the heat sources of direct solar radiation, Albedo radiation and the planet infrared radiation were considered while the impacts of conduction, convection, aero-thermal fluxes, and internal heat dissipation were neglected.

3.3 Orbital Periods

The radiative heats absorbed by panels of a CubeSat under various conditions are analyzed by performing on-orbit thermal simulations. Foremost, thermal simulations

are run dynamically for sun synchronous low earth orbits with different altitudes in order to put forward the durations of orbital, illuminated and shadow periods. Higher the altitudes satellites travel, longer the orbital periods they have, as presented in Figure 3.3.

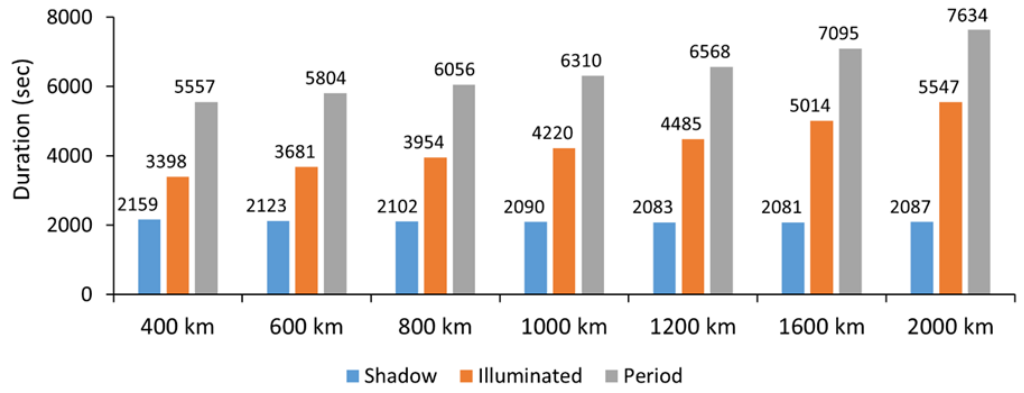

Figure 3.3 Durations of period, shadow and illuminated at different orbital altitudes

With increasing altitude, satellites spend more time within illuminated regions of space. Comparing the durations, the least time in shadow is appeared for satellites flying at 1600 km among the simulated altitudes. The altitude also dictates both umbral and penumbral durations. The ratio of the penumbral duration to the shadow is 0.78% at the altitude of 400 km while the ratio of that is 1.12% at the altitude of 2000 km. Satellites having orbits closer to the Earth stay less in penumbral regions due to the shadow geometry illustrated in Figure 2.1.

3.4 Orbital Altitudes

The effects of orbital altitudes on the heat loads received from space thermal environment are examined by means of thermal simulations for 1U CubeSats traveling at sun synchronous orbits with varying altitudes between 400 km to 2000 km. The highest contribution on the satellite heating for defined parameters is occurred by the direct solar radiation, as demonstrated in Figure 3.4 and the heat received through the direct solar radiation increases in direct proportion to the orbital altitude.

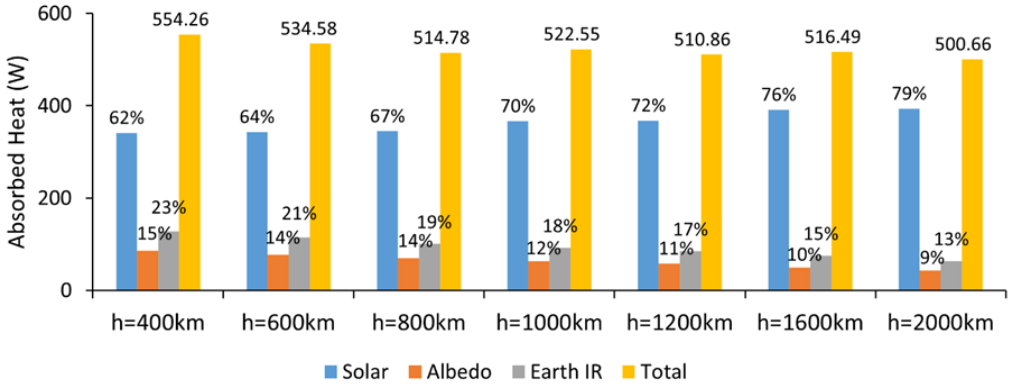

Figure 3.4 Absorbed heat from external sources with respect to the orbital altitudes

On the other hand, the contribution of the Albedo radiation and the Earth infrared radiation decreases as the distance between the CubeSat and the Earth increases. The altitude of 400 km leads to the highest total absorbed heat input while that of 1600 km leads the lowest. CubeSats traveling at higher orbital altitudes are more exposed to space thermal environment because their orbital periods are longer. That situation brings about a substantial alteration in the overall heat input received during each orbit.

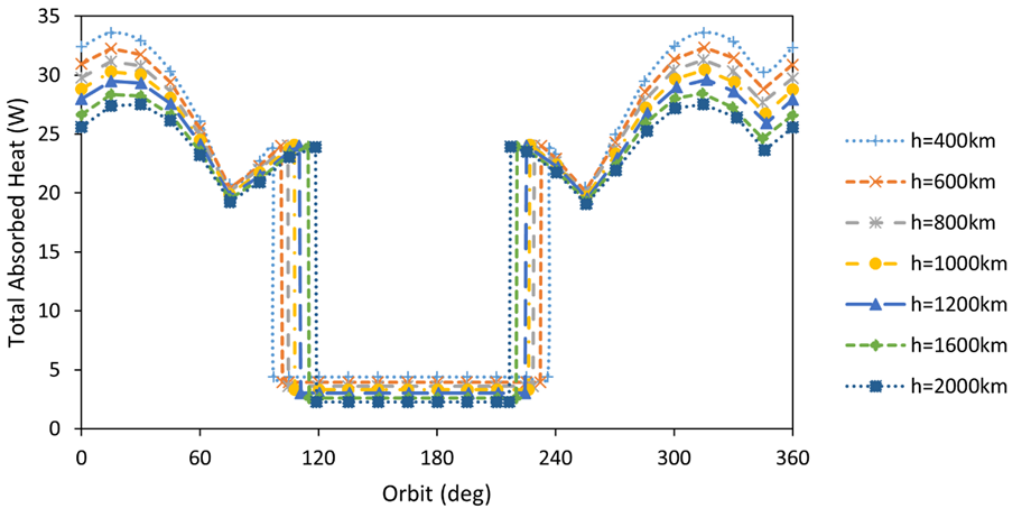

Figure 3.5 Total absorbed heat inputs with respect to the orbital altitudes

The change in the total heat absorbed by 1U CubeSat with respect to the orbital altitude is shown in Figure 3.5. Over an orbital period, the instantaneous heat input reaches the

maximum, 33.6 W, for the altitude of 400 km while that falls the minimum, 2.27 W, for the altitude of 2000 km during the eclipse.

3.5 Panel Directions

The amount of heat absorbed by the different panels of the satellite varies due to the fact that the effects and the magnitudes of external heat sources are changed over an orbital depending on the position and alignment of CubeSat panels. The overall heat amounts received by the different surface panels of a 1U CubeSat orbiting at the altitude of 400 km are illustrated in Figure 3.6.

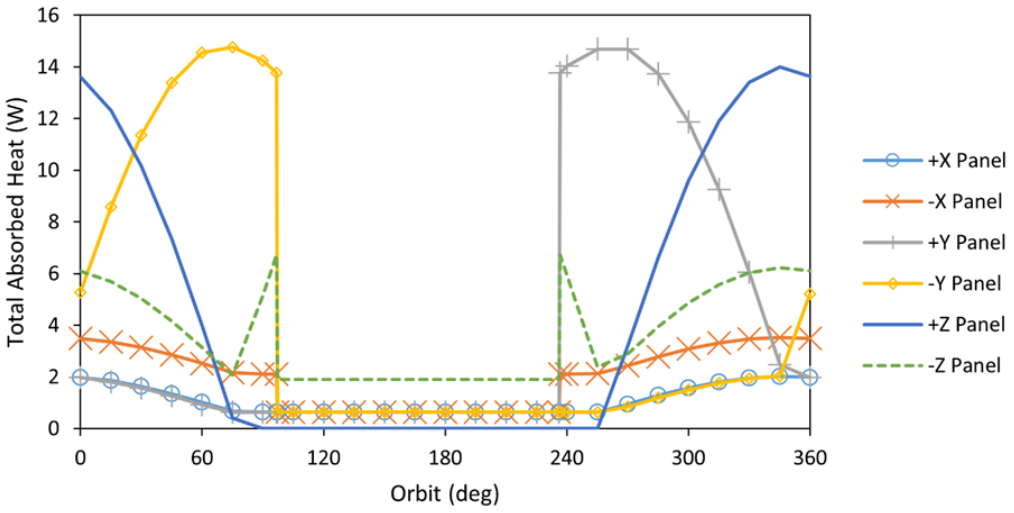

Figure 3.6 Total heat absorbed by different panels of 1U CubeSat at 400 km

The Earth-facing surface of the CubeSat is the -Z panel and therefore that receives more heat through Albedo and Earth infrared radiation compared to other satellite panels. Over an orbital period, it receives 37.14 W of energy from Albedo radiation and 55.11 W from Earth infrared radiation. On the contrary, the +Z panel that is on the opposite side, does not receive any heat from either of the external heat sources because the view factor is zero between the panel and the Earth as a result of the panel not facing the Earth. While the heat amounts absorbed through the Albedo radiation per orbit are 11.97 W for +X panel, 12.29 W for -X panel, 12.12 W for +Y panel, 12.21 W for -Y panel, the heat amounts absorbed through the Earth infrared radiation are constant along the orbit for these panels and that is 18.05 W per orbit for each panel.

The absorbed heat amount via the direct solar radiation is determined by both the orientation of the satellite with respect to the celestial bodies and the material properties [34]. The total solar heat amounts absorbed by various panels of a 1U CubeSat at 400 km are presented in Figure 3.7 by using the same material properties to investigate the influence of the panel position and orientation. The direct solar radiation contributes the most to the total absorbed heat by the CubeSat as discussed earlier and besides it dictates the heat profiles in Figure 3.7.

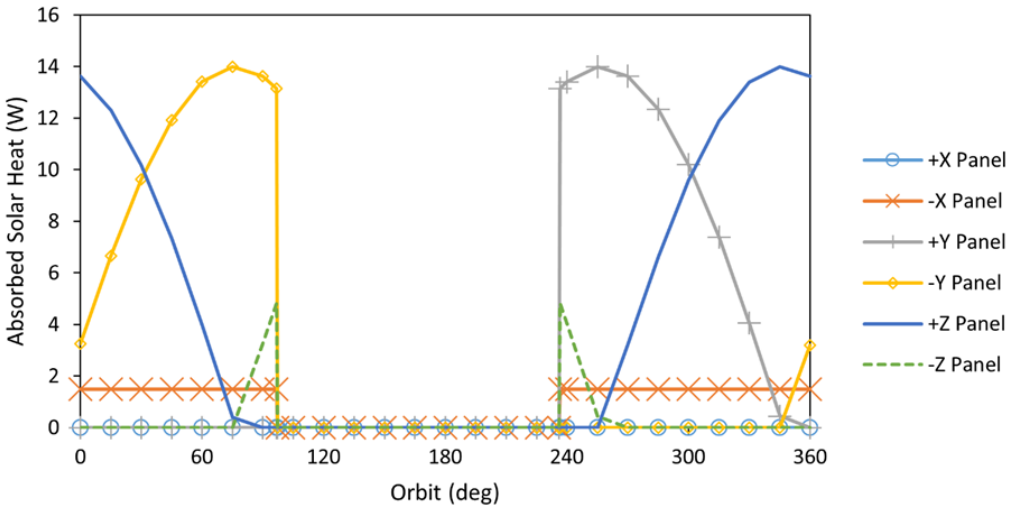

Figure 3.7 Total solar heat absorbed by different panels of 1U CubeSat at 400 km

The maximum number of CubeSat panels facing the sun is three at most as stated in the study of Dinh [41]. The result of this study validates that statement and only three panels absorb direct solar radiation along the illuminated passage. However, the panels absorb no direct solar radiation along the eclipse.

3.6 Beta Angles

Another essential parameter effecting the quantity of heat received from external thermal sources in space is beta angle. Thus, thermal analyses are conducted for the beta angles of 0, 15, 30, 45, 60, and 75 degrees for a 1U CubeSat deployed at an altitude of 800 km.

The durations the CubeSats stay in the passages of illuminated and shadow with respect to different Beta angles are stated in Table 3.1. Among the beta angles studied, the 0 degree has the longest shadow period. As the beta angle rises from 0 to 60 degrees, CubeSats spend less time in the eclipse. Moreover, they have less umbra intervals and more penumbra intervals for higher beta angles at the altitude of 800 km. When the beta angle of the satellite as high as 75 degrees, there is no ecliptic passage anymore and the orbit of the satellite is completely in the illuminated passage for the defined orbital configuration.

Table 3.1 Durations in illuminated and shadow for varying beta angles

Beta Angles	Illuminated	Shadow (U-Umbra; P-Penumbra)		
0°	65.19%	34.81%	U	99.15%
			P	0.85%
15°	65.77%	34.23%	U	99.08%
			P	0.92%
30°	67.78%	32.22%	U	98.87%
			P	1.13%
45°	72.44%	27.56%	U	98.20%
			P	1.80%
60°	86.51%	13.49%	U	90.21%
			P	9.79%
75°	100.00%	0.00%	U	0.00%
			P	0.00%

Satellites having smaller beta angles experience less direct solar fluxes and stay longer in the eclipse. On the other hand, they receive more solar fluxes per orbit when orbiting at higher beta angles and in the absence of appropriate thermal control measures they may be overheated [41]. Hence, it is very important to realize how external heat loads change with respect to the beta angle. To this end, various beta angles for a 1U CubeSat orbiting at the height of 800 km are studied and the total absorbed heats with respect to the beta angles are exhibited in Figure 3.8.

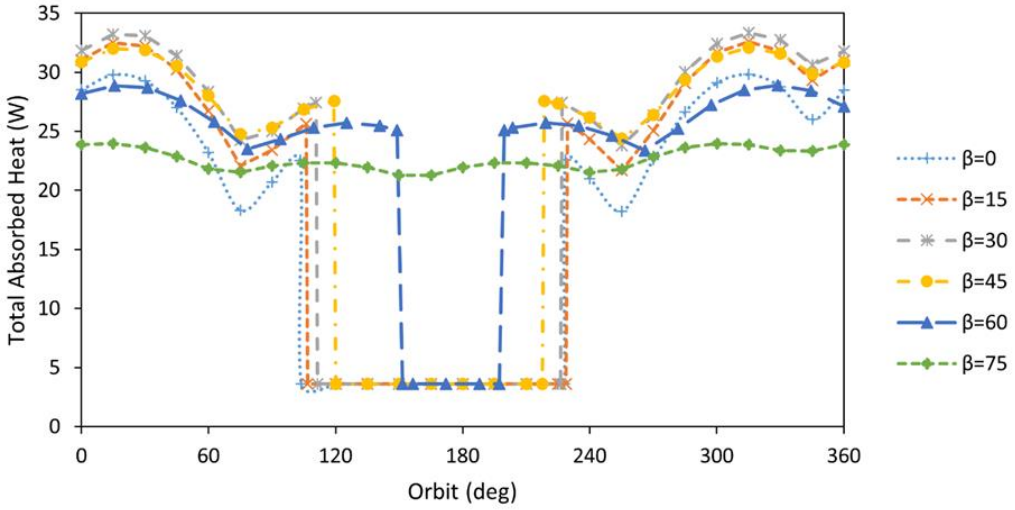

Figure 3.8 Total absorbed heat for different beat angles of 1U CubeSat at 800 km

The beta angle of 30 degrees has the maximum instantaneous heat input, which is 33.35 W, received by the CubeSat. Nevertheless, the beta angle of 60 degrees has the maximum total heat, which is 621.36 W, per orbit. The reason is that the CubeSat stay shorter in the eclipse while it absorbs more heat during the illuminated interval. For the beta angle of 75 degrees where no eclipse is present during the whole orbit, the satellite receives the heat of 565.82 W in total. The orbit-averaged total absorbed heat is 1.57 W per orbit for the angle of 75 degrees as well.

3.7 Satellite Sizes

The heat loads delivered from external thermal sources in space to the satellite is affected by the size of it since the absorbed heat rate is directly proportional to the areas of external satellite panels. In Figure 3.9, total absorbed heats for various CubeSat sizes at 800 km are demonstrated.

The -Z panel facing the nadir has the dimension of 0.1 m x 0.1 m for satellites having 1U, 2U, 3U and 5U sizes while that has the dimension of 0.1 m x 0.2 m and 0.2 m x 0.2 m for 6U and 12U, respectively. The 1U CubeSat having the least surface area among the studied sizes receives the minimum total heat while 12U having the greatest surface area receives the maximum from external thermal sources. Per orbital period, the total heat Albedo radiation heats are 69.60 W, 106.13 W, 142.68 W, 215.77 W,

230.36 W and 351.42 W while that of total Earth infrared radiation heats are 100.35 W, 153.10 W, 205.52 W, 310.80 W, 332.64 W and 507.08 W for 1U, 2U, 3U, 5U, 6U and 12U CubeSats, respectively.

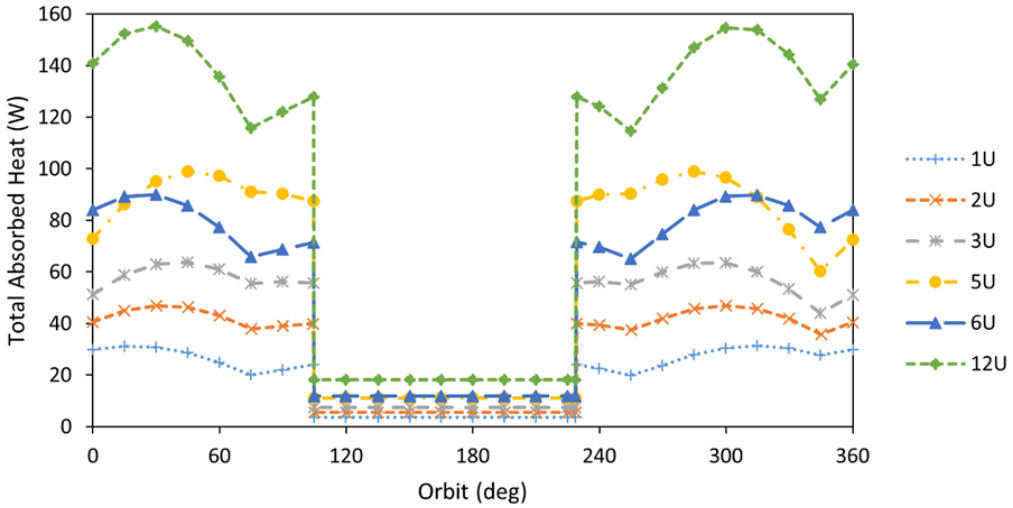

Figure 3.9 Total absorbed heat for different CubeSat sizes at 800 km

The total heat from both Albedo and Earth infrared radiation increases as the satellite size gets bigger and the size of panels interacted with Earth is more decisive on the total heat input through these sources.

3.8 Surface Coatings

The material properties are very influential on the amount of heat absorbed from space thermal environment to the satellite; therefore, the change in total absorbed heat with respect to the different coating materials applied to the outer surfaces of CubeSat panels is investigated.

Table 3.2 Solar absorptivity and IR emissivity of surface coatings

	White Paint	Black Paint	Kapton	MLI	OSR	Solar Cell
α	0.25	0.95	0.85	0.52	0.20	0.74
ε	0.81	0.90	0.85	0.71	0.81	0.82

The coatings of white paint, black paint, Kapton, MLI, OSR and solar cell, that are commonly used in satellites with purposes of thermal control and power management, are selected for thermal analyses and their properties are provided in Table 3.2.

The total heat inputs absorbed by 1U CubeSat at the altitude of 800 km are shown for different coating types in Figure 3.10. The total heats of 184.84 W, 483.98 W, 437.53 W, 286.72 W, 164.12 W and 388.93 W are received per orbital period for the coatings of white paint, black paint, Kapton, MLI, OSR and solar cell, respectively.

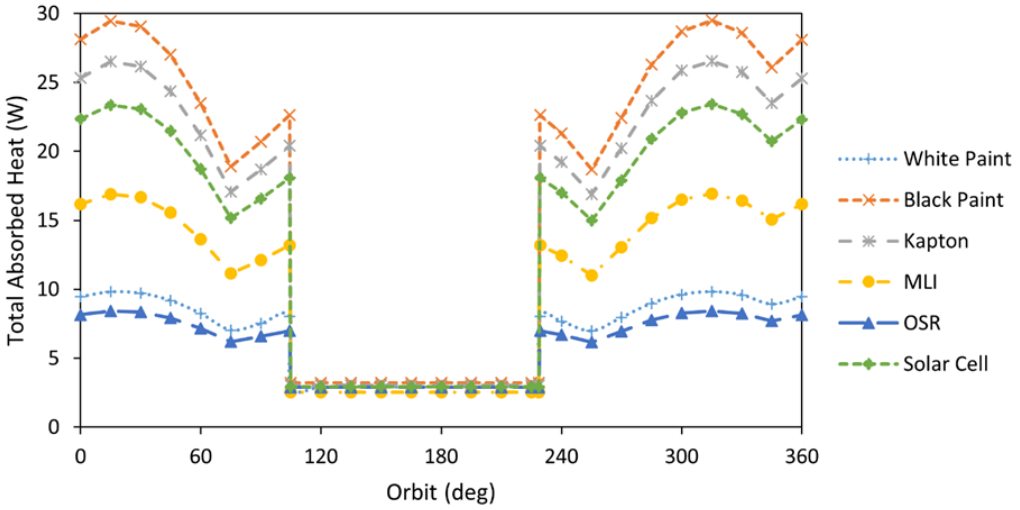

Figure 3.10 Total absorbed heat for different coatings applied to 1U CubeSat orbiting at 800 km

The black paint having the highest absorptivity to emissivity ratio among the coatings analyzed leads to the maximum heat absorption. As the ratio of absorptivity/emissivity of the external surfaces of satellite materials increases, the heat received by a satellite rises as well. Compared OSR and white paint, having same emissivity values, OSR absorbs less heat from space thermal environment since its absorptivity/emissivity ratio is lower. The application of coating with different solar absorptivity and IR emissivity values to satellite panels in accordance with the desired purpose is a very common and effective passive thermal control measure, especially for small satellites. Consequently, the outer panels of a CubeSat can be coated with OSR and white paint in order to minimize the heat load while they can be coated with black paint and Kapton to maximize that.

3.9 Conclusion

This chapter presents the effects of space thermal environment on CubeSats panels under various orbital conditions and satellite setups by conducting numerical analyses on Systema Thermica v4.9.0 software, employing Monte Carlo Ray Tracing technique. Various altitudes are simulated for sun synchronous orbits and the results exhibited that the heat input is changing with the altitude. As the orbital altitude gets higher, the absorbed heat from direct solar radiation rises while that from albedo and earth infrared radiation falls. Besides, CubeSats orbiting at lower heights experience longer shadow periods.

CubeSats receive different heat input according to the positions of their panels with respect to celestial bodies in space. When they are in the illuminated intervals, only three panels of them are exposed to direct solar radiation. In contrast, no panels get direct solar radiation when they are in the shadow.

Outcomes of this study also reveal that the beta angle has very influential on not only total absorbed heat but also eclipse durations. The maximum satellite heating is achieved for the beta angle of 60 degrees while there is no eclipse interval observed for the angle of 75 degrees.

Furthermore, the sizes of CubeSats change the total amount of absorbed heat power because the surface areas of CubeSat panels are directly proportional to the received heat rate. Thermal analyses show that the bigger the satellites are the more the heats are absorbed as well.

Finally, it is found that the surface properties of CubeSat panels significantly influence the satellite heating in space. The heat received by a satellite increases as the ratio of absorptivity/emissivity increases, and thus thermal management can be achieved, especially for small satellites, by changing the coating material having different surface properties.

To conclude, it is highly important to understand the influence of space thermal environment on satellite design and orbital configuration. An accurate thermal control system can only be designed and utilized upon detailed studies of the heat budget

effected on several parameters. The findings of this chapter can provide useful information for the early design phase of small satellites operating in similar orbits and help satellite thermal engineers to decide on design parameters and orbital configurations.

CHAPTER 4

INVESTIGATION OF SURFACE TEMPERATURES FOR CUBESATS AT VARIOUS LOW EARTH ORBITS

This chapter is based on [64], where the temperature profiles at surfaces of CubeSats sized 1U, 2U, 3U, 5U, 6U and 12U are examined for various low Earth orbits. The influences of orbital heights varying from 400 km to 2000 km and the beta angles varying from 0 to 75 degrees on thermal behaviors are systematically studied. In order to uncover the effects on satellite thermal budget, not only different types of coatings with varying solar absorptance and infrared emissivity but different amounts of internal heat dissipations are investigated as well. Results reveal that satellite surface temperatures greatly depend on those parameters. The heat amounts that a satellite absorbs from space thermal environment are impacted by the satellite design parameters and the orbital configurations. The findings of this study may be beneficial for defining the criteria of design that the satellite will have and orbit that it will fly at especially in the early engineering stage.

4.1 Introduction

Recent concepts and developments in satellite thermal modeling and analysis were reviewed [19] and various studies have been conducted focusing on thermal design and analysis to evaluate the thermal performance of small satellites [3, 27, 33, 41, 45, 48, 83-87]. However, there has been only limited number of studies addressing the influence of satellite design parameters and orbital configurations.

CubeSats with different panel configurations were investigated analytically for the orbital altitudes ranging from 500 km to 2000 km by Bulut and Sözbir [34]. Three different altitudes and three different orientations for a 3U CubeSat were simulated by Sanchez-Sanjuan et al [77] to reveal solar energy behavior. Considering 4 beta angles, Farrahi and Perez-Grande [28] presented the simplified thermal analysis for the angular velocity of a small satellite. To study the satellite thermal management by

Wallace et al, the 2U sized CubeSat at 400 km was analyzed [78] under steady conditions. The heat path from solar panels to the satellite was investigated by Almehisni and Naimat [79] in terms of effectiveness by means of thermal simulations. Nenarokomov et al [88] used inverse problems approach to evaluate radiative properties of materials with the real data of the satellite Meteor-2. Spinning small satellites were analyzed by Morsch Filho et al [89] using finite volume method to assess thermal scenarios. Experimental test results together with simulations were provided by Bulut [9] for TURKSAT-3USAT serving at low earth orbit. Another study related to TURKSAT-3USAT was conducted by Bulut and Sözbir [16] for estimating the thermal limits of satellite parts under worst-case scenarios. By using finite volume method, Morsch Filho et al [90] simulated a 1U sized CubeSat externally covered by solar panels to analyze the internal radiation within the satellite. Thermal simulations using finite difference method were performed by Malde et al [91] for 3U CubeSat to determine the temperature distribution. The impacts of beta angles and contact conductance were evaluated by Garzon et al [92] for 3U sized CubeSat at the orbital height of 732 km.

Despite the increasing interest in thermal analysis of small satellites, there are still limited studies in this area and there is no detailed research analyzing and comparing the surface temperature profiles of CubeSats at sun synchronous orbits with changing orbital heights for different satellite sizes, design, and orbital configurations all together. Between space thermal environment and the satellite, thermal interactions are investigated through numerical simulations by using Monte Carlo Ray Tracing method. In order to obtain temperature profiles of surface panels for different sized CubeSats orbiting at various altitudes in the range of low earth orbit, the analytical assessments are conducted. The motivation of this study is to reveal relationships among several factors of satellite design and orbital configuration. Furthermore, presenting valuable data and knowledge in thermal management of small satellites is aimed within this research.

4.2 Material and Methods

Satellites operating at orbits are exposed to heat loads varying greatly per orbital period over their lifespan. That situation leads to significant thermal gradients and instantaneous temperature changes, having negative effects on the integrity of satellites and their equipment. To reveal the thermal behavior of CubeSats with different sizes at various low earth orbits, the influences of space thermal environment are analyzed for varying parameters through on-orbit transient simulation by using Systema Thermica v4.9.0 software. The method used in estimating the external thermal loads for satellite surfaces is Monte Carlo Ray Tracing approach. In space thermal analysis, the nodal method, in which the satellite is divided into nodes, is used. As shown in Figure 4.1, each panel of the satellite is represented by a defined node, and it is assumed that each satellite panel is isothermal.

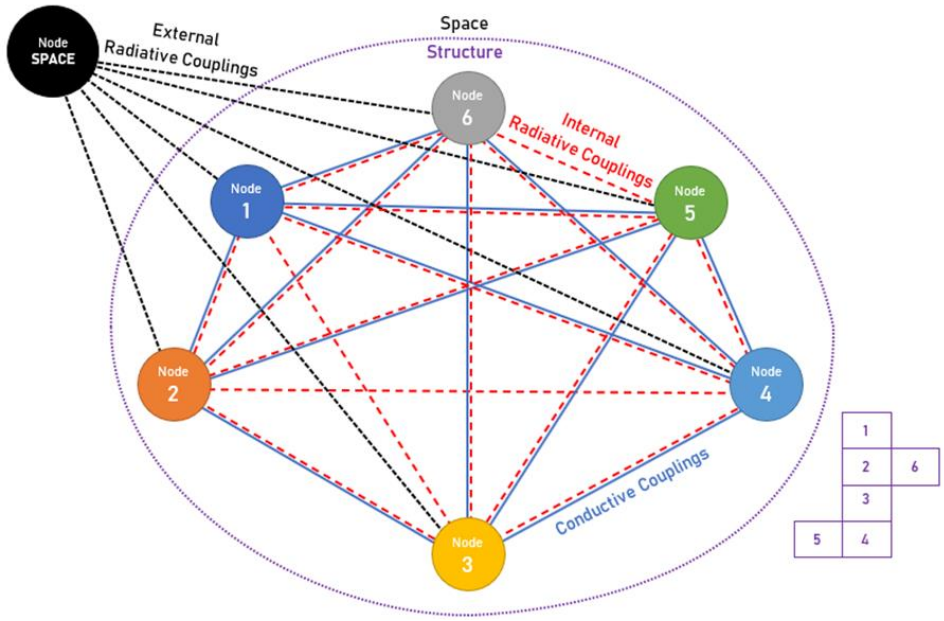

Figure 4.1 Thermal links for CubeSat panels in space

The sizes of 1U, 2U, 3U, 5U, 6U, and 12U having standard dimensions in the literature are considered in this study. All satellite panels are chosen as Al7075 aluminum alloy with the thickness of 1 mm. The density is 2800 kg/m3, the conductivity is 130 W/mK and the specific heat is 915 J/kgK for the selected alloy. To simulate the internal heat dissipation, the value of 3.8 W for TURKSAT-3USAT available in the literature [9] is

considered as reference. Accordingly, the heat dissipation of 0.63 W is applied to each panel of 3U CubeSat in thermal analyses and that value is linearly extended to all other sizes of CubeSats by applying equally to all their panels. Therefore, 1U CubeSat has the internal heat dissipation of 0.21 W per panel, leading to 1.26 W in total.

The altitude and the attitude are two important factors affecting the heat absorbed by the satellite. Altitudes are studied dynamically in 200 km increments for the range between 400 km and 2000 km corresponding to low earth orbits. In addition, the orbits are arranged sun synchronous. Satellites are modeled as they move with no spinning in space towards the +Y panels of them and their -Z panels always view the Earth.

Besides, six beta angles changing from 0 to 75 degrees are investigated in order to determine the effects of beta angles on temperature profiles at satellite panels due to the fact that beta angles change considerably over a year causing great changes in external heat inputs received by the satellite.

Satellite panels may have different surface properties according to the materials and the coatings applied. For the base simulations, the solar absorptivity and infrared emissivity of them are selected as ones. On the other hand, the impacts of surface properties on thermal behavior are examined applying commonly used coatings of white paint, black paint, multi-layer insulation (MLI), Kapton, optical solar reflector (OSR) and solar cell to all external surfaces and the properties of them are presented in Table 4.1.

Table 4.1 Solar absorptivity and IR emissivity values for coating types

Coatings	Solar Absorptivity, α	IR Emissivity, ε	ε/α
Black Paint	0.95	0.90	0.95
Kapton	0.85	0.85	1.00
Solar Cell	0.74	0.82	1.11
MLI	0.52	0.71	1.37
White Paint	0.25	0.81	3.24
OSR	0.20	0.81	4.05

The position of the Earth affects the available thermal environment in space. The Earth reaches its closest distance from the Sun approximately on the 3rd of January while it reaches its farthest distance approximately on the 4th of July. The mean distance, corresponding to the 1 AU, between the Earth and the Sun, on the other hand, takes place on about the 4th of April and the 5th of October, as shown in Figure 4.2 [93]. Hence, thermal simulations are performed for the date of April 4th.

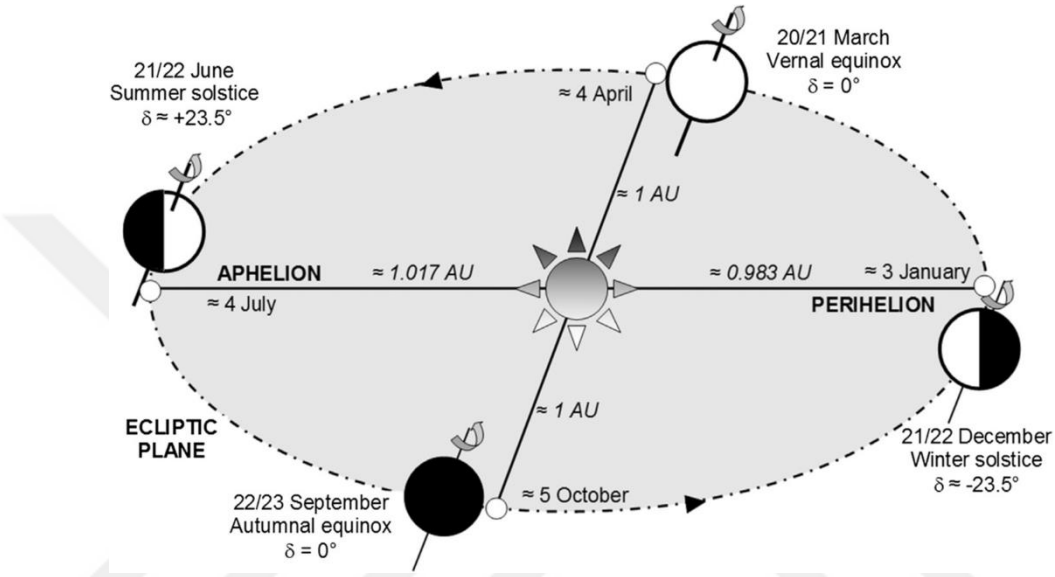

Figure 4.2 Changes in distance of the Earth from the Sun [93]

4.3 Orbital Altitudes

First, the total absorbed heats by the panels of 1U sized CubeSat are examined for changing orbital heights as shown in Figure 4.3. Satellites experience different external heats changing with respect to their position and orientation. Among all other thermal sources in space, the solar radiation is the most dominant. Satellites flying at higher altitudes absorb more heat since the contribution of solar radiation to the satellite heating increases as they get closer to the sun. However, the contributions of Albedo and Earth IR decrease significantly as they orbit farther from the Earth. It should be noted that their contributions are significant at lower altitudes and even they are negligible for altitudes higher than the range of low earth orbits.

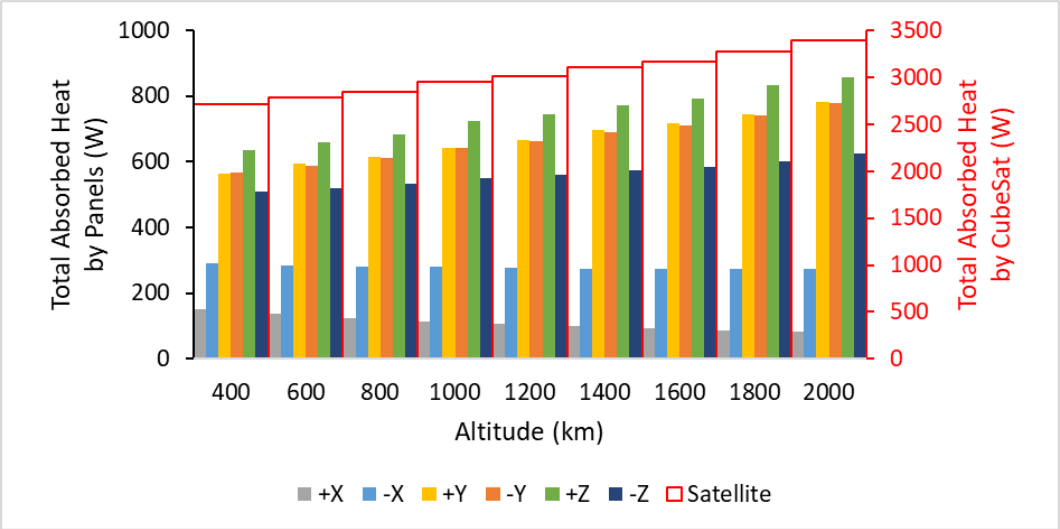

Figure 4.3 Total absorbed heat by 1U CubeSat panels

Satellite panels receive varying rates of heat fluxes from external thermal sources in space according to their position and orientation along the orbital period. Because the orbits of CubeSats in this study are selected as sun synchronous, +Z panel by facing the Sun stays longer duration and absorbs more direct solar radiation per orbit compared to other panels, as exhibited in Figure 4.4.

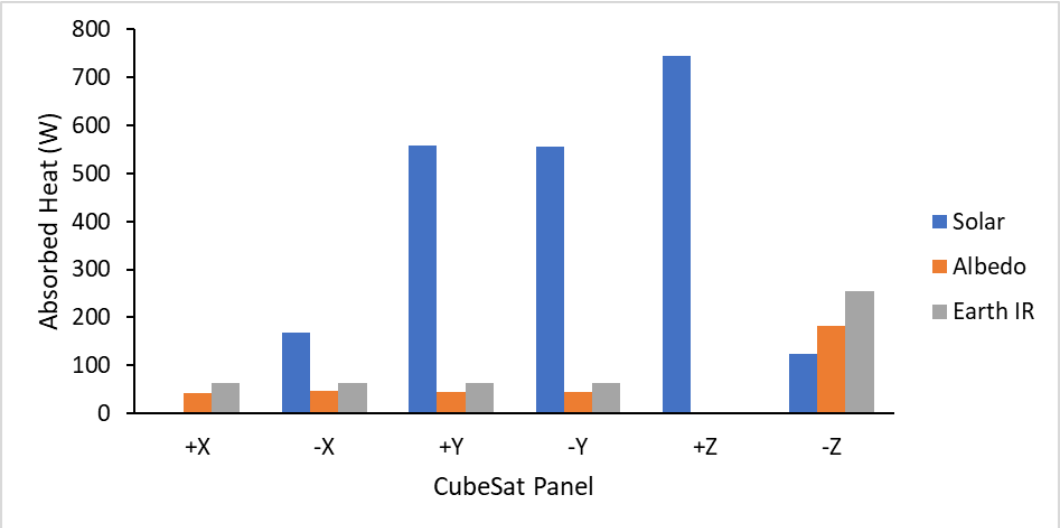

Figure 4.4 Absorbed heat by different panels of 1U CubeSat at 1200 km

The temperature profiles of 1U sized CubeSat panels are shown in Figure 4.5, Figure 4.6, Figure 4.7, Figure 4.8, Figure 4.9 and Figure 4.10 for orbital heights ranging from

400 km to 2000 km. The changes in thermal energy inlet result in different profiles of temperatures at satellite panels along an orbit. As satellites pass through the eclipse, the temperature values decrease and begin to rise again immediately after exiting the eclipse. That causes higher positive temperatures for illuminated intervals and lower negative temperatures for ecliptic intervals and eventually results in cyclic thermal stresses on satellites during their lifespans in service. Therefore, extrema temperatures together with thermal gradients should be considered not only to provide proper designs but also to choose durable materials for them.

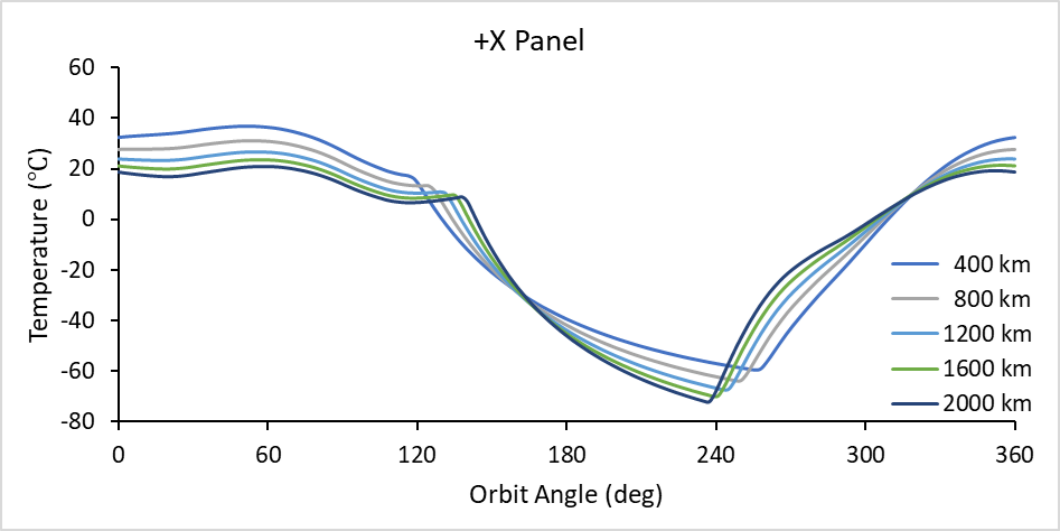

Figure 4.5 Temperature profiles for +X panel of 1U CubeSat at different altitudes

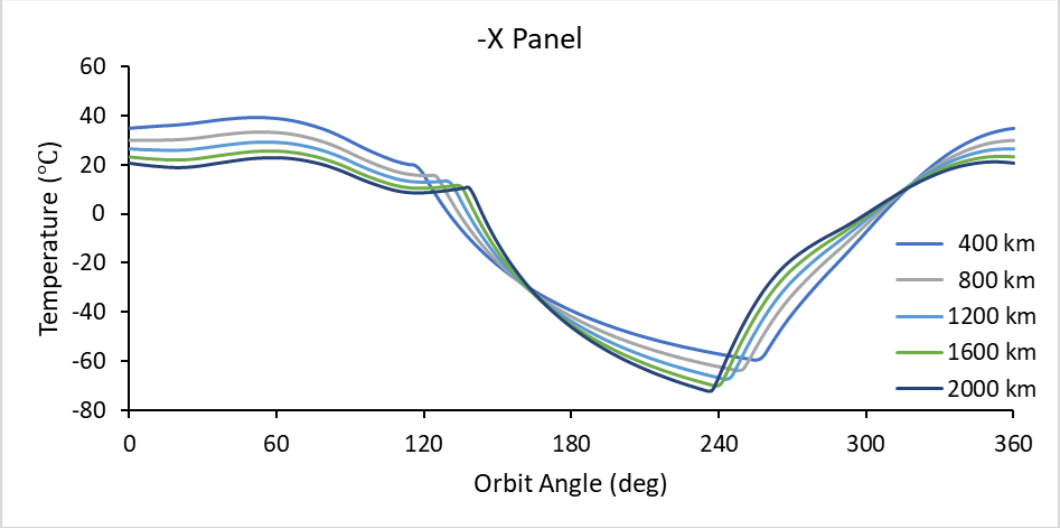

Figure 4.6 Temperature profiles for -X panel of 1U CubeSat at different altitudes

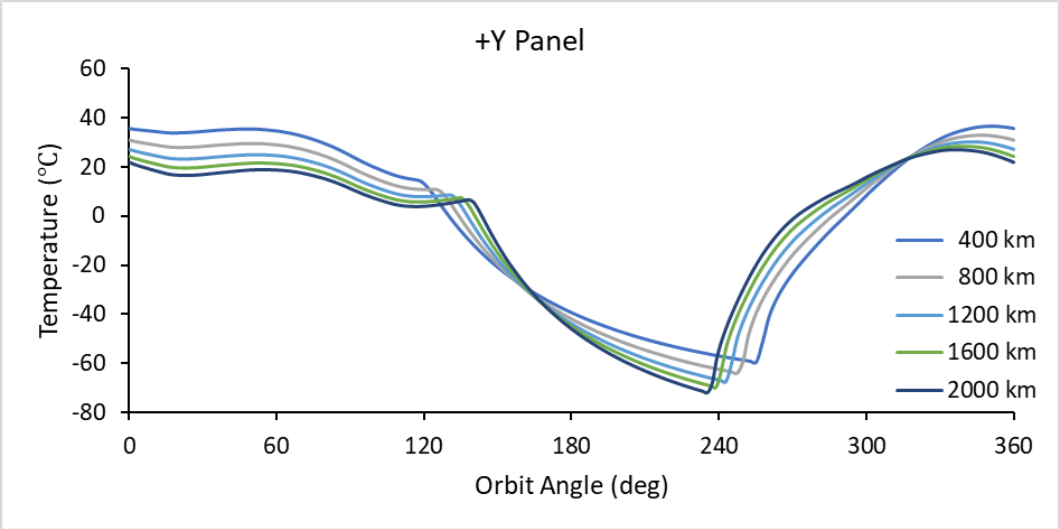

Figure 4.7 Temperature profiles for +Y panel of 1U CubeSat at different altitudes

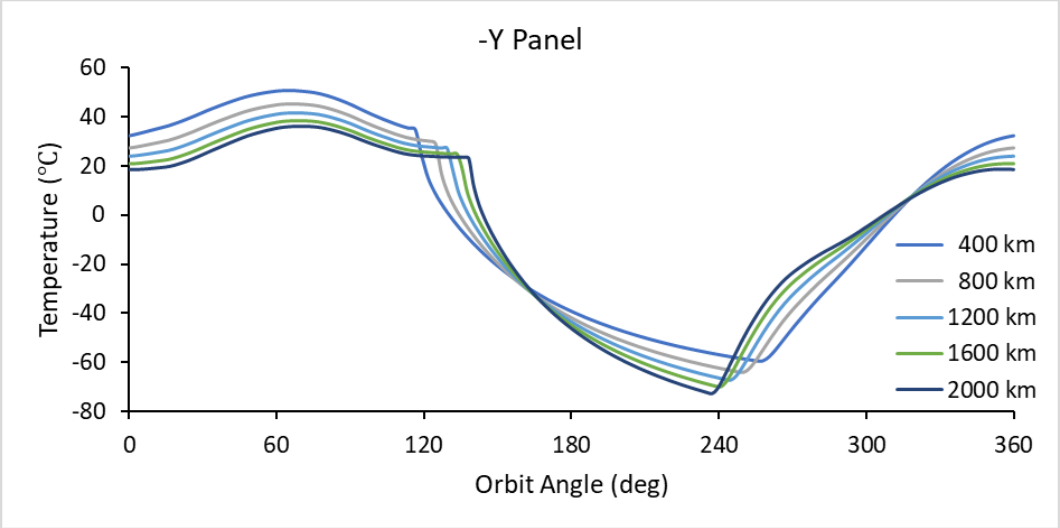

Figure 4.8 Temperature profiles for -Y panel of 1U CubeSat at different altitudes

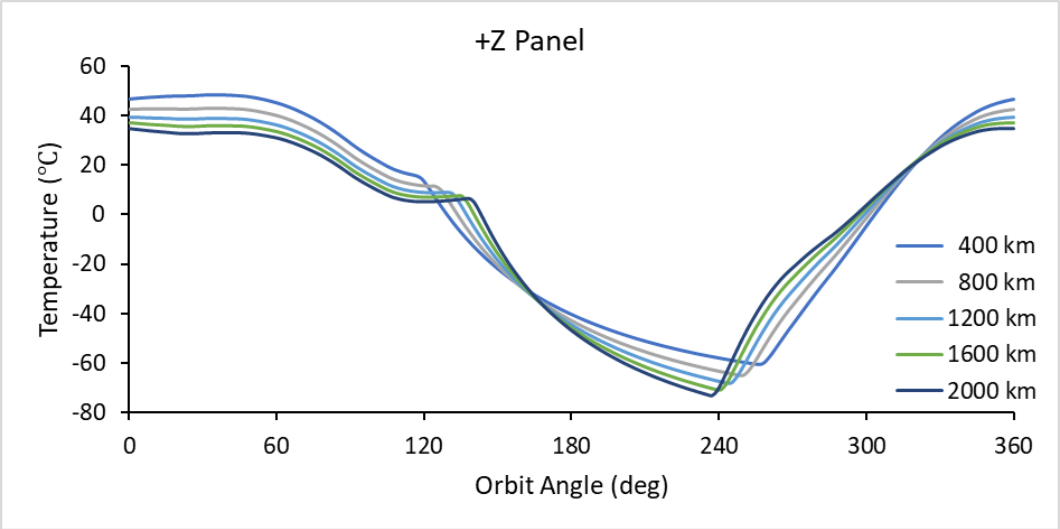

Figure 4.9 Temperature profiles of for +Z panel of 1U CubeSat at different altitudes

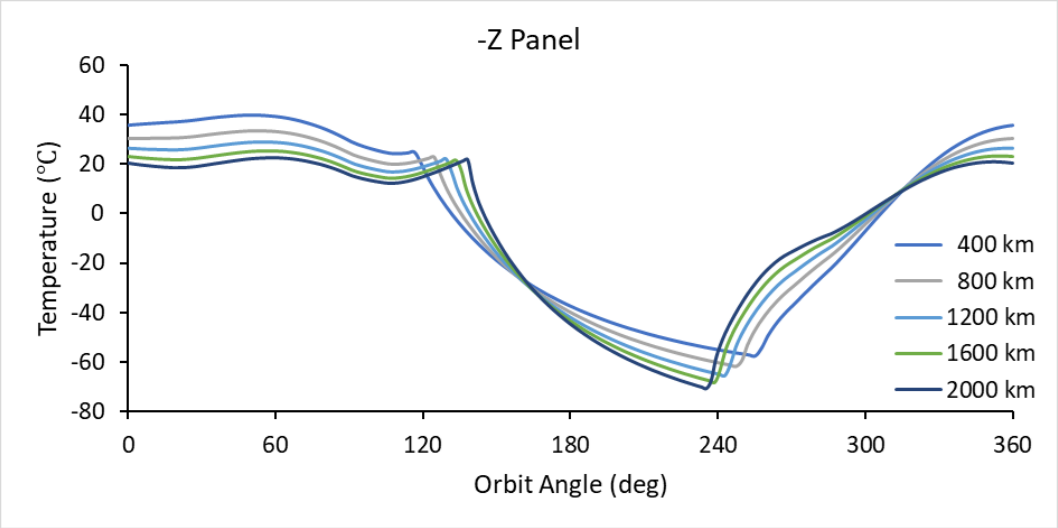

Figure 4.10 Temperature profiles for -Z panel of 1U CubeSat at different altitudes

4.4 Satellite Sizes

Another factor influencing the heat loads absorbed is the satellite size, as demonstrated in Figure 4.11, because transferred heat is directly proportional to the area of satellite panel surface. Panel areas are changing according to the sizes of satellites and that causes the amounts of heat absorbed to change. The bigger sizes the satellites have, the more heat loads they are exposed to per orbit. Nevertheless, the increase in the satellite heating is nonlinear because satellite panels viewing different directions

eventually receive different heat loads. The areas of +Z and -Z panels are same for 1U, 2U, 3U and 5U CubeSat sizes while they are twice larger for 6U size and four times larger for 12U size. As a result, the heat loads absorbed by +Z and -Z panels are doubled for 6U and quadrupled for 12U. The increase in surface areas of satellites boost satellite heating directly. However, the influence of satellite sizes on thermal performance should be examined together with the satellite orientation parameter. When analyzed the cases where the sizes of satellites are doubled, the increase in the absorbed heat is 1.57 times between 1U and 2U, 1.38 times between 3U and 6U, and 1.74 times between 6U and 12U. On the other hand, the increase in the heat amounts received from space thermal environment differently occurs although the total surface areas are equal for 5U and 6U sizes. It is due to the fact that different surface panels of satellites absorb different heat loads with respect to their orientation.

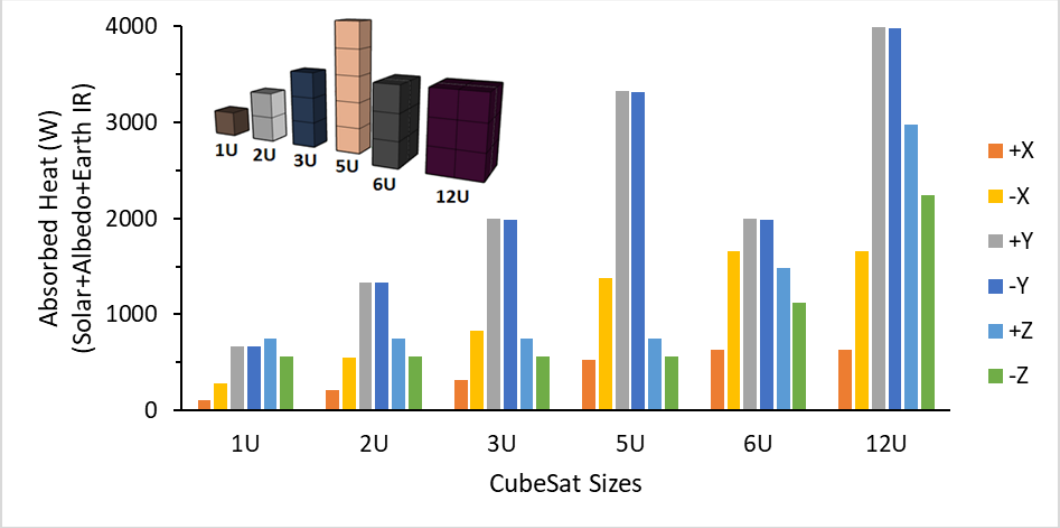

Figure 4.11 Absorbed heat by panels of different sized CubeSats at 1200 km

Different temperature profiles at satellite panels occur, as shown in Figure 4.12, because the heat loads are changing with respect to satellite sizes. It is revealed by analyzing the CubeSat sizes of 1U, 2U, 3U, 5U, 6U, and 12U that both total absorbed heat and surface temperatures are influenced by satellite sizes. Besides, the satellite heating as well as the temperature distribution is dictated by the satellite orientation.

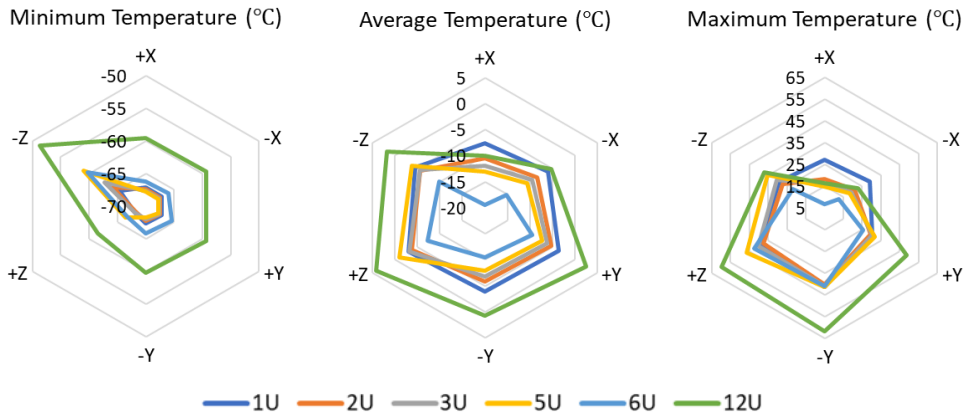

Figure 4.12 Minimum, average and maximum temperature profiles for different CubeSat sizes

4.5 Beta Angles

Beta angle, one of the parameters determining the illuminated interval per orbit, affects the surface temperature distribution, as in Figure 4.13 showing temperature profiles at Earth facing panel for different beta angles. The increase in beta angles leads to the decrease in ecliptic interval and consequently more heating for satellites flying at low earth orbits. The lowest temperature values encountered during an orbital period increase with the increase in the beta angle. They become positive for the beta angle of 75 degrees because no eclipse, where the lowest temperatures occurred, is present at this angle. The highest instantaneous temperature, however, is reached at the beta angle of 30 degrees since this angle has more heat load outside the eclipse. Yet the longer eclipse interval of this angle lowers the values of orbit-average temperature. The beta angle of 60 degrees having shorter eclipse interval and more heat load in the illuminated interval, on the other hand, offers the highest obit-averaged temperature.

Temperature gradients due to the cyclical changes in space thermal environment cause thermal stresses on satellites, and managing these gradients is another important concern in satellite thermal control, especially for small satellites. To keep satellites safe and operational in space conditions, lower levels of thermal changes are desired in terms of thermal design. The increase in beta angles leads to the decrease in temperature gradient magnitudes. Hence, the lowest changes in temperature gradients are observed at the beta angle of 75 degrees, because the orbiting satellite at this angle

does not experience an eclipse and is exposed to direct solar radiation throughout its entire orbital period.

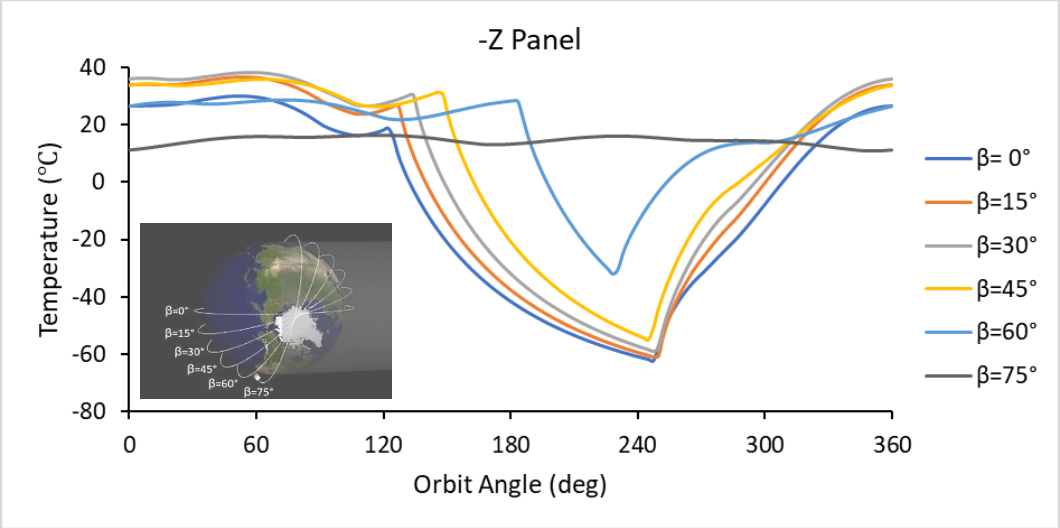

Figure 4.13 Temperature profiles for different beta angles of 1U CubeSat at 800 km

Ultimately, reducing the negative effects of space thermal environment on the satellite, or collecting more energy through solar panels placed on the satellite may be achieved by choosing appropriate beta angles.

4.6 Surface Coatings

Coatings influence temperature distributions at satellite panels, as shown in Figure 4.14, and the total absorbed heats by satellites. They are beneficial to sustain satellite thermal control by modifying the optical parameters of panel surfaces. The black paint with the lowest ratio of emissivity to absorptivity delivers the highest temperature profile while OSR with the highest ratio of that delivers the lowest. That is because of that fact that higher absorptivity values enable receiving more heat to the satellite from the space while lower emissivity values enable delivering less heat to the space from the satellite. Selecting the proper coating by evaluating its optical properties assists the satellite thermal control for the specific mission requirements and to sustain panel temperatures within safe operational levels. Satellite panels may be covered with Kapton or black paint to achieve higher temperatures while they may be covered with white paint or OSR to achieve lower temperatures.

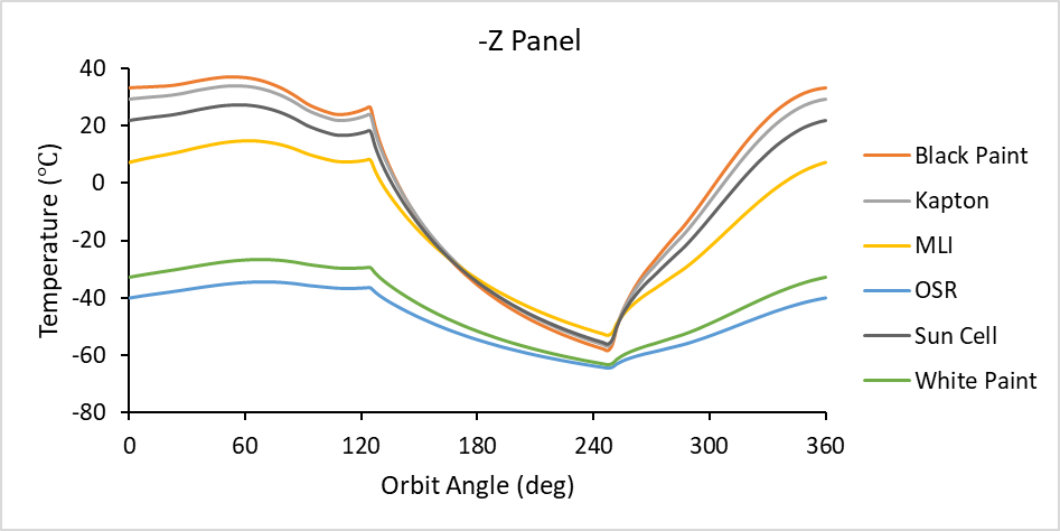

Figure 4.14 Temperature profiles for different coatings of 1U CubeSat at 800 km

4.7 Heat Dissipations

Satellites experience different internal heat dissipations resulted by electronics during their lifespans and the generated internal heat varies depending on types and efficiencies of these electronics. Especially for small satellites, the heat dissipated internally is an important concern for thermal management.

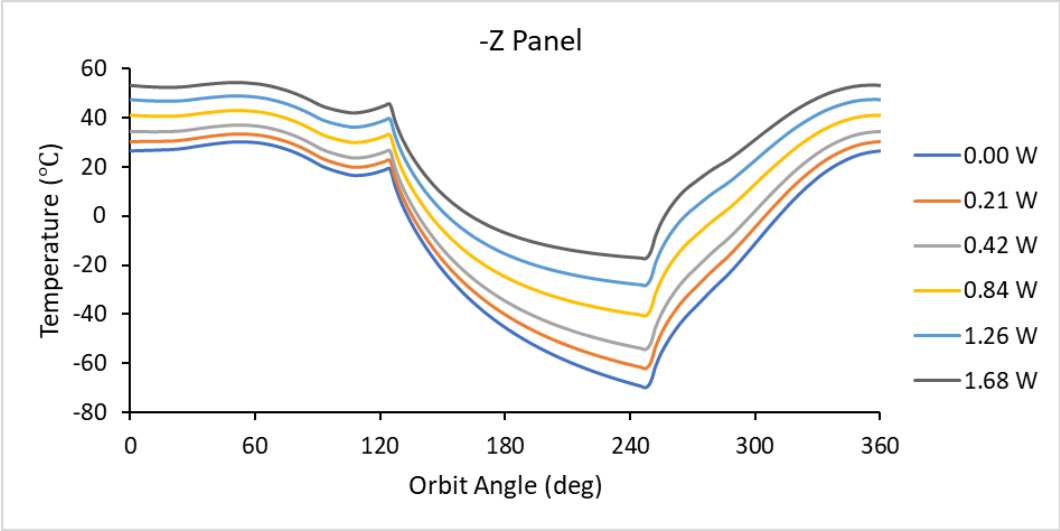

Figure 4.15 Temperature profiles at -Z Panel of 1U CubeSat for different heat dissipations

Therefore, the effect of heat dissipation is simulated by applying equal heats ranging from 0 W to 1.68 W (total 10.08 W for the satellite) to each satellite panels and then evaluated. Temperature profiles at nadir-viewing panel for different internal heats are demonstrated in Figure 4.15 for 1U CubeSat orbiting at an altitude of 800 km. It is presented that applied heat dissipations shift the temperature curves upwards and the influence of dissipated heat is more evident for the eclipse periods. In terms of the satellite thermal management, equipment dissipating heat may be placed near or adjacent to colder panels so that both panels and equipment may be kept within the desired thermal limits for safe and reliable space missions. Moreover, selecting electronics having better efficiencies and adjusting positions of electronics might be considered to optimize the thermal control system.

4.8 Conclusion

This chapter demonstrates the influence of satellite design parameters and orbital configurations on temperature profiles of CubeSat panels by modeling on-orbit conditions and conducting analytical investigations. Thermal analyses are performed by considering conduction in the structural parts of the satellite and radiation in the space thermal environment to understand how thermal behaviors of satellites are changing and the results are examined then.

It is an obvious fact that orbital configurations and different design parameters affect considerably the surface temperatures of CubeSats. A thermal management system that is safe, reliable, and effective can only be established with a full understanding of the heat transfer mechanisms between the satellite and the space thermal environment. That knowledge allows not only to keep the satellite within the desired operating temperature limits in the harsh space environment, but also to optimize the satellite design and orbital properties for longer and more efficient space services. This research can be further extended by including the internal equipment within the satellite and taking heat transfer among them into account.

To conclude, the outcomes of this chapter could support the engineering phase of small satellites in terms of selecting safe and reliable satellite design and orbital configuration.

CHAPTER 5

INVESTIGATION ON THERMAL INFLUENCE OF SOLAR PANEL DEPLOYMENT ANGLE

The studies focusing on CubeSats with deployed solar panels at different angles are extremely limited in the literature. This chapter based on [63] investigates the effects of solar panel deployment angle on radiative heat input for a 3U CubeSat orbiting at low Earth orbit. The solar panel deployment angles of 75, 60, 45, 30, 15, 0, -15, -30, -45, -60 and -75 degrees are modeled and simulated. Orbital positions for different earth days are examined for the 3U CubeSat with fully deployed solar panels. Besides, the heat absorbed by CubeSat panels and its solar panels are analyzed. The results show that solar panel deployment angle affects the satellite heating, and hence maximum heat input occurs at the deployment angle of 15 degrees. It can be here noted that the results may give rise to valuable contribution for optimizing the design and energy budget of CubeSats.

5.1 Introduction

Thermal investigations of CubeSats with deployable solar panels are extremely limited. A thermal analysis model of composite solar arrays with complex structures were simulated for selected two altitudes of 300 km and 35768 km to characterize the thermal response of the whole solar array system subjected to space heat flux [94]. The external heat flux of the solar array in LEO and GEO was covered together with the thermal analysis model incorporating the honeycomb panel, simplified hinges, composite frames, and yokes. The transient temperature fields in various orbits for all components and the impacts of thermal environmental factors on different components were addressed in the study. Additionally, a comparative analysis was conducted on the thermal response of the solar array when constructed with two commonly used materials.

The influence of deployable solar panels on power generation at a picosatellite was examined in another study [95]. The challenges of powering picosatellites with solar

energy, owing to the limited surface area available for solar cells and the intricacy of accurately aligning them with the sun, were examined. A method for achieving more precise calculations of accessible solar power was presented, and the design of efficient and dependable solar panels for CubeSats was described.

A simple thermal design procedure for microsatellites and nanosatellites with deployable solar array panels had been provided by using both two nodal and three nodal analysis methods [33]. The thermal design concepts and passive thermal control techniques used for the thermal design of a microsatellite with a deployable solar array panel were discussed. The steps involved in the two and three nodal thermal analyses of small satellites with deployable solar panels were provided in the flowcharts. The optical property region with reference to thermal design principles and the implementation of passive thermal control techniques were detailed in the study.

A comprehensive thermal analysis was undertaken for two nanosatellite missions, PICSAT and CIRCUS, with a primary focus on ensuring their resilience in harsh space environments [46]. The fundamental principles of heat transfer and the thermal conditions in space, along with simulation techniques, were discussed in the context of analyzing the PICSAT satellite. Two potential failure scenarios associated with the solar panel deployment mechanism were examined and recommendations for ensuring the survivability of the satellite in these circumstances were also offered.

Another study presented [96] the simplified thermal analysis of a 3U CubeSat having photovoltaic panels with different sizes. It was assessed how varying photovoltaic panel areas influence temperature fluctuations in extreme hot and cold scenarios, ensuring that all components remain within acceptable limits.

This chapter focuses on the thermal effects of solar panel deployment angles on thermal heat loads for CubeSats. The deployment angles of 75, 60, 45, 30, 15, 0, -15, -30, -45, -60 and -75 degrees are selected for thermal studies. The impacts of Earth positions orbiting the sun on the heat input received by a CubeSat were also analyzed. Additionally, the cases for various albedo coefficients and Earth surface temperatures were investigated to find out the worst-case scenarios that a satellite may encounter. In that way, the extrema situations were defined among the studied cases.

5.2 Material and Methods

A 3U sized CubeSat that its dimensions are 30 mm x 10 mm x 10 mm is chosen for thermal studies and the panel thickness is 1 mm. The CubeSat panels are aluminum alloy with multi-layer insulation coating while solar panels are honeycomb material with solar cells. The internal heat dissipation of 3.8 W in total was simulated by applying 0.27143 W per unit area to each CubeSat panels. No heat dissipation was applied to solar panels.

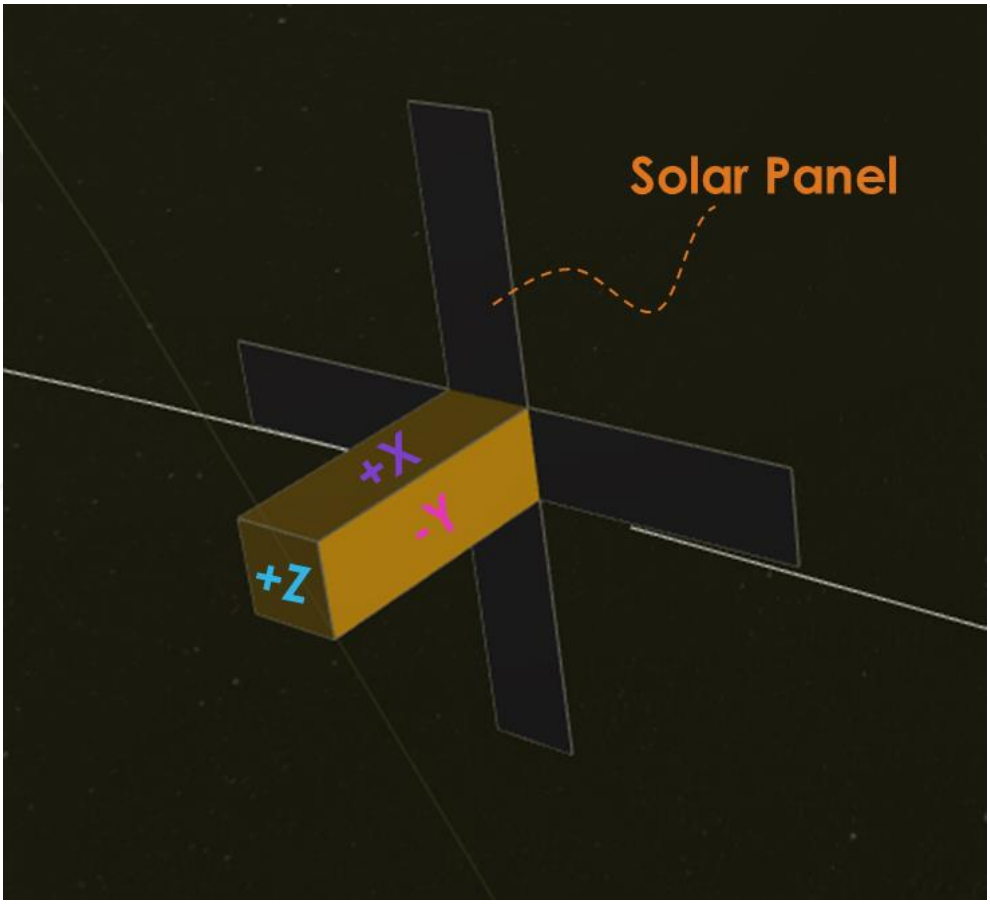

Figure 5.1 Panel directions of 3U CubeSat

The orbits were modeled as sun synchronous low earth orbits. The orbital height of 680 km was selected that is same with the TURKSAT-3USAT [16]. Satellite was modeled, that it moves towards +Y panel and its +Z panel faces the Earth, as illustrated in Figure 5.1 and Figure 5.2.

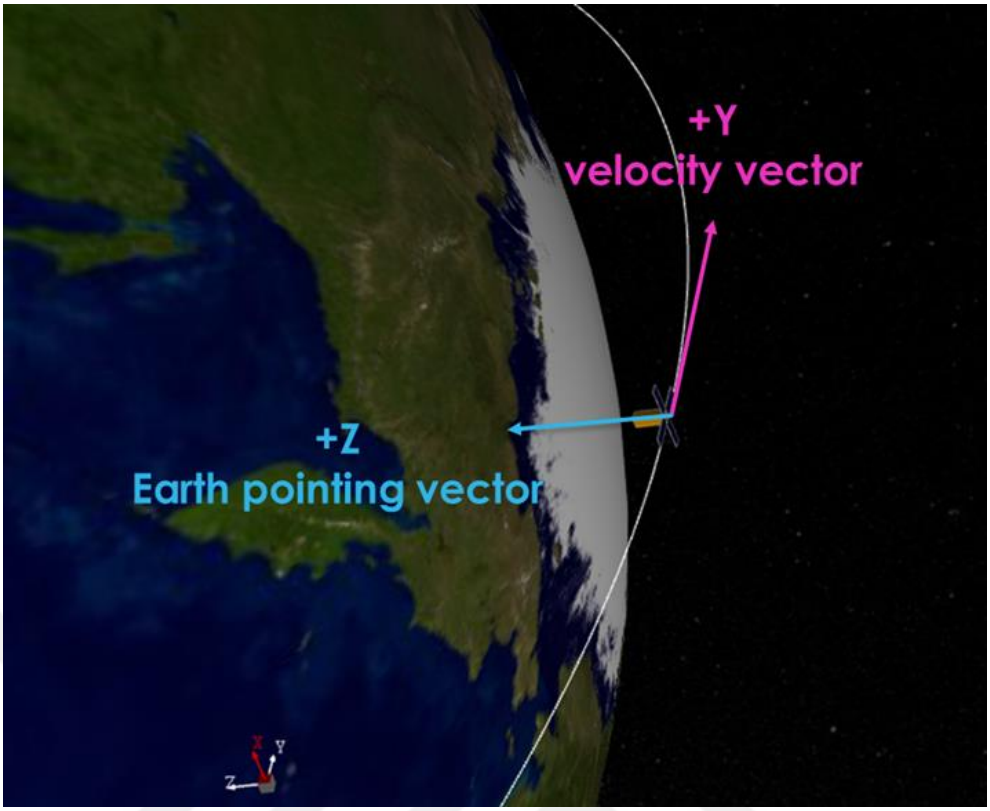

Figure 5.2 Kinematics of 3U CubeSat

Earth orbiting satellites receive heat fluxes varying according to the position of the Earth around the Sun [3]. The simulations were performed for different Earth days, given in Table 5.1.

Table 5.1 Earth days

January 3rd	$\approx 0.983\ AU$; Perihelion
March 20th	Spring Equinox
April 4th	$\approx 1\ AU$
June 21st	Summer Solstice
July 4th	$\approx 1.017\ AU$; Aphelion
September 22nd	Fall Equinox
October 5th	$\approx 1\ AU$
December 21st	Winter Solstice

The heat fluxes of Albedo and Earth infrared radiation are depended on several factors. Hence, the albedo coefficients and the earth surface temperatures, presented in Table 5.2, are examined. The deep space temperature was set to -269 degrees of Celsius.

Table 5.2 Albedo coefficients and earth surface temperatures

T	-25.00 ℃		-20.75 ℃	
a	0.35	0.30	0.25	0.20

CubeSats are modeled with four deployable solar panels at eleven angles, as illustrated in Figure 5.3. Thermal simulations were performed using Systema Thermica to evaluate heat fluxes and their change under parameters of deployment angles, earth days, albedo coefficients and earth surface temperatures.

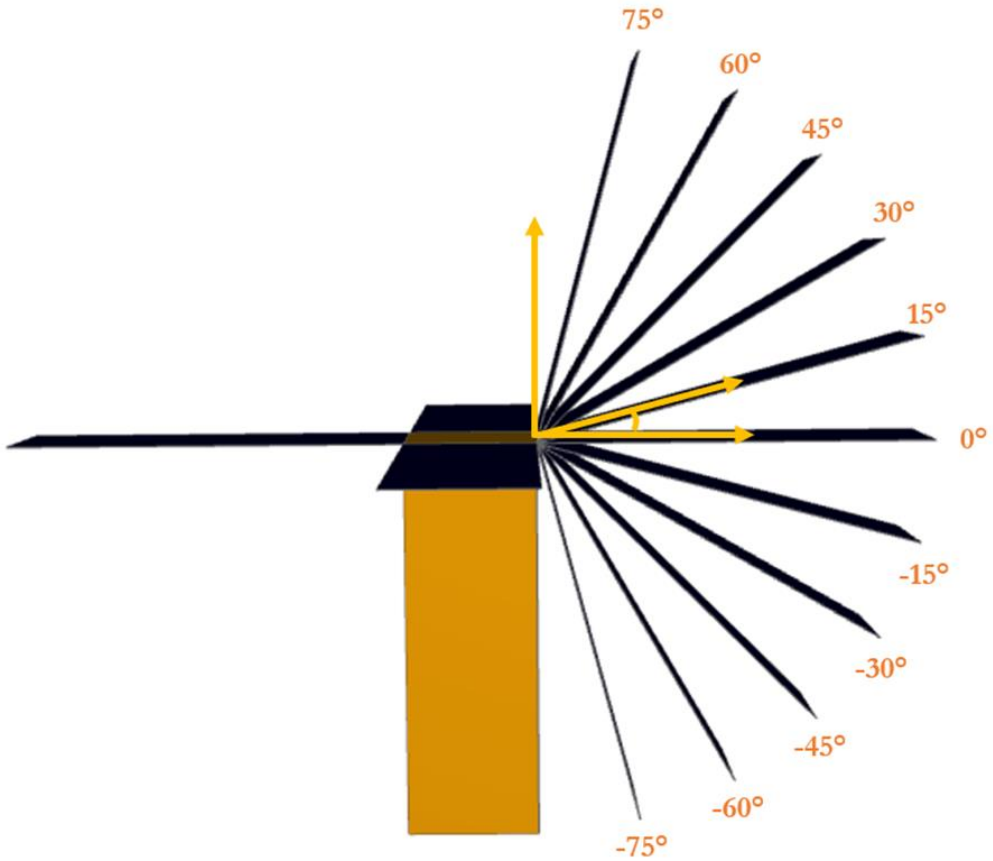

Figure 5.3 Solar panel deployment angle

The amounts of heat absorbed by CubeSat panels, solar panels and the satellite in total were computed separately. The temperature profiles at CubeSat panels and solar panels were also studied.

5.3 Heat Sources

In order to obtain heat loads for on-orbit conditions, several numerical studies were conducted. The change in total absorbed heat by 3U CubeSat with fully deployed solar panels at 0 degree on 3rd of January is exhibited in Figure 5.4. The satellite in the eclipse receives only planetary infrared radiation. It starts to receive heat from solar and albedo radiation together with planetary infrared radiation as leaving the eclipse.

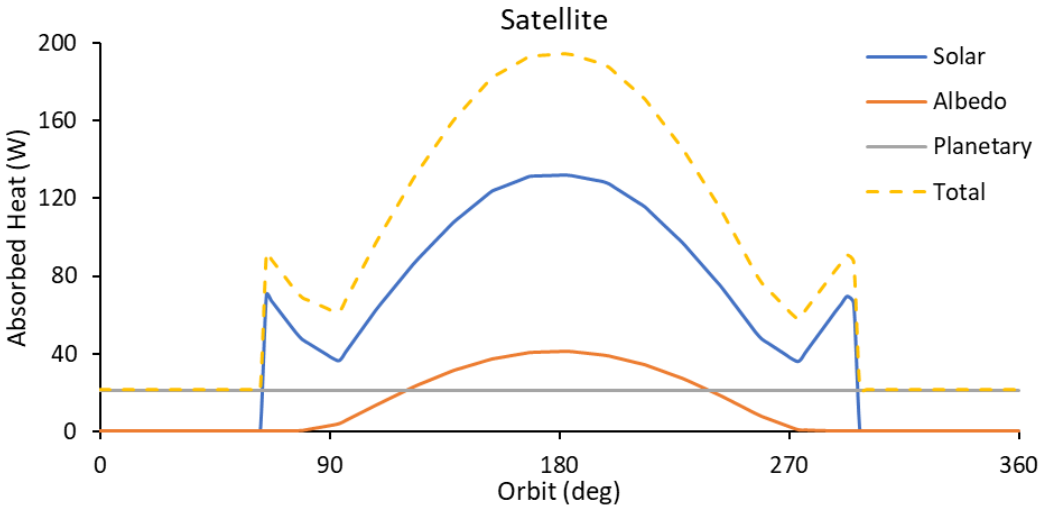

Figure 5.4 Heat absorbed by the satellite per orbit on January 3rd

CubeSat panels and solar panels have different absorbed heat profiles, as shown in Figure 5.5 and Figure 5.6, separately. For illuminated period, the absorbed heat through solar radiation reached the maximum level for solar panels while it reached the minimum for CubeSat panels. That happened because of the orientation of exposed panels and the shadowing impact of solar panels on CubeSat panels.

While the albedo radiation rose for both panels, the planetary infrared radiation remained constant during the orbit. Per orbit 77% of heat inputs from space thermal

environment to the satellite (10.418 kW) was received by solar panels when 23% of that (3.104 kW) was received by CubeSat panels.

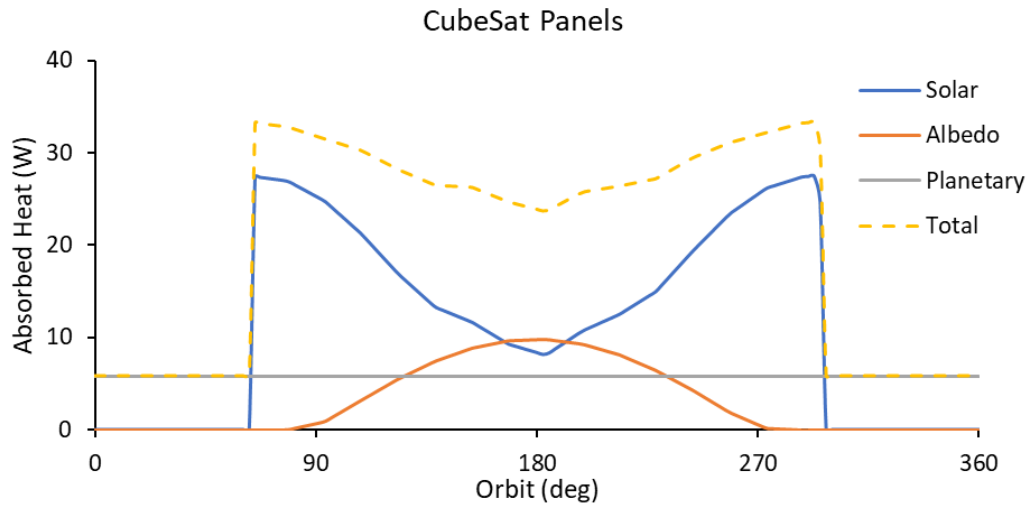

Figure 5.5 Heat absorbed by CubeSat panels per orbit on January 3rd

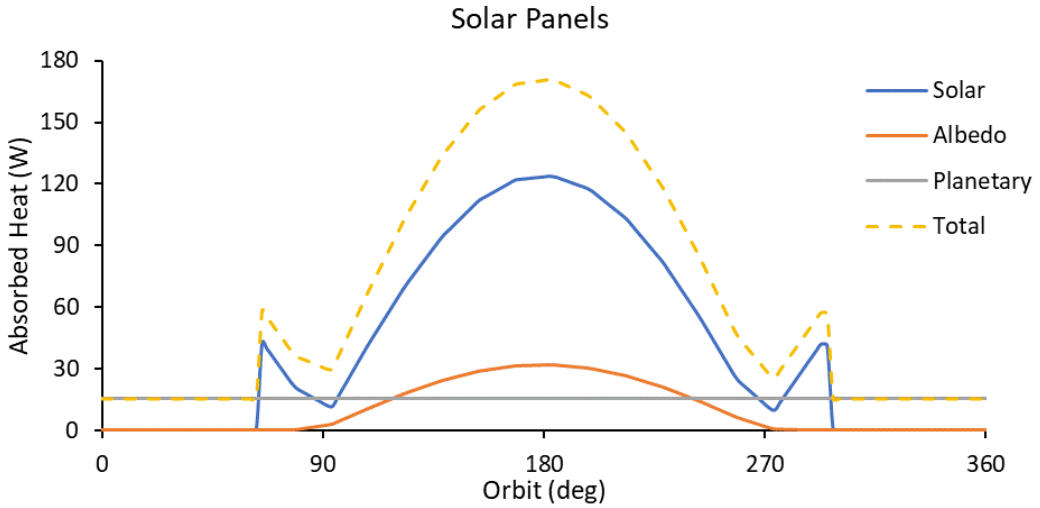

Figure 5.6 Heat absorbed by solar panels per orbit on January 3rd

5.4 Earth Days

According to the position of Earth around the sun, satellites that are servicing around the earth receive different amounts of solar fluxes. The change in solar flux regarding to the earth days is presented in Table 5.3. Solar flux is the maximum on January 3rd

because the earth is at its closest position to the sun. On the other hand, it is minimum on July 4th since the earth is at the farthest.

Table 5.3 Solar fluxes for different earth days

Earth Days	Solar Flux (W/m^2)
Jan 3rd	1418.15
Mar 20th	1382.76
Apr 4th	1371.27
Jun 21st	1327.88
Jul 4th	1326.56
Sep 22nd	1361.39
Oct 5th	1370.80
Dec 21st	1416.98

The earth days influence the received heat for satellites operating in space thermal environment. The amounts of total radiative heat absorbed by the satellite having fully deployed solar panels at an angle of 0 degree are given in Table 5.4 for eight significant days.

Table 5.4 Total absorbed heat by the satellite for different earth days

Earth Days	Total Absorbed Heat (W)			
	Solar	Albedo	Planetary	Total
Jan 3rd	8306.95	1998.28	3217.30	13522.53
Mar 20th	8006.87	1965.47	3217.30	13189.65
Apr 4th	7944.91	1947.79	3217.30	13110.00
Jun 21st	7565.10	1893.49	3217.30	12675.90
Jul 4th	7541.05	1892.37	3217.30	12650.72
Sep 22nd	7979.99	1915.66	3217.30	13112.95
Oct 5th	8044.52	1917.72	3217.30	13179.54
Dec 21st	8375.98	1987.88	3217.30	13581.15

The values of albedo coefficient and the earth surface temperature were set constant in simulations to evaluate the effect of earth days. That caused constant heat input on

satellite panels via earth infrared radiation. However, the heat inputs caused by solar and albedo radiation changed considerably.

The amounts of total incoming radiative heat for both CubeSat and solar panels were found higher for Dec 21st and Jan 3rd while those were lower for June 21st and July 4th. The highest heat energy was achieved on January 3rd for solar panels and on Dec 21st for CubeSat panels. The incoming heat was averaged as 13127.81 W while the greatest difference was calculated as 930.43 W over a year period.

5.5 Deployment Angles

In order to investigate the thermal influence of solar panel deployment angle on satellite heating, CubeSats having 11 different angles varying from -75 to +75, as shown in Figure 5.3, were modeled and simulated. The absorbed total radiative heat profiles were demonstrated in Figure 5.7 over an orbit period. The deployment angle of 0 degree represents fully deployed solar panels horizontally on the top of the CubeSat. The positive deployment angles are for inclined solar panels upward where negative angles are vice versa.

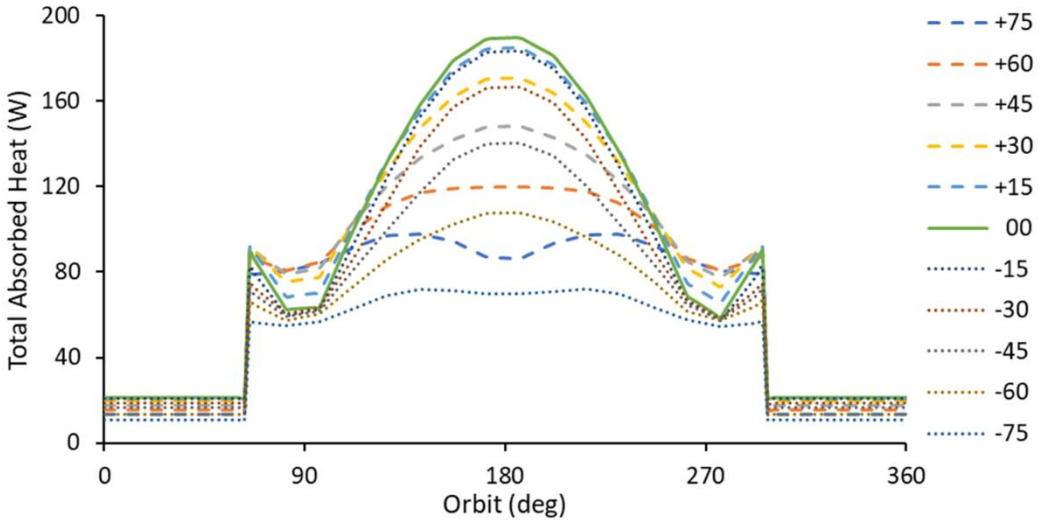

Figure 5.7 Total absorbed heat by the satellite for different deployment angles

The deployment angles changed the view factors; consequently, heat profiles were obtained differently for each angle. The shadowing effect of solar panels on the

CubeSat panels was another reason for varying total heat inputs. The maximum instantaneous heat absorption was achieved for the deployment angle of 0 degree in the middle of the illuminated passage. The angle of -75 degrees, on the other hand, had the minimum instantaneous heat inputs along the orbit compared to other cases.

In addition, the amounts of total heat absorbed by the satellite from different thermal sources in space with respect to the solar panel deployment angles were given in Table 5.5. The analyses were performed by setting the earth day as April 4th to examine the effects of deployment angles.

Table 5.5 Total heat absorbed by the satellite for different deployment angles

Deployment Angles (deg)	Absorbed Total Radiative Heat (W)			
	Solar	Albedo	Planetary	Total
+75	6170.32	1178.17	2027.18	9375.67
+60	7093.76	1393.14	2366.80	10853.70
+45	7690.05	1595.41	2683.79	11969.24
+30	8030.82	1781.16	2972.26	12784.24
+15	8103.52	1908.62	3165.51	13177.65
0	7944.91	1947.79	3217.30	13110.00
-15	7568.37	1884.16	3101.37	12553.89
-30	7028.16	1728.46	2833.96	11590.58
-45	6277.61	1512.72	2469.74	10260.06
-60	5357.53	1271.55	2061.31	8690.38
-75	4237.87	990.31	1595.00	6823.18

Although solar panels received more heat for the angle of 0 degree, the greatest total absorbed heat per orbit was obtained for the deployment angle of +15 degrees. Because the CubeSat panels had less shadowing caused by solar panels for the angle of +15 degrees. The lowest amount of incoming heat was obtained for the angle of -75 degrees. The increase in absolute value of solar panel deployment angle led the decrease in total absorbed heat per orbit, except the case with the angle of +15 degrees.

Finally, radiative heat inputs from space thermal environment were studied for various cases to reveal possible worst-case scenarios. With this purpose, the parameters defined in Table 5.2 and the earth days of January 3rd, October 5th and July 4th were used for thermal simulations. The worst-case analyses were performed for the deployment angles of +15 degrees and -75 degrees where previously the maximum and the minimum amounts of absorbed heat were obtained, respectively. By means of that, it was tried to determine the extreme conditions having the greatest and the lowest heat inputs within the studied parameters.

5.6 Worst-Case Scenario Analysis

The amounts of radiative heat absorbed by the satellite are presented in Table 5.6.

Table 5.6 Worst-Case scenario analysis

Earth Days	Albedo Coefficient	Earth Surface Temperature (°C)	Deployment Angle (deg)	Absorbed Total Radiative Heat (W)			
				Solar	Albedo	Planetary	Total
Jul 4th	0.20	-25.00	+15	7716.1	1059.6	3165.5	11941.3
			-75	3838.5	549.7	1595.0	5983.3
Jul 4th	0.25	-25.00	+15	7716.1	1324.5	3165.5	12206.2
			-75	3838.5	687.2	1595.0	6120.7
Jul 4th	0.30	-25.00	+15	7716.1	1589.4	3165.5	12471.1
			-75	3838.5	824.7	1595.0	6258.2
Jul 4th	0.35	-25.00	+15	7716.1	1854.3	3165.5	12736.0
			-75	3838.5	962.1	1595.0	6395.7
Jul 4th	0.35	-20.75	+15	7716.1	1854.3	3388.0	12958.5
			-75	3838.5	962.1	1707.1	6507.8
Oct 5th	0.35	-25.00	+15	8225.0	1879.1	3165.5	13269.7
			-75	2784.7	786.05	1697.73	5268.4
Jan 3rd	0.35	-20.75	+15	8459.9	1958.07	3388.01	13806.0
			-75	4669.4	1016.16	1707.11	7392.7

For the same earth day and the same earth surface temperature, the higher albedo coefficients increased the incoming heat through the albedo radiation, and the total heat input, accordingly. The increase in earth surface temperature caused the increase in absorbed heat amount through the planetary infrared radiation under the condition with the same earth day and the same albedo coefficient. Changing only the earth day effected the heat received through solar and albedo radiation mechanisms.

5.7 Conclusion

This chapter investigates the influences of solar panel deployment angle on radiative heat input for a 3U CubeSat orbiting at low Earth orbit. To reveal how satellite heating is influenced with respect to the solar panel deployment angle, the solar panel deployment angles of 75, 60, 45, 30, 15, 0, -15, -30, -45, -60, and -75 degrees were studied by modeling a 3U CubeSat with fully deployed solar panels. Besides, various satellite positions on orbit on different Earth days are analyzed to find out how heat budget of a satellite changes. The results demonstrated that solar panel deployment angle is highly significant on the satellite heating and maximum heat input occurs at the deployment angle of 15 degrees. It is believed that the outcomes might be valuable for designing CubeSats with deployable solar panels and managing their thermal performance. This research can be extended with further studies to evaluate the panel temperature distributions and to estimate the available solar energy that can be harnessed by solar panels.

CHAPTER 6

DEVELOPMENT OF A SPREADSHEET ANALYSIS TOOL FOR THERMAL TESTING OF CUBESATS

The successful operation of satellites in space relies on effective thermal design, which must account for both extreme temperature conditions and rapid temperature fluctuations. These challenges can generate significant thermal stresses that may potentially harm satellite components and the satellite itself. In order to guarantee the secure functioning of satellites in space, it is imperative to develop a numerical thermal simulation tool capable of offering reasonably precise forecasts of temperature distributions during the early phases of design. First, the studies on the development of numerical tools for thermal analysis of satellites are presented in this chapter. After introducing the PiriSat, a 6U CubeSat used in thermal studies related to tool verifications, the developed analysis tool within an Excel-based spreadsheet solver, called TheSpAn - Thermal Spreadsheet Analyzer for satellites in thermal vacuum chamber, is explained in detail. The thermal results obtained by the tool compared to the data of thermal testing and thermal analysis using commercial software.

6.1 Introduction

Maintaining the temperature of a satellite is of utmost importance for the success of space missions. Each component within the spacecraft must adhere to specified temperature limits, encompassing both operational and non-operational ranges. These limits are not mere technicalities; they are critical to the functionality and survivability of the spacecraft. At the heart of thermal management in satellites lies the thermal control system, a sophisticated and meticulously engineered subsystem tasked with the responsibility of ensuring that every component operates within the specified temperature bounds. To ensure the efficacy of this thermal control system, it is crucial to conduct precise thermal modeling throughout the satellite design and testing phases.

In the complex and rigorous world of satellite design, the evaluation of component temperatures and thermal analyses is an ongoing and iterative process. At every stage

of satellite development, from the initial conceptualization to the final pre-launch preparations, engineers and scientists meticulously assess the thermal characteristics of various satellite elements. This process is essential to validate that each component can endure the harsh temperature variations experienced during the mission.

Numerous sophisticated commercial software tools designed to facilitate extensive thermal analysis of satellites are offered by the aerospace industry. These tools are indispensable aids for predicting and optimizing thermal performance to ensure satellites serve at optimally serviced and remain operational in space conditions. Although they are highly effective for meeting the demands of advanced stages in satellite development, they might not propose the most advantageous solutions during the initial stages because of being costly and complex. Moreover, constructing accurate and safe satellite models when relying solely on human computation are challenging. As a result, organizations operating within the space industry commonly create their own proprietary tools to facilitate the satellite thermal analysis procedure in preliminary phases.

ThermXL, which became available by Thomas et al [97, 98], marked a significant development by being the first thermal analysis tool fully integrated into a spreadsheet. It is an integrated tool within MS Excel that functions as a generic environment provider and a thermal lumped parameter network solver. It also comes equipped with predefined routines for conducting analyses in both steady-state and transient conditions, employing the widely accepted finite difference method. Separate worksheets are designated to store the node information and each specific type of conductive link, including linear for simulating solid and convective heat transfer, radiative, which is influenced by the fourth power of temperature differences.

SatTherm is a thermal analysis tool designed for small spacecraft, developed by Allison et al [99] through a collaboration between the Mission Design Center at NASA Ames and San Jose State University. This tool employs the finite difference method to calculate the time-dependent temperatures of various components within spacecraft. It relies on MATLAB and Excel for its operation. It is essentially a combination of MATLAB scripts seamlessly integrated with an Excel user interface, with this

integration made possible through the utilization of the MATLAB toolbox known as Excel Link.

An in-house computer code based on Thermal Network Method was built by Turkish Aerospace Industries, Inc. [100] to predict the thermal behavior of satellites in extreme space conditions. The code was employed the Method of Lines for solving energy transfer equations. It was used to analyze a test scenario featuring a satellite in orbit around the Earth at an altitude of 700 km and achieved a good confidence.

Satellite Thermal Modeling Software (STMS) was developed by Shirazi and Mirshams [101], using MATLAB GUI, for the purpose of designing and analyzing a satellite model. The thermal analysis of a satellite with specific configuration and thermophysical properties is compared in the STMS software and SatTherm software.

6.2 Overview of PiriSat – 6U CubeSat

The PiriSat is a Turkish 6U CubeSat, currently under development by STM Defense Technologies Engineering and Trade Inc. to operate within Low Earth Orbit, with the primary objective of delivering space-based Automatic Identification System (AIS) data. The core function of this satellite primarily involves showcasing the capabilities of AIS. An exterior view of PiriSat is given in Figure 6.1.

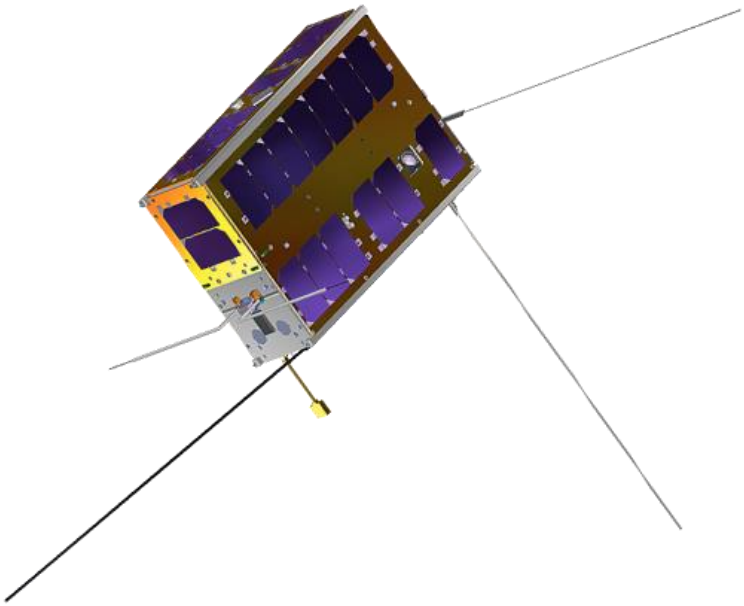

Figure 6.1 An exterior illustration of PiriSat

This involves receiving AIS signals while in orbit, recording these signals, transmitting the gathered data back to the ground station, and conducting data processing to identify vessels. In addition to its primary objective, PiriSat will also accommodate various secondary payloads, including an X-ray detector, a linear transponder, a Langmuire probe, and instruments for measuring radiation levels.

Table 6.1 Technical specifications of PiriSat

Core Mission	Space-Based AIS Data Detection
Mission Lifespan	A minimum of 1 year with no propulsion system
Configuration	6U CubeSat
Coverage	Global coverage between 80°N - 80°S latitude
Orbit	Sun synchronous orbit
Satellite Mass	A maximum of 10 kg
Power Systems	Solar cells and batteries
Payload Volume	2U
Payload Mass	A maximum of 4 kg

PiriSat operates with its capacity to execute diverse satellite missions within the framework of a nano-satellite platform aligned with 6U cube satellite standards. It possesses a set of skills and proficiencies encompassing mission and satellite design and analysis, system integration and testing, software, and hardware development, as well as satellite communication. Furthermore, it will function as a prototype for acquiring historical data to support the development of future multi-satellite missions. Technical specifications of PiriSat are provided in Table 6.1.

The CubeSat consists of 31 structural components. These are frames, ribs and panels positioned on three directions of X, Y and Z.

An interior demonstration of PiriSat is given in Figure 6.2. Inside the satellite, on the other hand, there are 26 pieces of equipment, including power batteries, battery electrical power systems, satellite data control systems, heat sinks, satellite automatic

identifier systems, communication systems, orbit and altitude determination control systems, satellite reaction wheels, star sensors, and satellite antennas.

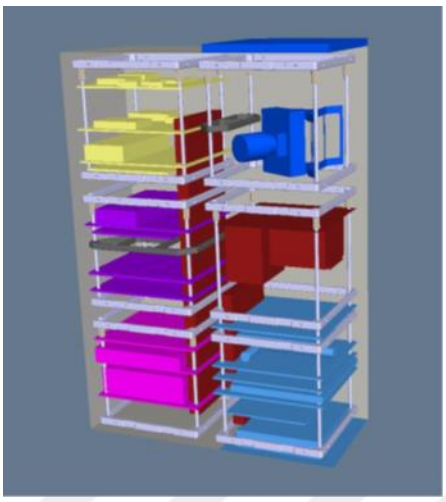

Figure 6.2 Interior demonstration of PiriSat

6.3 Thermal Testing of PiriSat

The assessment of the PiriSat 6U CubeSat involved subjecting it to testing within a thermal vacuum chamber, which is a controlled environment for simulating the harsh conditions of space. Within the chamber, there were specific components utilized to simulate the thermal interactions between the chamber and the satellite. These components included one shroud cylinder and two disks, strategically positioned to replicate the heat exchange mechanisms between the satellite and its external environment.

The testing procedure consisted of two distinct cycles. In the first cycle, known as the hot cycle, the surface temperatures of the thermal vacuum chamber were deliberately elevated to 50℃. This elevated temperature was chosen to replicate the conditions of the satellite being exposed to a high-temperature environment. Conversely, in the second cycle, referred to as the cold cycle, the surface temperatures of the chamber were adjusted to a frigid -20℃. This extreme cold temperature emulated the exposure of the satellite to sub-zero temperatures in space. Through these carefully controlled test cycles, the performance of the PiriSat 6U CubeSat and thermal responses were rigorously evaluated under varying thermal conditions.

6.4 TheSpAn - MS Excel Based Analysis Tool

The spreadsheet solver tool, called TheSpAn, was created on MS Excel platform to predict the thermal performance of CubeSats for thermal testing in preliminary phases. It was aimed to develop a tool fast and accurate enough for analyzing thermal behavior of small satellites under TVC test conditions.

The tool, TheSpAn, has 8 sheets including “Home” for main parameters, “C” for the capacitance values, “Qint” for internal heat dissipation values, “GL” for conductive coupling values, “GR” for radiative coupling values, “TSolver” for calculations, “Results” for results, and “Graph” for graphical presentations.

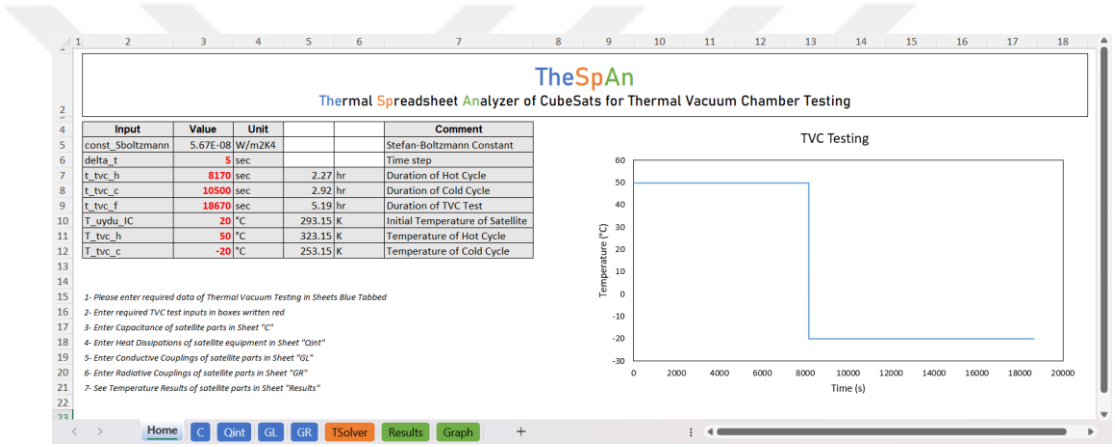

Figure 6.3 Home sheet of TheSpAn

A view for Home sheet of TheSpAn is presented in Figure 6.3. In Home sheet, time step for calculation, durations of hot and cold cycles, the initial temperature values of satellite items, temperature values of hot and cold cycles can be introduced. The test cycles are illustrated in a temperature-time graph for visualization of the test.

The satellite items are introduced in C sheet and their capacitances are defined here while introduced items are appeared on all sheets automatically. The capacitance values are defined as a function of mass and specific heat as in Equation 6.2.

Only some equipment leads to heat generation, therefore their internal heat dissipation values are also specified in Qint sheet. The current version of TheSpAn considers only

constant internal dissipation from the satellite items. In terms of TVC testing, safe modes of satellites can be assessed by turning internal heat dissipation on and off.

	1	15	16	17	18	19	20
1	**GL (W/K)**	-X_1U_FRAME_5	-X_1U_FRAME_6	+Y_FRAME	-Y_FRAME	+X_RIB_1	+X_RIB_2
15	-X_1U_FRAME_5	0.000	0.000	0.100	0.250	0.000	0.000
16	-X_1U_FRAME_6	0.000	0.000	0.250	0.250	0.000	0.000
17	+Y_FRAME	0.100	0.250	0.000	0.000	0.520	0.520
18	-Y_FRAME	0.250	0.250	0.000	0.000	0.520	0.520
19	+X_RIB_1	0.000	0.000	0.520	0.520	0.000	0.000
20	+X_RIB_2	0.000	0.000	0.520	0.520	0.000	0.000
21	+X_RIB_3	0.000	0.000	0.520	0.520	0.000	0.000
22	+X_RIB_4	0.000	0.000	0.520	0.520	0.000	0.000
23	-X_RIB_1	0.000	0.000	0.520	0.520	0.000	0.000
24	-X_RIB_2	0.000	0.000	0.520	0.520	0.000	0.000
25	-X_RIB_3	0.000	0.000	0.520	0.520	0.000	0.000
26	-X_RIB_4	0.000	0.000	0.520	0.520	0.000	0.000
27	+Z_RIB_1	0.000	0.000	0.260	0.260	0.000	0.000
28	+Z_RIB_2	0.000	0.000	0.235	0.235	0.000	0.000
29	-Z_RIB_1	0.000	0.000	0.260	0.260	0.000	0.000
30	+X_PANEL	0.000	0.000	0.000	0.000	0.150	0.150
31	-X_EARTH_PANEL	0.000	0.000	0.000	0.000	0.000	0.000
32	+Y_PANEL	0.000	0.000	0.500	0.000	0.000	0.000
33	-Y_PANEL	0.000	0.000	0.000	0.500	0.000	0.000
34	+Z_PANEL	0.000	0.000	0.250	0.250	0.000	0.000
35	-Z_PANEL	0.000	0.000	0.250	0.250	0.250	0.000
36	POWER_BAT	0.000	0.000	0.000	0.000	0.000	0.000
37	POWER_EPS	0.000	0.000	0.000	0.000	0.000	0.000
38	CDHS_SMC	0.000	0.000	0.000	0.000	0.000	0.000
39	CDHS_OBC	0.000	0.000	0.000	0.000	0.000	0.000
40	CDHS_NANOSATPRO	0.000	0.000	0.000	0.000	0.000	0.000
41	HEAT_SINK_UHF	0.000	0.000	0.000	0.000	0.000	0.000

Home C Qint GL GR TSolver Results

Figure 6.4 GL sheet of TheSpAn

In terms of conduction, the conductive couplings are being introduced to TheSpAn in GL sheet, shown in Figure 6.4 for the satellite items whose surface are in contact.

	1	30	31	32	33	34	35
1	**GR (m^2)**	+X_PANEL	-X_EARTH_PANEL	+Y_PANEL	-Y_PANEL	+Z_PANEL	-Z_PANEL
30	+X_PANEL	0.0000000	0.0000227	0.0007190	0.0003654	0.0001961	0.0001052
31	-X_EARTH_PANEL	0.0000227	0.0000000	0.0008722	0.0004459	0.0000437	0.0000012
32	+Y_PANEL	0.0007190	0.0008722	0.0000000	0.0006701	0.0003067	0.0001346
33	-Y_PANEL	0.0003654	0.0004459	0.0006701	0.0000000	0.0001760	0.0000703
34	+Z_PANEL	0.0001961	0.0000437	0.0003067	0.0001760	0.0000000	0.0000011
35	-Z_PANEL	0.0001052	0.0000012	0.0001346	0.0000703	0.0000011	0.0000000
36	POWER_BAT	0.0008626	0.0000061	0.0010445	0.0005253	0.0000000	0.0007926
37	POWER_EPS	0.0005155	0.0000000	0.0006324	0.0003100	0.0000000	0.0000095
38	CDHS_SMC	0.0004520	0.0000000	0.0005650	0.0003155	0.0000010	0.0000028
39	CDHS_OBC	0.0005058	0.0000045	0.0006046	0.0003134	0.0000000	0.0000019
40	CDHS_NANOSATPRO	0.0005268	0.0000077	0.0005983	0.0003018	0.0000034	0.0000006
41	HEAT_SINK_UHF	0.0000677	0.0000005	0.0001024	0.0000481	0.0000000	0.0000000
42	UHF_VHF	0.0006922	0.0000146	0.0006929	0.0003461	0.0000019	0.0000012
43	HEAT_SINK_S	0.0000726	0.0000007	0.0001085	0.0000549	0.0000000	0.0000000
44	S_BANT	0.0005811	0.0000123	0.0005582	0.0002796	0.0000086	0.0000012
45	EXPERIMENTAL_AIS	0.0004988	0.0000196	0.0007195	0.0003979	0.0000460	0.0000000
46	AIS	0.0004880	0.0000356	0.0006741	0.0003406	0.0017709	0.0000000
47	LANGMUIR_PLATE	0.0000014	0.0000508	0.0000524	0.0000258	0.0000000	0.0000000
48	LANGMUIR_BOARD	0.0000119	0.0004220	0.0005270	0.0002464	0.0000000	0.0000348
49	ADCS_COMPUTER	0.0000000	0.0003461	0.0004737	0.0002213	0.0000000	0.0000410
50	ADCS_COIL	0.0000000	0.0002283	0.0002327	0.0001123	0.0000000	0.0000000
51	ADCS_SENSE	0.0000000	0.0001741	0.0002386	0.0001405	0.0000000	0.0000072
52	ADCS_CONTROL	0.0000000	0.0004175	0.0005448	0.0002572	0.0000000	0.0000032
53	GPS	0.0000000	0.0000399	0.0000493	0.0000144	0.0000000	0.0000000
54	ADCS_CONNECT	0.0000000	0.0006458	0.0007774	0.0003924	0.0000037	0.0000025
55	REACTION WHEEL 1	0.0000000	0.0001700	0.0001286	0.0000079	0.0000000	0.0000000
56	REACTION WHEEL 2	0.0000000	0.0000911	0.0000179	0.0001340	0.0000000	0.0000000

Home C Qint GL GR TSolver Results

Figure 6.5 GR sheet of TheSpAn

Similarly, the radiative couplings between satellite nodes are being defined in GR sheet, illustrated in Figure 6.5 to consider radiative heat transfer.

Basically, a square matrix sized by satellite nodes is utilized in both GL an GR sheets in order to define these thermal couplings. Conductive couplings can be estimated by multiplying the effective conductivity by the effective heat transfer area and dividing it by the effective distance between nodes. Radiative couplings, on the other hand, can be estimated by multiplying the radiative exchange factor, the emissivity, and the surface area. However, the coupling values to define into TheSpAn should be either estimated manually or retrieved from another software performing this task.

The walls of TVC were simulated with three nodes as TVC Shroud Cylinder, TVC Shroud Disk 1 and TVC Shroud Disk 2 in the tool. These are only in thermal relation with satellite elements facing outside. Radiative coupling calculations between the satellite and the TVC were conducted based on the radiative exchange factor values. On the other hand, there are no values of capacitance, internal heat dissipation or conductive coupling since the heat transfer between the satellite and the TVC occurs only through the radiation.

	1	30	31	32	33	34	35	36	37
1	Time (s)	+X_PANEL	-X_EARTH_PANEL	+Y_PANEL	-Y_PANEL	+Z_PANEL	-Z_PANEL	POWER_BAT	POWER_EPS
2	0	20.000	20.000	20.000	20.000	20.000	20.000	20.000	20.000
3	5	20.142	20.101	20.122	20.245	20.013	20.169	20.006	20.027
4	10	20.280	20.199	20.244	20.487	20.025	20.327	20.012	20.054
5	15	20.416	20.295	20.364	20.725	20.037	20.475	20.018	20.081
6	20	20.549	20.389	20.483	20.961	20.049	20.613	20.025	20.107
7	25	20.680	20.480	20.601	21.194	20.060	20.744	20.031	20.133
8	30	20.808	20.569	20.717	21.424	20.072	20.868	20.038	20.159
9	35	20.934	20.656	20.833	21.651	20.085	20.985	20.045	20.184
10	40	21.058	20.742	20.948	21.875	20.098	21.097	20.052	20.210
11	45	21.179	20.826	21.061	22.097	20.112	21.202	20.060	20.236
12	50	21.299	20.908	21.174	22.316	20.126	21.303	20.068	20.261
13	55	21.417	20.988	21.286	22.533	20.142	21.399	20.076	20.287
14	60	21.532	21.068	21.397	22.747	20.158	21.490	20.084	20.313
15	65	21.646	21.145	21.507	22.958	20.175	21.578	20.092	20.339
16	70	21.758	21.222	21.616	23.167	20.194	21.662	20.100	20.366
17	75	21.868	21.297	21.724	23.373	20.213	21.743	20.109	20.392
18	80	21.977	21.372	21.831	23.577	20.233	21.821	20.118	20.418
19	85	22.083	21.445	21.937	23.778	20.254	21.897	20.127	20.445
20	90	22.189	21.517	22.043	23.977	20.277	21.969	20.136	20.472
21	95	22.292	21.588	22.147	24.174	20.300	22.040	20.146	20.499
22	100	22.394	21.658	22.251	24.368	20.324	22.108	20.155	20.526
23	105	22.495	21.727	22.354	24.560	20.350	22.175	20.165	20.554
24	110	22.594	21.796	22.457	24.750	20.376	22.240	20.175	20.581
25	115	22.692	21.864	22.558	24.938	20.404	22.303	20.185	20.609
26	120	22.789	21.930	22.659	25.124	20.432	22.365	20.195	20.637
27	125	22.884	21.996	22.759	25.307	20.461	22.425	20.206	20.664
28	130	22.978	22.062	22.858	25.488	20.491	22.484	20.216	20.693
29	135	23.071	22.127	22.956	25.667	20.523	22.542	20.227	20.721

Home C Qint GL GR TSolver Results Graph

Figure 6.6 Results sheet of TheSpAn

The calculations are run in TSolver sheet and finally the results are presented in Results sheet of TheSpAn, as demonstrated in Figure 6.6. All temperature data with respect to

time is presented in this sheet for each satellite item included in the simulation of thermal testing.

An illustration is given in Figure 6.7 for Graph sheet of TheSpAn. It provides a graphical demonstration how the thermal behavior of the selected satellite item varies with respect to time. Moreover, over a test period, the maximum, minimum and average temperature values for a particular item are presented in a table together with the temperature gradient. This helps one to visualize the thermal range and profile easily and quickly experienced by a selected satellite item, within the defined test period and parameters.

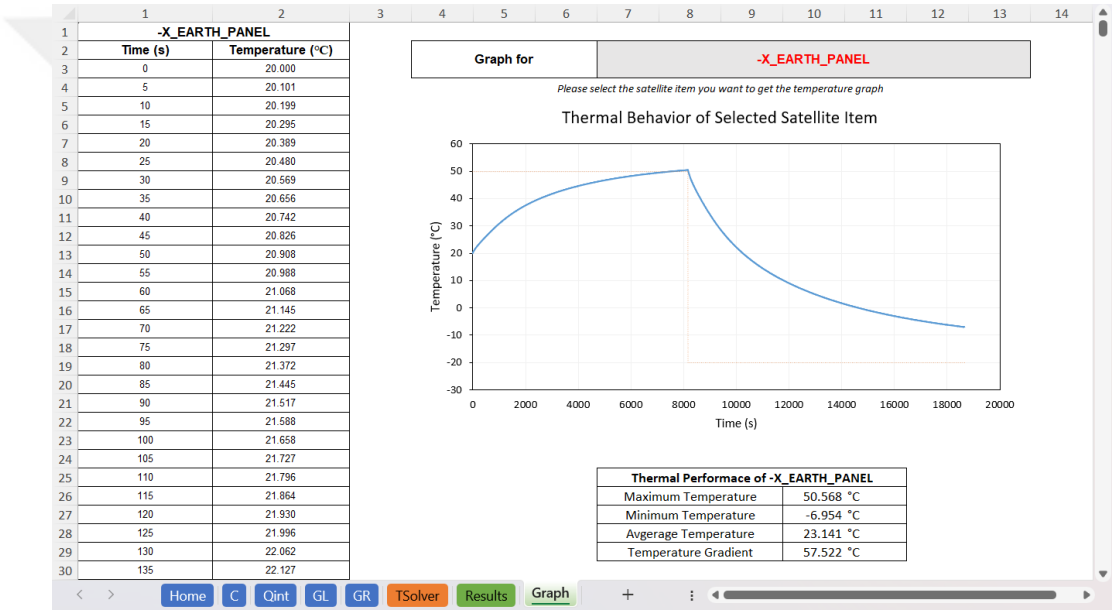

Figure 6.7 Graph sheet of TheSpAn

In brief, TheSpAn, containing 60 nodes, was developed based on MS spreadsheets to perform thermal testing of small satellites so that it was possible to simulate various scenarios and equipment at low cost in the preliminary design phase before going for real TVC testing that is quite expensive.

6.5 Numerical Background of TheSpAn

The energy balance for each node is solved by applying explicit finite difference methods to find the rate of temperature change. A forward differencing scheme is used

to calculate temperatures at node points. The reason for using explicit forward differencing scheme is that this approach is easy to implement, requires less computation times and is faster when compared to other approaches. This scheme establishes the solution for a finite difference model used to approximate the behavior of a physical object. In this approach, it is assumed that the nodes are isothermal and physical properties are considered constant within each node. The links between nodes are maintained by conduction and/or radiation. A finite difference mesh is constructed through the transforming partial differential equations into finite difference equations [22]. The discretization of space and time within a finite difference grid is illustrated in Figure 6.8.

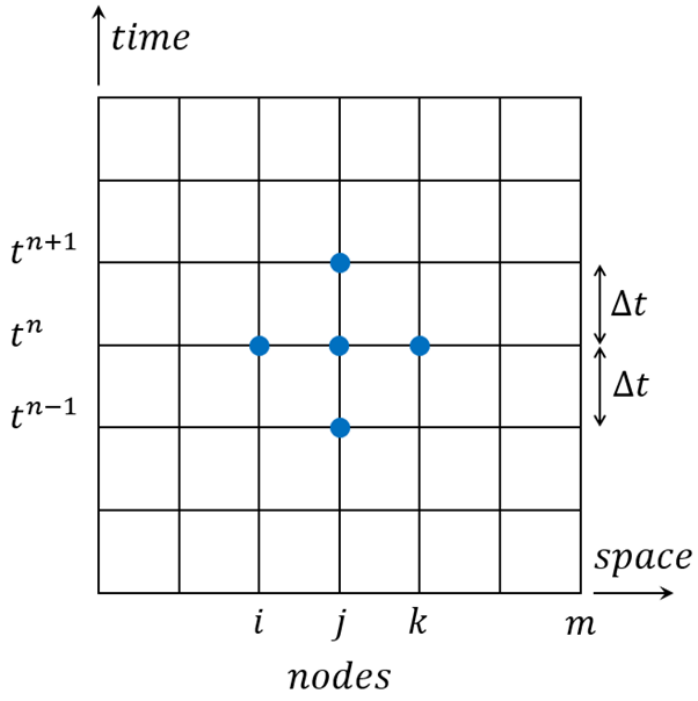

Figure 6.8 Discretization of space and time within a finite difference grid

The energy balance equation can be presented as shown is Equation 6.1 where C is capacitance, T is temperature, t is time, Q is the receiving heat, σ is the Stefan-Boltzmann constant while GL and GR are conductive and radiative couplings between node i and j, respectively.

$$C_i \frac{\partial T_i}{\partial t_i} = \sum_{j=1}^{n} GL_{ij}\left(T_j - T_i\right) + \sigma \sum_{j=0}^{n} GR_{ij}\left({T_j}^4 - {T_i}^4\right) + Q_i \qquad \textbf{(6.1)}$$

The capacitance of node i can be defined as the product of density, volume, and specific heat, and it can alternatively be expressed as the product of mass and specific heat, as in Equation 6.2.

$$C_i = \rho \cdot \Delta x \cdot \Delta y \cdot \Delta z \cdot C_p = m_i \cdot C_p \quad \textbf{(6.2)}$$

The time derivative can be approximated, as in Equation 6.3, with θ serving as a variable-weighted implicit factor, and the forward-explicit, Crank-Nicolson, and backward-implicit approximations can be obtained for θ values of 0, ½, and 1, respectively [22].

$$T_i(t+\Delta t) = T_i(t) + \theta \cdot \frac{\partial T_i}{\partial t_i}\Big|_{t+\Delta t} \cdot \Delta t + (1-\theta) \cdot \frac{\partial T_i}{\partial t_i}\Big|_{t} \cdot \Delta t \quad \textbf{(6.3)}$$

The MS Excel-based analysis tool in this study is created by using forward-explicit approach, taking the value of θ as 0. Hence, it can be written as in Equation 6.4.

$$C_i \frac{T_i(t+\Delta t) - T_i(t)}{\Delta t} = \sum_{j=1}^{m} GL_{ij}\left(T_j(t) - T_i(t)\right) + \sigma \sum_{j=0}^{m} GR_{ij}\left(T_j(t)^4 - T_i(t)^4\right) + Q_i(t) \quad \textbf{(6.4)}$$

The energy balance equation can be further represented as given in Equation 6.5 by utilizing forward-explicit scheme.

$$T_i(t+\Delta t) = T_i(t) + \frac{\Delta t}{C_i}\left[\sum_{j=1}^{m} GL_{ij}\left(T_j(t) - T_i(t)\right) + \sigma \sum_{j=0}^{m} GR_{ij}\left(T_j(t)^4 - T_i(t)^4\right) + Q_i(t)\right] \quad \textbf{(6.5)}$$

The receiving heat at node i is defined as the summation of heat loads transferred to the node from external and internal sources, as shown in Equation 6.6. It should be noted that the heat transfer among nodes is considered through conductive and/or radiative terms in Equation 6.5.

$$Q_i(t) = Q_{Solar,i}(t) + Q_{Albedo,i}(t) + Q_{EarthIR,i}(t) + Q_{Internal,i}(t) \quad \textbf{(6.6)}$$

Future, present, and past time can be denoted by $n+1$, n, and $n-1$, respectively as in Equation 6.7.

$$t^{n+1} - \Delta t = t^{n} = t^{n-1} + \Delta t \quad \textbf{(6.7)}$$

Eventually, the energy balance equation yields to the discrete-time representation of the satellite thermal system as in Equation 6.8 and this form is used in the solver tool.

$$T_{i,n+1} = T_{i,n} + \frac{\Delta t}{C_i}\left[\sum_{j=1}^{m} GL_{ij}\left(T_{j,n} - T_{i,n}\right) + \sigma \sum_{j=0}^{m} GR_{ij}\left({T_{j,n}}^{4} - {T_{i,n}}^{4}\right) + Q_{i,n}\right] \quad \textbf{(6.8)}$$

This equation can be utilized to simulate the transient thermal characteristics of a satellite. It enables the monitoring the temperature changes of each element over time through diverse heat transfer mechanisms. Based on known temperatures, all other temperature values with respect to time for each node can be estimated by means of this form.

The computer that operates the spreadsheet solver, TheSpAn, was equipped with the Windows 11 Home operating system, designed for 64-bit architecture. It boasted an 11th Generation Intel Core i7 processor, providing robust computing power for efficient calculations. Additionally, the computer was outfitted with a substantial 16 GB of installed random access memory, ensuring sufficient memory resources for smooth and responsive performance while running the solver.

6.6 Results

In order to validate TheSpAn, the developed tool, the aim was to evaluate its performance by comparing data from both a commercial software and an actual TVC test as well as to examine the results obtained by TheSpAn whether fall within an acceptable range when compared to them. For this purpose, statistical approach and graphical analyzes were applied.

First, the thermal results of a hypothetical satellite were created by means of SINDA, the commercial software for satellite thermal modeling. This hypothetical satellite consisted of 7 structural elements that are six satellite panels and one solar panel mounted on one of the panels, and 8 equipment. In this simple case, a hot thermal cycle of 50℃ for a period of 10,000 seconds was considered. The initial temperature values

of satellite elements were set to 20°C. Internal heat dissipations were applied as 3.00 W for EQ2, 1.00 W for EQ3, 2.00 W for EQ7 and 0.75 W for EQ8, in the imaginary model. Conduction heat transfer was considered between structural elements to structural elements as well as between structural elements to equipment. The values of capacitances, conductive and radiative couplings were taken from the software into TheSpAn.

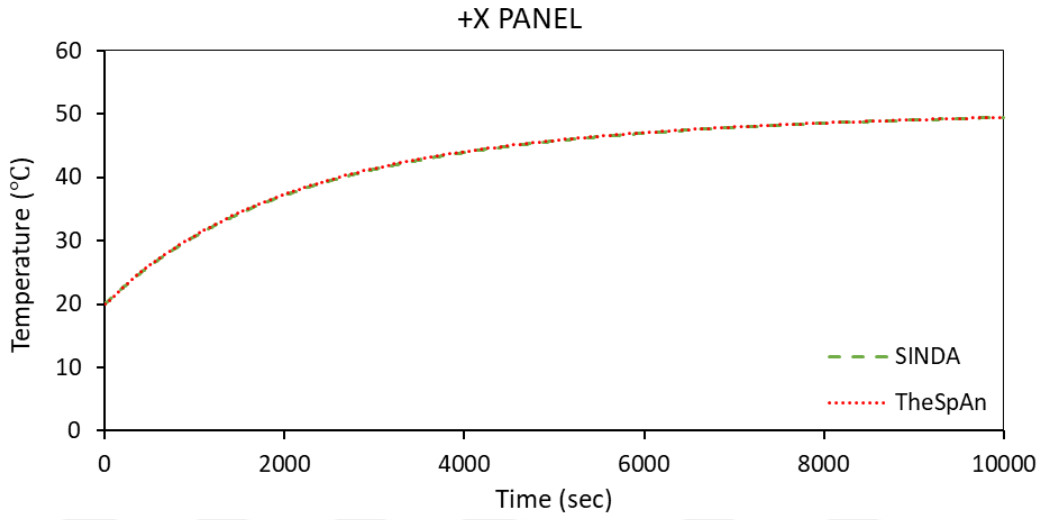

Figure 6.9 Temperature profiles of +X Panel, obtained by SINDA and TheSpAn

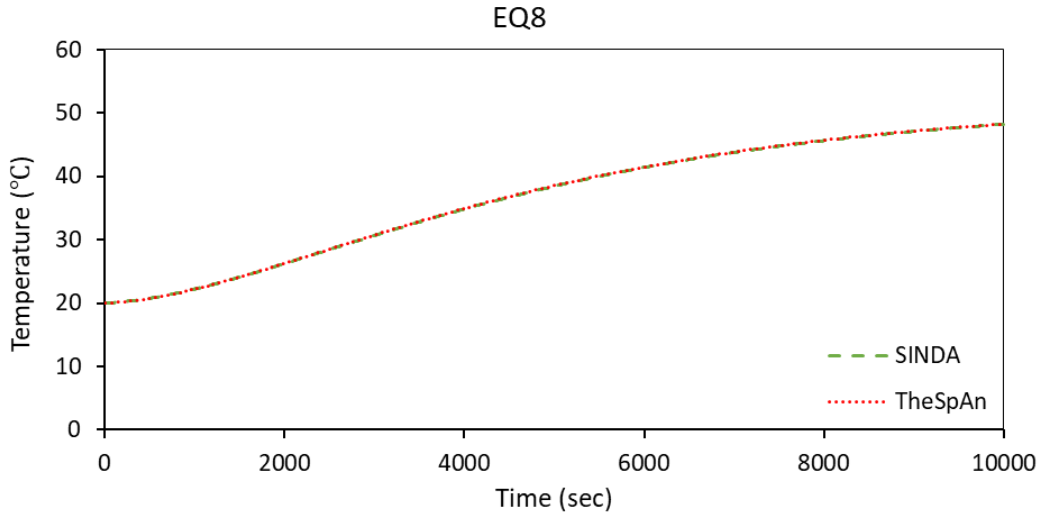

Figure 6.10 Temperature profiles of EQ8, obtained by SINDA and TheSpAn

The temperature profiles of the +X Panel, obtained through SINDA and TheSpAn, were shown in Figure 6.9. In Figure 6.10, on the other hand, the thermal characteristics of imaginary satellite equipment, EQ8, were presented based on data retrieved from SINDA and TheSpAn.

It was noted that both curves consistently displayed alignment upon analyzing the graphical representation of any given satellite component. As a result, TheSpAn was able to match the results of SINDA for the imaginary satellite TVC test.

Then, the real TVC test data of the 6U-sized PiriSat was compared with the results of TheSpAn to evaluate whether the developed tool could predict the thermal behavior of a small satellite quickly and accurately enough. The temperature values of all satellite components were 20℃ initially. The TVC testing of PiriSat was performed as the hot cycle of 50℃ for 8,170 seconds and the cold cycle of -20℃ for following 10,500 seconds, for a test time of 18,670 seconds in total.

To simulate the space thermal environment in the TVC testing, there were 3 nodes corresponding the walls of TVC. For the satellite, there were a total of 57 satellite components, including 31 structural satellite elements and 26 satellite equipment. Batteries, command and data handling systems, attitude determination and control systems and reaction wheels were the heat dissipating components of the satellite.

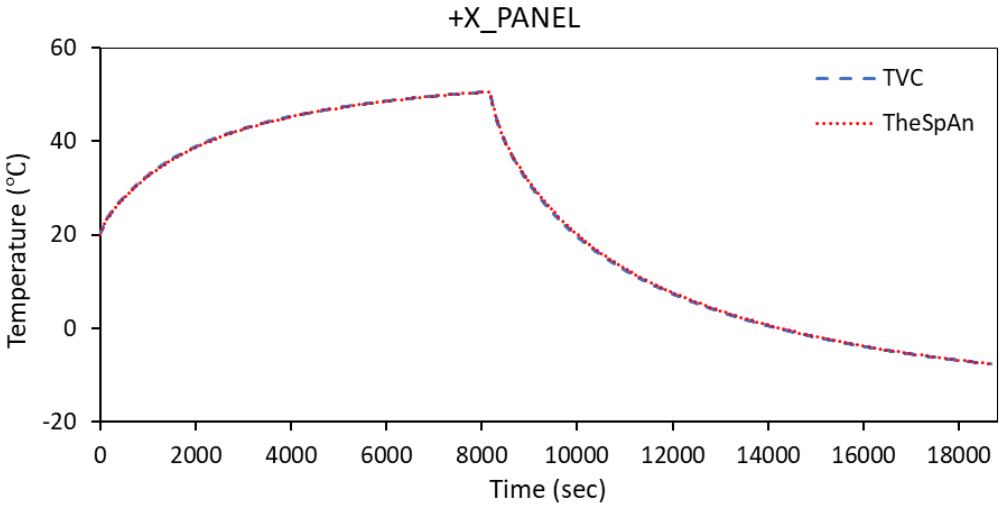

Figure 6.11 Temperature profiles of +X Panel, obtained by TVC test and TheSpAn

The thermal characteristics obtained by the real TVC test data and TheSpAn were demonstrated in Figure 6.11 for the +X Panel. For the +X panel, the temperature began to increase during the hot cycle phase of the test and subsequently decreased as soon as the cold cycle commenced. The maximum temperature was calculated by TheSpAn as 50.61℃ while the minimum temperature was -7.58°C. That caused a temperature gradient of 58.19°C. The average temperature over the test period was found as 22.63°C with TheSpAn. The highest inconsistency between temperature values obtained by TVC and TheSpAn for +X Panel was 0.196°C while the average inconsistency was 0.038°C as per the test period.

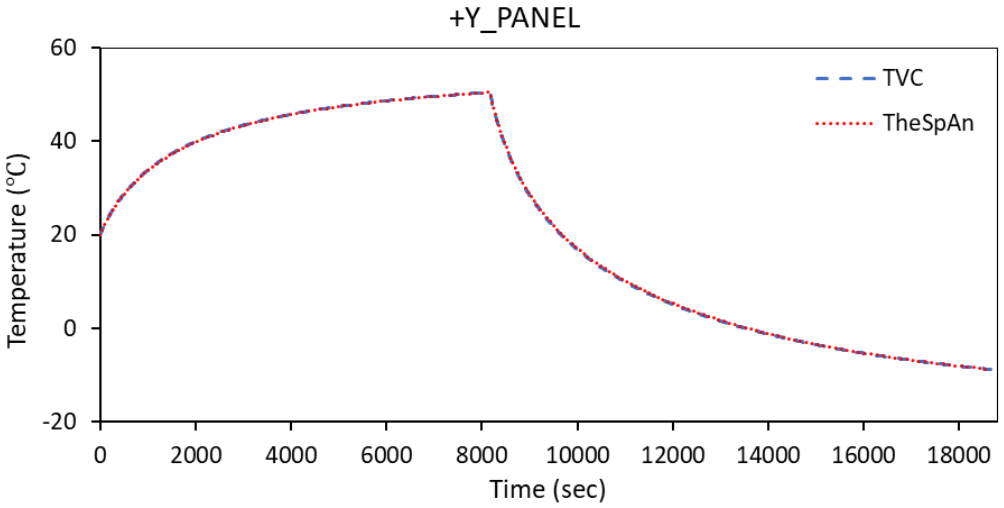

Figure 6.12 Temperature profiles of +Y Panel, obtained by TVC test and TheSpAn

Figure 6.12 exhibited the temperature distribution curves for +Y Panel obtained by TVC testing and TheSpAn. In the simulation performed by means of the developed tool, it was found that the maximum temperature was 50.44℃ where the minimum was -8.77℃. The maximum temperature deviation between the data of TVC test and TheSpAn was appeared as 0.121℃. Thus, a good match was observed between two curves, supporting the validity of the developed tool, TheSpAn.

In Figure 6.13, the temperature variations over time for the +Z Panel were presented, comparing data from the real TVC test and TheSpAn. The average temperature inconsistency between methods was found 0.240°C throughout the test period.

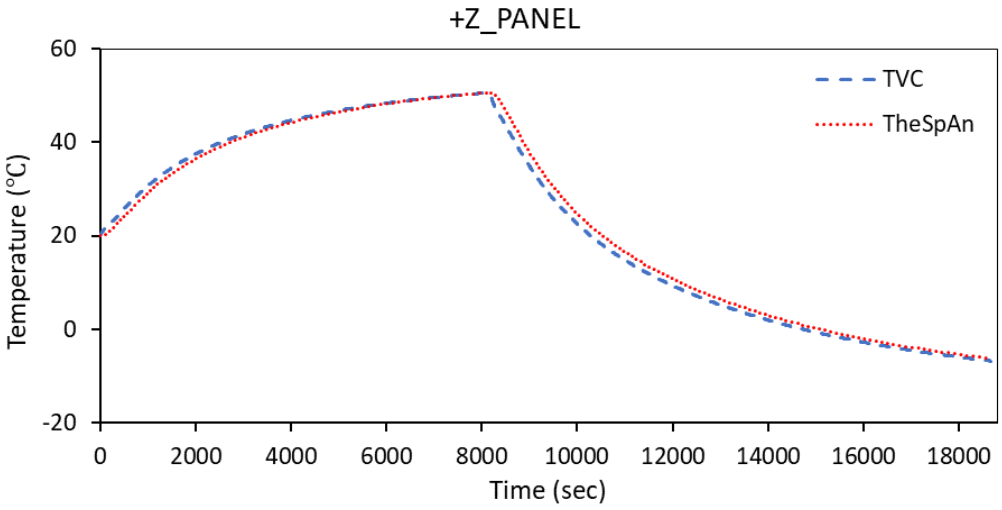

Figure 6.13 Temperature profiles of +Z Panel, obtained by TVC test and TheSpAn

From the statistical point of view, datasets of structural components was compared by means of independent samples t-test. The hypothesis formulated for this statistical test that there was no difference between the temperature data from the real TVC test and by TheSpAn. To evaluate the hypothesis by performing statistical analyses, IBM SPSS Statistics software was used, and the confidence interval level in the analyzes was set to 95%. Comparing the data of the TVC test and TheSpAn, a significance of 0.272 ($p>0.05$) was found that means there was no significant difference between two datasets. As shown in Table 6.2, the significance values were found above the significance level of 0.05 for all satellite panels, meaning that the developed tool provided consistent results with the TVC test.

Table 6.2 Significance values of 2-tailed test for satellite panels

2-tailed test	+X Panel	-X Panel	+Y Panel	-Y Panel	+Z Panel	-Z Panel
Significance	0.871	0.889	0.909	0.931	0.272	0.480

It was observed that there was a good match between the TVC test and TheSpAn for satellite panels as well as other structural components when thermal characteristics were examined both graphical illustrations and statistical findings.

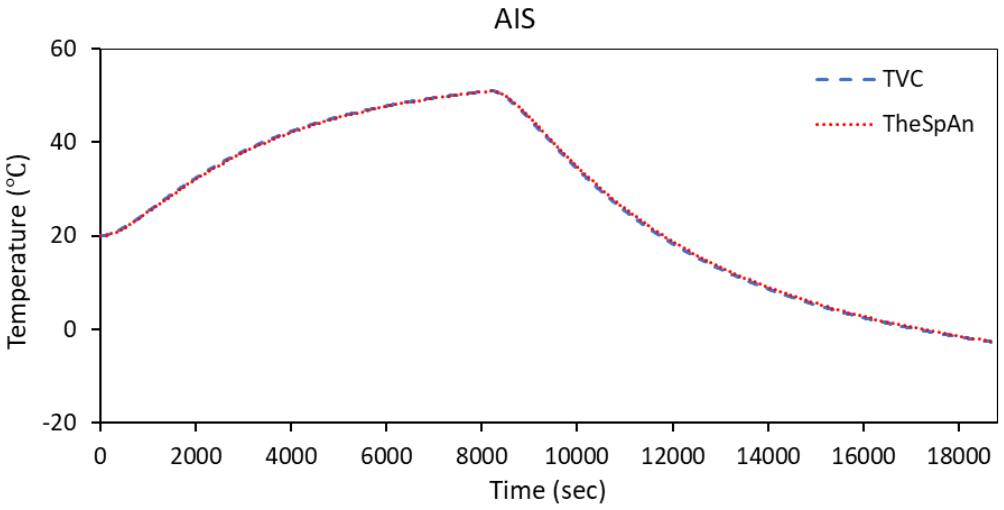

Figure 6.14 Temperature profiles of AIS, obtained by TVC test and TheSpAn

The graphical representation of the temperature curves obtained by TVC test and TheSpAn showed a good match for Automatic Identification System (AIS), as shown in Figure 6.14.

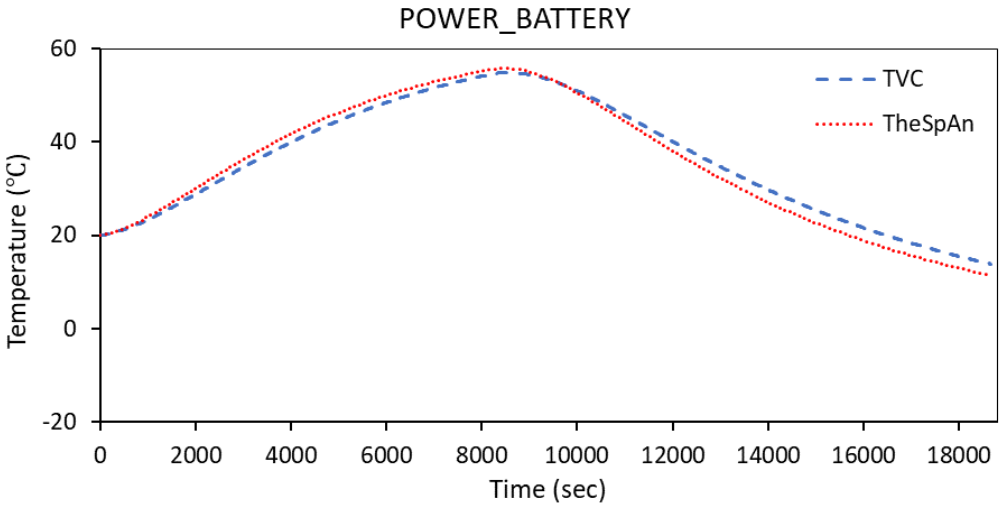

Figure 6.15 Temperature profiles of Power Battery, obtained by TVC test and TheSpAn

Thermal behavior of Power Battery acquired through the TVC test and TheSpAn was illustrated in Figure 6.15. Both datasets were observed matched to each other with minor variations.

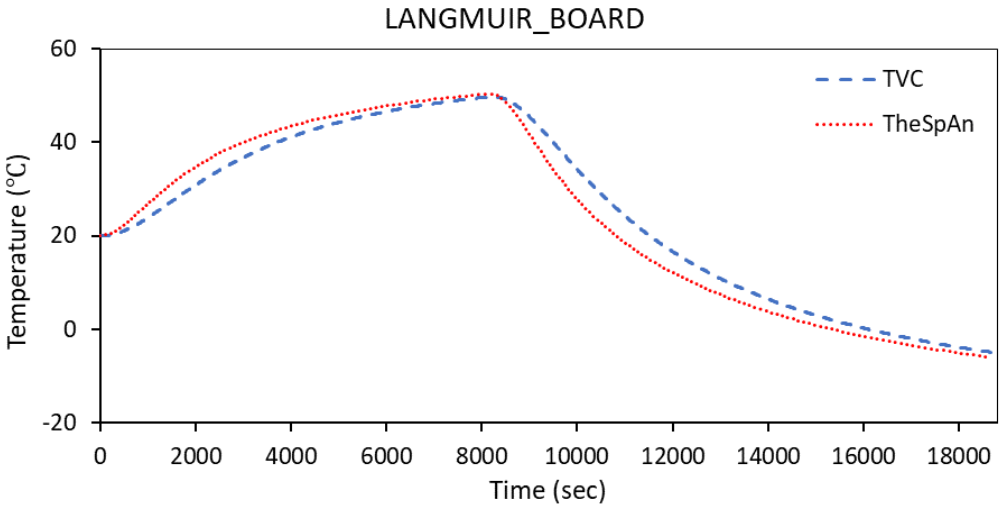

Figure 6.16 Temperature profiles of Langmuir Board, obtained by TVC test and TheSpAn

On the other hand, there were some deviations noticed in the temperature profiles of Langmuir Board obtained by the TVC test and TheSpAn. Yet, the thermal behaviors in both datasets showed similar curves in Figure 6.16. The maximum temperature of this component was found as 50.40℃ and the minimum was -5.95℃ by means of TheSpAn while the maximum was 49.78℃ and the minimum was -4.87℃ at the TVC test data. The averaged inconsistency in the data over the testing period was found 0.415℃ although it reached as high as 6.35℃ at instantaneously.

The statistical analyses using independent samples t-test method were conducted to evaluate the datasets obtained from the TVC test and TheSpAn. The significance values of satellite equipment were presented in Table 6.3.

Table 6.3 Significance values of 2-tailed test for satellite equipment

2-tailed test	AIS	Power Battery	Langmuir Board	GPS	Star Tracker	Reaction Wheel
Significance	0.760	0.140	0.052	0.914	0.881	0.842

The significance values as given in Table 6.3 were found above the significance level of 0.05 for all satellite panels, meaning that the developed tool provided consistent

enough results with the TVC test. Even though the overall temperature distributions exhibited slight inconsistencies when considering all satellite equipment, TheSpAn was found to provide a good approximation in terms of thermal characteristics throughout the test.

To conclude, TheSpAn was developed to perform thermal testing of a 6U sized CubeSat. The tool was used to analyze thermal performance of small satellites in the preliminary design phase by obtaining temperature values of both satellite structures and equipment at a particular test time. It was compared with both the results of a hypothetical satellite obtained by SINDA and the real TVC results of 6U sized PiriSat. The graphical illustrations showed that there were good matches in terms of thermal characteristics between both datasets of the TVC test and TheSpAn. It was seen that TheSpAn can predict the thermal behavior of a CubeSat at an average 94% confidence with an averaged error deviation of 0.7℃. Moreover, analyzing both datasets confirmed that there was no statistically significant difference between the outcomes of TheSpAn and the data of TVC test at the confidence interval level of 95%. Therefore, the tool was validated to analyze temperature data of the satellite fast, easy, and accurate enough for preliminary design tasks. It was resulted that the thermal behavior of any satellite item under various test setups can be assessed within stated error margin through this tool. Moreover, it can be used for 3U, 12U and 24U sized CubeSats as well since they are symmetrical in geometry with 6U sized satellites.

6.7 Conclusion

In this chapter, the development of a spreadsheet analysis tool for thermal testing of CubeSats is presented. The primary objective is to ensure the secure functioning of satellites in space by accurately predicting temperature distributions during the design phase. This is crucial because extreme temperature conditions and rapid fluctuations can generate thermal stresses that may harm satellite components. The study discusses the importance of thermal management in satellite design and the iterative process of assessing thermal characteristics throughout development. An overview of existing thermal analysis tools used in the aerospace industry is presented by highlighting their effectiveness but also their limitations in the early stages of satellite design.

The development of the MS Excel-based analysis tool is explained, which uses VBA to predict CubeSat thermal performance during preliminary testing. It employs finite difference methods, isothermal node assumptions, and conduction/radiation mechanisms for heat transfer modeling. The methodology of the MS Excel-based analysis tool is detailed, including the use of a forward-explicit approach and the energy balance equation to simulate the transient thermal characteristics of the satellite. The study also outlines the material and methods used in testing the PiriSat 6U CubeSat, a Turkish satellite designed to operate within low earth orbit, within a thermal vacuum chamber, replicating the extreme temperature conditions of space.

To sum up, the development of an MS Excel-based analysis tool for CubeSat thermal testing is a valuable contribution to the field of satellite design. It offers a cost-effective and accessible solution for predicting thermal performance in the early stages of development, ensuring the safe operation of satellites in the harsh conditions of space. The application of the study to the PiriSat CubeSat demonstrates the practicality of the tool and its ability to accurately model thermal behavior under varying conditions, contributing to the success of space missions.

CHAPTER 7

DISCUSSION AND CONCLUSION

This thesis study systematically investigates the thermal modeling and analysis of small satellites, with a particular emphasis on CubeSats operating at low Earth orbits, within the complex space environment. The research objectives cover the areas of understanding the connections between external heat loads and orbit characteristics, conducting comparative studies on thermal effects influenced by various design parameters and orbital configurations, evaluating the impact of deployable solar panels on external heat and surface temperature distributions, and developing a spreadsheet analyzing tool for thermal vacuum testing of these small satellites.

The first chapter of this study, the fundamental concepts related to satellites were introduced for a comprehensive understanding of the presented work. The basics of satellites, their types and orbits were explained with this aim. Then, the major aspects of thermal design and thermal control systems for satellites were described as well as the methodologies of satellite thermal modeling and analysis. Next, in Chapter 2, the basic elements of the space thermal environment were discussed by detailing the heat sources of satellites, the orbital parameters affecting them and heat transfer mechanisms. In order to be used in thermal analysis, a general heat balance equation was derived specific to satellites servicing in orbits.

CubeSats at various LEOs were investigated to discuss the effects of external heat loads in Chapter 3 and the surface temperatures in Chapter 4 since there was no detailed study considering both orbital and structural parameters of CubeSats together in the literature, to the best of my knowledge. The findings revealed that orbital altitude, beta angle, CubeSat size and surface properties significantly influence the absorbed heat by satellite panels and temperature distribution on the panels. Beta angles, especially, were found to have great effects on eclipse duration and heat loads received to the satellite consequently. In terms of passive thermal control systems in CubeSats, it was identified that the surface properties, including the ratio of absorptivity to emissivity, play a crucial role to ensure safe operational conditions.

Deployable solar panels at different angles were studied for a 3U CubeSat regarding to their effects on radiative heat input in Chapter 5. The outcomes showed that the deployment angles of solar panels influence the satellite heat budgets and they are practical for optimizing both thermal behavior of satellite parts and harnessing energy through solar panels. Additionally, the worst-case scenario analyses were performed for different earth days, albedo coefficients and earth surface temperatures together with the deployment angles. The results clearly exhibited that Earth orbiting CubeSats experience great variations in external heats from space thermal environment along a year period in space due to the presence of elliptical Earth orbit around the Sun.

Finally, in Chapter 6, a spreadsheet thermal analysis tool, called as TheSpAn, was developed by employing finite difference methods, isothermal node assumptions and considering conductive and radiative heat transfer mechanisms, as a remarkable contribution to the field of thermal testing of CubeSats. It was aimed with the analyzer tool to provide cost-effective and efficient predictions of thermal performance for CubeSats in the early design stages. The practical application of TheSpAn was demonstrated on PiriSat, a 6U CubeSat, to compare the results of real TVC testing with that obtained by TheSpAn and the findings proved its effectiveness in accurately enough modeling thermal behavior for changing conditions.

The presented studies and methods in this thesis have potential opportunities to be extended into a variety of new works. The following ideas for further studies can be proposed:

- A comprehensive thermal study on heat absorption by satellite panels from space thermal environment was provided in the work. The investigations can be extended by including internal equipment of CubeSat and considering the heat transfer among them to investigate more detailed thermal behaviors inside the satellite.

- Solar panels were considered within this thesis. However, there are various types of solar panel arrangements. In order to reveal optimal design, further studies on these arrangements can be conducted.

- In this thesis, deployable solar panels were analyzed to outline the thermal behavior of both the satellite and its solar panels. The research on available solar energy to be harnessed by solar panels can be further studied.

- The thermal analyzer tool in this thesis was developed to predict thermal behavior of CubeSat for TVC testing. The tool can be upgraded to perform on-orbit thermal simulations in the early design stage.

In conclusion, the outcomes provided in this thesis prove that there is a complex interplay among external heat sources, orbital parameters, and satellite design by offering meaningful perspectives for thermal engineers and scientists working in satellite thermal design. The importance of understanding the relationship among variables to build effective thermal control systems was demonstrated. A spreadsheet thermal analysis tool was developed to predict thermal behavior of CubeSats fast, accurate and practical in TVC tests in the early thermal design stage, with desire to enhance the success of space missions. Overall, the study contributes significantly to improving the understanding and effective management of thermal considerations in design and operation of small satellites.

REFERENCES

[1] Maini, A. K., Agrawal, V. "*Satellite technology: principles and applications*" (3rd Edition). John Wiley & Sons Ltd, England, ISBN: 978-1118636473, June 2014.

[2] Kopacz, J. R., Herschitz, R. & Roney, J. Small satellites an overview and assessment. Acta Astronautica, *(170)*, 93-105. 2020

[3] Atar, C., Aktaş, M. & Sözbir, N. Investigation of external heats for CubeSats at various low earth orbits. Pamukkale University Journal of Engineering Sciences, *(29)*, (4) 314-321. 2023

[4] European Space Agency (ESA), Enabling & Support, Space Engineering & Technology, "*The PICosatellite for Atmospheric and Space Science Observations (PICASSO) CubeSat*". (2020, June 16). Accessed 12 November 2023. [Online]. Retrieved from https://www.esa.int/Enabling_Support/Space_Engineering_Technology/PICASSO_CubeSat_to_sift_secrets_from_sunrise

[5] The National Aeronautics and Space Administration (NASA), "*What are SmallSats and CubeSats?*". (2023, August 23). Accessed 9 November 2023. [Online]. Retrieved from https://www.nasa.gov/content/what-are-smallsats-and-cubesats

[6] Garino, B. W., Lanphear, J. D. "Chapter 22 Spacecraft design, structure, and operations". *AU-18 Space Primer*. (1st Edition) pp. (283-298). Alabama, USA: Air University Press. 2009

[7] Karim, S. M. R., Sakib, S., Islam, M. T. & Ahamed, F. A. S. A review of communications satellite by focusing on 'Bangabandhu Satellite-1', the first GEO communications satellite of Bangladesh. International Journal of Networks and Communications. *(8)*, (5), 123-128. 2018

[8] Foster, I. "*Small Satellite Thermal Modeling Guide*". Air Force Research Laboratory, Space Vehicles Directorate, Virginia, USA, July 2022.

[9] Bulut, M. Thermal design, analysis, and testing of the first Turkish 3U communication CubeSat in low earth orbit. Journal of Thermal Analysis and Calorimetry. *(143),* (6) 4341-4353. 2021

[10] Martinez, I. "*Spacecraft thermal control, modelling and testing*". (2023, January 02). Accessed 10 September 2023. [Online]. Retrieved from http://imartinez.etsiae.upm.es/~isidoro/tc3/Spacecraft%20Thermal%20Modelling%20and%20Testing.pdf

[11] Mermer, E. & Ünal, R. Passive thermal control systems in spacecrafts. Journal of the Brazilian Society of Mechanical Sciences and Engineering. *(45),* (3), 1-23. 2023

[12] Soliman, M. A. "Effect of thermo-optical properties on microsatellites passive thermal design". *AIAA SCITECH 2023 Forum*. pp. (1726). Maryland, USA: American Institute of Aeronautics and Astronautics, Inc. 2023

[13] Elshaer, A. M., Soliman, A. M. A., Kassab, M., Mori, S. & Hawwash, A. A. Numerical study about thermal performance evaluation of PCM and PCM/fins composite-based thermal control module at microgravity conditions. International Journal of Thermofluids. *(20),* (100419), 1-14. 2023

[14] NASA Mission Design Division Staff. Small Spacecraft Technology - State of the Art (NASA/TP-2014-216648/REV1). California, USA: NASA Ames Research Center. 2014

[15] Meseguer, J., Pérez-Grande, I. & Sanz-Andrés, A. "20 - Thermal control testing". *Spacecraft Thermal Control*. (1st Edition) pp. (349-371). Cambridge, UK: Woodhead Publishing Ltd. 2012

[16] Bulut, M. & Sözbir, N. Thermal design, analysis and test validation of Turksat-3USAT satellite. Journal of Thermal Engineering. *(7),* (3) 468-482. 2021

[17] Quirino, M., Sciarrone, G., Piazzolla, R., Fuschino, F., Evangelista, Y., Morgante, G., et al. HERMES CubeSat payload thermal balance test and comparison with finite volume thermal model. Applied Sciences. *(13)*, (9) 1-28. 2023

[18] Chisabas, R. S. S., Loureiro, G., Lino, C. O. & Cantor, D. F. "Method for CubeSat thermal-vacuum cycling test specification". *47th International Conference on Environmental Systems*. pp. (1-15). South Carolina, USA: ICES. 2017

[19] Atar, C. & Aktaş, M. Advances in thermal modeling and analysis of satellites. Gazi University Journal of Science. *(35)*, (1) 42-58. 2022

[20] Oshima, K. & Oshima, Y. An analytical approach to the thermal design of spacecrafts. ISAS report/Institute of Space and Aeronautical Science. *(33)*, (1), 1-39. 1968

[21] Arduini, C., Laneve, G. & Folco, S. Linearized techniques for solving the inverse problem in the satellite thermal control. Acta Astronautica. *(43)*, (9-10) 473-479. 1998

[22] Gilmore, D. G. "*Spacecraft Thermal Control Handbook, Volume 1: Fundamental Technologies*" (2nd Revised Edition). AIAA & The Aerospace Press, California, USA, ISBN: 978-1-884989-11-7, December 2002.

[23] Tsai, J. R. Overview of satellite thermal analytical model. Journal of Spacecraft and Rockets. *(41)*, (1) 120-125. 2004

[24] Ziebart, M., Adhya, S., Sibthorpe, A., Edwards, S. & Cross, P. Combined radiation pressure and thermal modelling of complex satellites: Algorithms and on-orbit tests. Advances in Space Research. *(36)*, (3) 424-430. 2005

[25] Gadalla, M. A. Prediction of temperature variation in a rotating spacecraft in space environment. Applied Thermal Engineering. *(25)*, (14) 2379-2397. 2005

[26] Prajapati, J. C., Kachhia, K. B. & Kosta, S. P. Fractional calculus approach to study temperature distribution within a spinning satellite. Alexandria Engineering Journal. *(55)*, (3) 2345-2350. 2016

[27] Chung, P. N., Anh, N. D., Hieu, N. N. & Manh, D. V. Extension of dual equivalent linearization to nonlinear analysis of thermal behavior of a two-node model for small satellites in low earth orbit. International Journal of Mechanical Sciences. *(133)*, 513-523. 2017

[28] Farrahi, A. & Pérez-Grande, I. Simplified analysis of the thermal behavior of a spinning satellite flying over sun-synchronous orbits. Applied Thermal Engineering. *(125)*, 1146-1156. 2017

[29] Pérez-Grande, I., Sanz-Andrés, A., Guerra, C. & Alonso, G. Analytical study of the thermal behaviour and stability of a small satellite. Applied Thermal Engineering. *(29)*, (11-12) 2567-2573. 2009

[30] Gaite, J., Sanz-Andrés, A. & Pérez-Grande, I. Nonlinear analysis of a simple model of temperature evolution in a satellite. Nonlinear Dynamics. *(58)*, (1-2) 405-415. 2009

[31] Gaite, J. Nonlinear analysis of spacecraft thermal models. Nonlinear Dynamics. *(65)*, (3) 283-300. 2011

[32] Baturkin, V. Micro-satellites thermal control – concepts and components. Acta Astronautica. *(56)*, (1-2) 161-170. 2005

[33] Das, T. K., Totani, T., Wakita, M. & Nagata, H. "A simple thermal design procedure for micro- and nano-satellites with deployable solar array panel". *45th International Conference on Environmental Systems*. pp. (1-20). Washington, USA: ICES. 2015

[34] Bulut, M. & Sözbir, N. Analytical investigation of a nanosatellite panel surface temperatures for different altitudes and panel combinations. Applied Thermal Engineering. *(75)*, 1076-1083. 2015

[35] Krishnaprakas, C. K. A comparison of ode solution methods for spacecraft thermal problems. Heat Transfer Engineering. *(19),* (3) 103-109. 1998

[36] Lyon, R., Sellers, J. & Underwood, C. “Small satellite thermal modeling and design at USAFA: FalconSat-2 applications”. *IEEE Aerospace Conference*. pp. (3391-3399). Montana, USA: IEEE. 2002

[37] Diaz-Aguado, M. F., Greenbaum, J., Fowler, W. T. & Lightsey, E. G. “Small satellite thermal design, test, and analysis”. *Proceedings Volume 6221, Modeling, Simulation, and Verification of Space-based Systems III*. pp. (74-85). Florida, USA: SPIE. 2006

[38] Narayana, K. B. & Reddy, V. V. Thermal design and performance of HAMSAT. Acta Astronautica. *(60),* (1) 7-16. 2007

[39] Sözbir, N., Bulut, M., Oktem, M., Kahriman, A. & Chaix, A. Design of thermal control subsystem for TUSAT telecommunication satellite. International Journal of Computer and Systems Engineering. *(2),* (7) 1370-1373. 2008

[40] Bulut, M., Kahriman, A. & Sözbir, N. "Design and analysis for thermal control system of nanosatellite". *Proceedings of the ASME 2010 International Mechanical Engineering Congress and Exposition*. pp. (863-866). British Columbia, Canada: ASME. 2010

[41] Dinh, D. Thermal Modeling of Nanosat. Unpublished master thesis, San Jose State University. 2012

[42] Garzon, M. M. Development and analysis of the thermal design for the OSIRIS-3U CubeSat. Unpublished master thesis, Pennsylvania State University. 2012

[43] Athirah, N., Afendi, M., Hafizan, K., Amin, N. A. M. & Majid, M. S. A. Stress and thermal analysis of CubeSat structure. Applied Mechanics and Materials. *(554),* 426-430. 2014

[44] Silva, D. F. D., Muraoka, I. & Garcia, E. C. Thermal control design conception of the Amazonia-1 satellite. Journal of Aerospace Technology and Management. *(6)*, (2) 169-176. 2014

[45] Wachche, S., Marne, A., Singare, S., Naik, P., Bhide, O., Chaudhari, G., et al. "Thermal modelling and simulation of a Pico-satellite using finite element method". *5th International Conference on Thermal Process Modeling and Computer Simulation*. pp. (65-74). Florida, USA: ASM International. 2014

[46] Flecht, T. Thermal modelling of the PICSAT nanosatellite platform and synergetic prestudies of the CIRCUS nanosatellite. Unpublished master thesis, Lulea University of Technology. 2016

[47] Chandrashekar, S. Thermal analysis and control of MIST CubeSat. Unpublished master thesis, KTH Royal Institute of Technology. 2017

[48] Bulut, M., Sözbir, Ö. & Sözbir, N. "Thermal control of Turksat 3U nanosatellite". *5th International Symposium on Innovative Technologies in Engineering and Science*. pp. (26-32). Baku, Azerbaijan: Azerbaijan University of Architecture and Construction. 2017

[49] Still, V. Thermal control design and simulation of a space mission. Unpublished master thesis, Lulea University of Technology. 2018

[50] Bonnici, M., Mollicone, P., Fenech, M. & Azzopardi, M. A. Analytical and numerical models for thermal related design of a new pico-satellite. Applied Thermal Engineering. *(159)*, (113908) 1-9. 2019

[51] Elhefnawy, A. & Elweteedy, A. thermal analysis of a small satellite in post-mission phase. Journal of Multidisciplinary Engineering Science and Technology. *(6)*, (2) 9495-9504. 2019

[52] Salazar-Salinas, G., Botello-Ramírez, E. & Avalos-Gauna, E. "Thermal analysis of a 3U-CubeSat, a case study of Pakal satellite". *Proceedings of the 8th International Conference on Fluid Flow, Heat and Mass Transfer*. pp. (1-8). Ontario, Canada: International ASET Inc. 2021

[53] Akka, A., Benabdelouahab, F. & Yerrou, R. Low earth orbit nanosatellite: influence of heat dissipation on passive thermal analysis. Acta Polytechnica. *(62)*, (5) 498-504. 2022

[54] Narimane, B. & Bah, A. “Thermal control: Case study of 3U CubeSat”. 2023 *Advances in Science and Engineering Technology International Conferences*. pp. (1-5). Dubai, UAE: IEEE. 2023

[55] Hernández, A., Ferrer, J. A., Gaviria, D., Romo, C. & Chávez, R. G. Calculation of environmental loads for a CubeSat using MATLAB. Journal of Physics: Conference Series. *(2475)*, (1) 1-12. 2023

[56] Seyedzadeh, A., Aasim, W. F. A. W., Okasha, M., Jallad, A. H. & Sulaeman, E. “Numerical analysis and experimental validation of the thermal subsytem of Alainsat-1”. *2023 IEEE International Geoscience and Remote Sensing Symposium*. pp. (368-371). California, USA: IEEE. 2023

[57] Zhou, Y., Zhang, X., Xu, C. & Yang, X. Thermal design and analysis of JZJ-5 CubeSat. Journal of Physics: Conference Series. *(2472)*, (1) 1-6. 2023

[58] Hosny, I., Mokhtar, A. & Safwat, I. M. Comparative study of energy balance for a 3U CubeSat for different orientation flight scenarios. Journal of Physics: Conference Series. *(2616)*, (1) 1-9. 2023

[59] Chippalkatti, V. S., Biradar, R. C., Chandrashekar, B. K., Suresha, K. R. & Joteppa, S. Structural and thermal modeling, verification, and optimization of space TR module for radar imaging. International Journal on Interactive Design and Manufacturing. *(17)*, (6) 1-11. 2022

[60] Hipp-Méndez, J. R., Sánchez-Varela, V., Galindo-Rosales, R. J. & Zorto-Aguilera, F. J. “Morazán MRZ-SAT CubeSat: Thermal modelling and analysis guide for academic CubeSat missions”. *73rd International Astronautical Congress*. pp. (1-15). Paris, France: International Astronautical Federation. 2022

[61] Zheng, H. R., Ma, Y., Zhang, S., Wang, J. C. & Qu, Y. Y. Calculation of orbit heat flow and research on radiation characteristics of space target. Chinese Optics. *(16)*, (6) 1-11. 2023

[62] Li, Y., Feng, T., Wang, Y., Zhu, Z., Peng, H. X., Xu, P., et al. Real-time evaluating temperature-dependent interfacial shear strength of thermoplastic composites based on interfacial stress impedance effect of magnetic fibers. Composites Part A: Applied Science and Manufacturing. *(176)*, 1-9. 2023

[63] Atar, C., Aktaş, M., Sözbir, N. & Çamdalı, Ü. "Effects of solar panel deployment angle on radiative heat input for a 3U CubeSat at LEO". *2nd International Congress on Multidisciplinary Natural Sciences and Engineering*. pp. (51-51). Ankara, Türkiye: BIDGEDER. 2022

[64] Atar, C., Aktaş, M., Sözbir, N. & Bulut, M. Analytical investigation of surface temperatures for different sized CubeSats at varying low earth orbits. ASME Journal of Thermal Science and Engineering Applications. *(15)*, (8) 1-6. 2023

[65] Birur, G. C., Siebes, G., Swanson, T. D. & Powers, E.I. "*Spacecraft Thermal Control*" (3rd Edition). Academic Press, California, USA, March 2001.

[66] Bárcena, D. G. Planetary and low orbit thermal environment for space thermal design. Unpublished doctoral dissertation, Universidad Politécnica de Madrid. 2022.

[67] Meseguer, J., Pérez-Grande, I. & Sanz-Andrés, A. "2 - Space environment". *Spacecraft Thermal Control*. (1st Edition) pp. (15-38). Cambridge, UK: Woodhead Publishing Ltd. 2012

[68] Arroyo, P. S. Mission and thermal analysis of UPC CubeSat. Unpublished master thesis, Universitat Politecnica de Catalunya. 2009.

[69] Meseguer, J., Pérez-Grande, I. & Sanz-Andrés, A. "19 - Thermal mathematical models". *Spacecraft Thermal Control*. (1st Edition) pp. (339-348). Cambridge, UK: Woodhead Publishing Ltd. 2012

[70] Garmendia, I. & Anglada, E. Transient thermal parameters correlation of spacecraft thermal models against test results. Acta Astronautica. *(199)*, 49-57. 2022

[71] Shibukawa, T. & Nakasuka, S. "A system-level spacecraft thermal model reduction method applicable to transient analysis". *52nd International Conference on Environmental Systems*. pp. (1-14). Alberta, Canada: ICES. 2023

[72] NASA Environmental and Thermal Systems Section Applied Mechanics Department. Thermal network modelling handbook. (Report No. TRW-14690-H003-RO-00). Texas, USA: NASA. 2013

[73] Peabody, H. "Use of TSS as a neutral format for geometry model conversions: An alternative to STEP-TAS". *16th European Workshop on Thermal and ECLS Software*. pp. (1-9). Noordwijk, The Netherlands: ESA European Space Research and Technology Centre. 2002

[74] Panczak, T., Rickman, S., Fried, L. & Welch, M. Thermal synthesizer system: An integrated approach to spacecraft thermal analysis. SAE Transactions. *(100)*, (1) 1851-1867. 1991

[75] Yang, K. "*The anatomy of ESATAN and ESARAD thermal model files*" (1st Edition). BiblioGov, California, USA, ISBN: 978-1289063030, June 2013.

[76] Duffy, K. "Introduction to NX TMG Space Thermal". *20th European Workshop on Thermal and ECLS Software*. pp. (169-188). Noordwijk, The Netherlands: ESA European Space Research and Technology Centre. 2006

[77] Sanchez-Sanjuan, S., Gonzalez-Llorente, J. & Hurtado-Velasco, R. Comparison of the incident solar energy and battery storage in a 3U CubeSat satellite for different orientation scenarios. Journal of Aerospace Technology and Management. *(8)*, (1) 91-102. 2016

[78] Wallace, P., Kalapura, A. & Kim, S. I. "Thermal modelling and analysis of a cube satellite, EIRSAT-1: Steady analysis". *2018 AIAA SPACE and Astronautics Forum and Exposition*. pp. (1-15). Florida, USA: AIAA. 2018.

[79] Almehisni, R. & Naimat, F. A. “Heat transfer influence of solar panel on spacecraft”. *2018 Advances in Science and Engineering Technology International Conferences*. pp. (1-6). Dubai, UAE: IEEE. 2018

[80] Lu, Y., Shao, Q., Yue, H. & Yang, F. A review of the space environment effects on spacecraft in different orbits. IEEE Access. *(7)*, 93473-93488. 2019

[81] Nenarokomov, A. V., Dombrovsky, L. A., Krainova, I. V., Alifanov, O. M. & Budnik, S. A. Identification of radiative heat transfer parameters in multilayer thermal insulation of spacecraft. International Journal of Numerical Methods for Heat & Fluid Flow. *(27)*, (3) 598-614. 2017

[82] Sundu, H. & Döner, N. Detailed thermal design and control of an observation satellite in low earth orbit. European Mechanical Science. *(4)*, (4) 171-178, 2020

[83] Reiss, P. and Hager, P., Bewick (Lucking), C. & Macdonald, M. "New Methodologies for the Thermal Modeling of CubeSats". *26th Annual AIAA/USU Conference on Small Satellites*. pp. (1-12). Utah, USA: AIAA & Utah State University. 2012

[84] Corpino, S., Caldera, M., Nichele, F., Masoero, M. & Viola, N. Thermal design and analysis of a nanosatellite in low earth orbit. Acta Astronautica. *(115)*, 247-261. 2015

[85] Anh, N. D., Hieu, N. N., Chung, P. N. & Anh, N. T. Thermal radiation analysis for small satellites with single-node model using techniques of equivalent linearization. Applied Thermal Engineering. *(94)*, 607-614. 2016

[86] Steven, H. & Huzain, M. F. Requirements and design structure for Surya Satellite-1. IOP Conference Series: Earth and Environmental Science. *(149)*, 1-10. 2018

[87] Kovács, R. & Józsa, V. Thermal analysis of the SMOG-1 PocketQube satellite. Applied Thermal Engineering. *(139)*, 506-513. 2018

[88] Nenarokomov, A. V., Alifanov, O. M., Krainova, I. V., Titov, D. M. & Morzhukhina, A. V. Estimation of environmental influence on spacecraft materials radiative properties by inverse problems technique. Acta Astronautica. *(160)*, 323-330. 2019

[89] Filho, E. M., Nicolau, V. P., Paiva, K. V. & Possamai, T. S. A comprehensive attitude formulation with spin for numerical model of irradiance for CubeSats and Picosats. Applied Thermal Engineering. *(168)*, 1-14. 2020

[90] Filho, E. M., Seman, L. O. & Nicolau, V. P. Simulation of a CubeSat with internal heat transfer using finite volume method. Applied Thermal Engineering. *(193)*, 1-15. 2021

[91] Malde, C. K., Sharma, G. & Aneesh, A, M. "Development and testing of computational model for the thermal analysis of a CubeSat Nanosatellite". *2021 IEEE Aerospace Conference (50100)*. pp. (1-9). Montana, USA: IEEE. 2021

[92] Garzón, A., Tami, J. A., Campos-Julca, C. D. & Acero-Niño, I. F. Effect of beta angle and contact conductances on the temperature distribution of a 3U CubeSat. Thermal Science and Engineering Progress. *(29)*, 1-16. 2022

[93] Notton, G. "Solar radiation for energy applications". *Encyclopedia of Sustainable Technologies* (1st Edition). pp. (339-356) Ohio, USA: Elsevier. 2017

[94] Li, J., Yan, S. & Cai, R. Thermal analysis of composite solar array subjected to space heat flux. Aerospace Science and Technology. *(27)*, (1) 84-94. 2013

[95] Vertat, I. & Vobornik, A. Efficient and reliable solar panels for small CubeSat Picosatellites. International Journal of Photoenergy. *(2014)*, 1-8. 2014

[96] Narimane, B., Daghouri, A., Bah, A. & El Hani, S. "Analysis of CubeSat thermal performance using various PV panel configurations". *2023 IEEE 10th International Workshop on Metrology for AeroSpace*. pp. (125-130). Milan, Italy: IEEE. 2023

[97] Knight, R., Pin, O. & Thomas, J. “ThermXL: A thermal modelling tool integrated within Microsoft® Excel”. *30th International Conference on Environmental Systems*. pp. (1-10). Toulouse, France: SAE International. 2000

[98] Thomas, J., Robson, A. & Price, S. “Spreadsheet analysis for early phase thermal design”. *31st International Conference on Environmental Systems*. pp. (1-9). Florida, USA: SAE International. 2001

[99] Allison, C., Diaz-Aguado, M. F. & Jaroux, B. A. “SatTherm: A thermal analysis and design tool for small spacecraft”. *23rd Annual AIAA/USU Conference on Small Satellites*. pp. (1-9). Utah, USA: AIAA & Utah State University. 2009

[100] Işık, H. G., Uygur, A. B., Ömür, C. & Solakoğlu, E. “The thermal analysis of a satellite by an in-house computer code based on thermal network method and Monte Carlo Ray Tracing technique”. *Proceedings of 5th International Conference on Recent Advances in Space Technologies*. pp. (978-983). Istanbul, Türkiye: IEEE. 2011

[101] Shirazi, A. & Mirshams, M. Software development for satellite thermal design. Applied Mechanics and Materials. *(390)*, 703-707. 2013

[102] NASA Ames Research Center. Small-Satellite Mission Failure Rates (NASA/TM-2018-220034). California, USA: NASA. 2019

[103] Busch, S., Bangert, P., Dombrovski, S. & Schilling, K. UWE-3, in-orbit performance and lessons learned of a modular and flexible satellite bus for future pico-satellite formations. Acta Astronautica. *(117)*, 73-89. 2015

APPENDICES

Appendix A: Some Real Examples on Satellite Thermal Issues

Appendix A – Some Real Examples on Satellite Thermal Issues

Small satellites are sensitive to thermal challenges. Due to these facts, several historical incidents have occurred in some years. Various examples below illustrate how thermal issues have impacted them. These mainly point to the significance and problematic of the thesis study.

1. QuakeSat (2003)

QuakeSat, a 3U CubeSat successfully launched on June 30, 2003, was a collaborative nanosatellite project involving Stanford University's Space Systems Development Laboratory and the QuakeFinder Team. Its primary objective is to identify earthquake signatures through the detection of extremely low frequency magnetic signals. It operated in a Sun-Synchronous Orbit with an average altitude of around 820 km.

Six months after the launch, both batteries were lost, leading to the reliance on solar power alone to sustain the mission. The probable cause was overheating, with temperatures reaching 120 degrees Fahrenheit. This overheating likely damaged the batteries, possibly leading to the evaporation of the electrolyte because the batteries lacked additional sealing beyond the standard factory packaging.

Regarding thermal design and control, the incident underscored the importance of addressing and mitigating high-temperature conditions to ensure the proper functioning and longevity of critical components [102].

2. SpriteSat (2009)

SpriteSat, an Earth observation satellite developed by Tohoku University in Sendai, Japan, was launched in early 2009 as a secondary payload on a Japanese H-2A-202 rocket. The small satellite, weighing 50 kg, was placed into the sun-synchronous orbit with an altitude of 600 km. It was designed to monitor Sprites, which are lightning-related phenomena in the upper atmosphere.

After reaching orbit, SpriteSat has been renamed Raijin, but faced a premature failure within just 12 days. The issue was attributed to a malfunction in the battery charging

system, led to critical temperature levels. That situation highlighted the significance of effective management of satellite thermal conditions [102].

3. TET-1 (2012)

TET-1, Technology Experiment Carrier 1, was a microsatellite launched in 2012 from the Baikonur Cosmodrome and operated by the German Space Operations Center of the German Aerospace Center. The satellite, positioned approximately 520 kilometers above Earth in its orbit, was designed with a 90-minute orbital period, including 60 minutes of exposure to solar radiation. The primary goal of TET-1 was to perform test and verification activities for a lithium-polymer battery system, a GPS receiver, and innovative solar cells.

The satellite experienced a temperature increase beyond the anticipated level, leading to a slight surpassing of the battery voltage. This issue was resolved by adjusting the orientation of the satellite [102].

4. UWE-3 (2013)

UWE-3 was a 1U-sized picosatellite developed as the third generation of a micro-satellite series by the University of Würzburg. The main technical goal of the satellite mission was to enhance the current attitude determination system and expand a basic position control system. This effort aimed to lay down the technical groundwork for developing durable and robust pico-swarms. Moreover, it was aimed to assess the performance of recent developments in hardware and software designs, covering the implementation of a real-time miniature attitude determination and control system onboard the satellite. That involved utilizing a range of sensors, magnetic torques, and a single reaction wheel.

The thermal control of UWE-3 encountered unforeseen challenges with its deployable solar panel. It led to unexpected thermal effects. These issues affected the power generation and overall thermal equilibrium of the satellite. This situation underlined the significance of meticulous thermal management for deployable components in the design of small satellites and further thermal investigations and enhancements were advised in preparation for future missions [103].

These incidents showcase some real examples for practical challenges that small satellites encounter regarding thermal control, drawing attention to the significance of implementing efficient thermal management strategies in both their design and operation.